Geometric Path-Planning Algorithm in Cluttered 2D Environments Using Convex Hulls

Nafiseh Masoudi
Clemson University

GEOMETRIC PATH-PLANNING ALGORITHM IN CLUTTERED 2D ENVIRONMENTS USING CONVEX HULLS

A Thesis
Presented to
the Graduate School of
Clemson University

In Partial Fulfillment
of the Requirements for the Degree
Master of Science
Mechanical Engineering

---

by
Nafiseh Masoudi
December 2017

ABSTRACT

Routing or path planning is the problem of finding a collision-free path in an environment usually scattered with multiple objects. Finding the shortest route in a planar (2D) or spatial (3D) environment has a variety of applications such as robot motion planning, navigating autonomous vehicles, routing of cables, wires, and harnesses in vehicles, routing of pipes in chemical process plants, etc. The problem often times is decomposed into two main sub-problems: modeling and representation of the workspace geometrically and optimization of the path. Geometric modeling and representation of the workspace is paramount in any path planning problem since it builds the data structures and provides the means for solving the optimization problem. The optimization aspect of the path planning involves satisfying some constraints, the most important of which is to avoid intersections with the interior of any object, and optimizing one or more criteria. The most common criterion in path planning problems is to minimize the length of the path between a source and a destination point of the workspace while other criteria such as minimizing the number of links or curves could also be taken into account.

Planar path planning is mainly about modeling the workspace of the problem as a collision free graph. The graph is later on searched for the optimal path using network optimization techniques such as branch-and-bound or search algorithms such as Dijkstra's. Previous methods developed to construct the collision free graph explore the entire workspace of the problem which usually results in some unnecessary information that has no value but to increase the time complexity of the algorithm, hence, affecting the efficiency significantly. For example, the fastest known algorithm to construct the visibility graph, which is the most common method of modeling the collision free space, in a workspace with a total of n vertices has a time complexity of order $O(n^2)$.

In this research, first, the 2D workspace of the problem is modeled using the tessellated format of the objects in a CAD software which facilitates handling of any free form object. Then, an algorithm is developed to construct the collision free graph of the workspace using the convex hulls of the intersecting obstacles. The proposed algorithm focuses only on a portion of the workspace involved in the straight line connecting the source and destination points. Considering the worst case that all the objects of the workspace are intersecting, the algorithm yields a time complexity of $O(n\log(n/f))$, with n being the total number of vertices and f being the number of objects. The collision free graph is later searched for the shortest path between the two given nodes using a search algorithm known as Dijkstra's.

TABLE OF CONTENTS

LIST OF TABLES

LIST OF FIGURES

NOMENCLATURE

C-hull	Convex hull
E	Set of edges of a graph
f	Total number of obstacles in the workspace
L	Total number of links or line segments in a workspace
m	Number of intersecting obstacles
n	Total number of vertices in a workspace
N	Total number of facilities in the facility location problem
n_{ave}	Average number of vertices per object
n_{max}	Maximum number of vertices per object
P	Polygon or set of disjoint polygons
V	Set of vertices of a graph

Chapter One
INTRODUCTION

In today's highly competitive business environment, industries strive to develop smaller and lighter products while increasing their performance. One critical issue is how to assemble the required subcomponents in tighter enclosures while ensuring ease of assembly and full functionality. Compact packaging of a finite number of components in an enclosed domain is an example of such assembly planning for smaller systems.

In an attempt to design a compact package, Dandurand et. al. [1] formulate the problem of designing a layout for hybrid vehicles as a bi-level optimization problem. In their article, the compact packaging of components in vehicle under-hood to achieve an optimum center of gravity, accessibility, survivability, dynamic behavior, and other objectives is undertaken. Before Dandurand, other research studies have been done on addressing different types of packaging problem. for example, Wodziak and Fadel [2], propose a methodology based on the Genetic Algorithm (GA), a heuristic optimization technique, to solve the optimal packing of rectangular boxes in a rectangular shaped enclosure. The objective of this optimization problem is to find the optimal location for the center of gravity of the system. In a separate study, Grignon and Fadel [3], take more complex shapes (including non-convex and hollow shapes) into account in the packaging problem and find the optimal configuration for a system of components (based on their locations) using GA. The objectives of this optimization problem, in addition to the location of the center of gravity (balance), are compactness and maintainability, hence, making the problem multi-criteria. Furthermore, in all packaging problems, the most important constraint is to avoid any interference between the components to be packed. In view of multiple objective packaging problem, Miao et.al. [4] use Multiple Objective Genetic Algorithm (MOGA) to optimize the configuration based on the ground clearance and dynamic behavior and apply the method to the design of a midsize truck. For the multiple criteria optimization problems, since the criteria are in conflict, the solution will be a Pareto front (rather than a single point in the domain) and a solution can be selected based on a trade-off between the criteria. As a new solution method to the packaging problem, Dong et.al. [5] propose using the rubber band analogy. Their method simulates the movement of the components based on the elastic force of the rubber band (2D) or rubber balloon (3D) and a reaction force by the components to avoid collisions between them. Following this approach, they are able to find the locations of the components such that the maximum compactness is achieved. Tiwari et.al.[6] move on to a step further and propose a GA-based optimization algorithm to find both the compact packing and the sequence of packing a set of 3D free form components inside an arbitrary enclosure. Finally from a different perspective, Katragadda et.al. [7] investigate the thermal performance of a vehicle under-hood packaging optimization. Hence, in addition to the packaging optimization criteria of minimizing the height of the center of gravity and maximizing the accessibility and survivability, they include the thermal performance of the vehicle under-hood. Exploitation of a CFD analysis, leads them to the temperatures of various components under different configurations. Finally, an optimizer identifies optimal configuration based on the lower thermal risk for the components.

After the identification of an optimal way to pack components and devices under the hood, the problem of how to connect them efficiently arises; this is the wire, hose or pipe routing problem.

Wires or cables and hoses or pipes are used in every electro-mechanical system to connect subsystems and components. For example, under the hood of an automobile or in ships and aircraft engines, hundreds to thousands of wires, hoses, and pipes are used, adding significant weight to the system. Wires are often times bundled together in cable harnesses for protection and ease of assembly. As new features are continuously added to the vehicles, their cable harnesses are becoming heavier and more complex to design. According to Matheus in his book "Automotive Ethernet" [8], cabling is the third heaviest and costliest component in a car after its engine and chassis. Therefore, an optimal cable and hose routing is required to reduce their length and therefore minimize the total weight of a vehicle while at the same time directly impacting fuel efficiency.

Traditionally, cables and hoses have been routed using a manual trial-and-error approach in a CAD system. It was sometimes tested on prototypes, but it is mostly based on the experience of the skilled engineers. This manual approach is time-consuming, tedious, and error-prone. In addition, most of the time, it results in suboptimal solutions. Automating the optimal routing of these cables and hoses has been a challenging question for decades.

Routing or path planning, the problem of finding the shortest collision-free path in an environment (e.g. a graph or a geometric space), appears not only in the vehicle assembly planning but also in other disciplines including pipe routing in chemical process plants, robot motion planning, navigating autonomous vehicles, routing on networks, and so on. In all these instances there are some criteria (e.g., minimization of the length of the path) to be optimized and constraints to be satisfied (such as collision avoidance). These constraints and criteria could differ depending on the discipline and problem specifics.

The definition of the path planning problem implies a decomposition of the general problem into three interactive domains as shown in Figure 1.1.

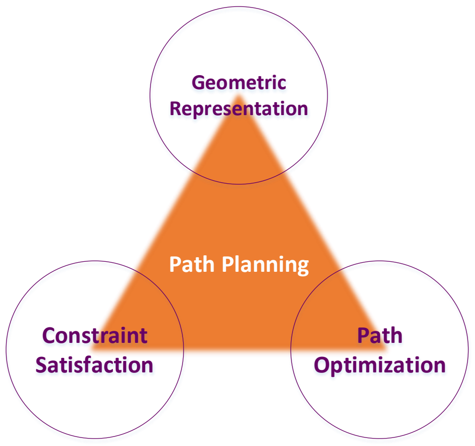

Figure 1.1 Path Planning Problem Domains

The first step in solving any path planning problem is to represent the environment of the problem geometrically or graphically. Geometric representation is a fundamental aspect of path planning problems, which provides a basis for the other domains. An appropriate representation of the complex environment provides meaningful data, which could be manipulated and utilized in the constraint checking and optimization domains.

The environment of a path planning problem typically consists of an enclosed domain with several cluttered objects that have to be avoided. Collision avoidance is an example of different constraints required to be satisfied. The Constraint handling domain takes care of the possible interferences as well as any other constraints and guarantees the feasibility of the path. Path planning on networks and graphs is not concerned with the collision avoidance constraint and this type of constraint is only critical in problems dealing with geometric environments cluttered with obstacles.

The Path optimization domain deals with solving a routing problem. Some of the optimization objectives include the length of the path (e.g., Euclidian length), number of turns in the path, the sharpness of the turns, and time to complete the path.

The Path planning problem could occur in any n-dimensional space. The addition of one dimension to the problem would significantly affect the computational complexity of the problem. Therefore, it is reasonable to start solving the path planning problem in lower dimensions and after testing different cases and validating the solutions, adapt the approach to the higher dimensions.

The 2D path planning problem is the simplest case of a routing problem which mainly involves finding the shortest path on the graph of the collision-free space. In order to satisfy the collision avoidance constraint in 2D geometric workspaces cluttered with obstacles, the problem is converted to constructing a network or graph from the free space and searching that graph for the optimal solution. The free space is the region of the workspace not occupied by any of the obstacles.

Path planning on networks for transportation and communication problems is an example of the 2D planning in which there usually exists a known set of nodes and segments that connect those nodes forming a graph. For example, the nodes could represent cities (locations of supply and demand) and the segments represent the flow of goods, information or signal between the two nodes.

A well-known and most-studied example of graph routing is the Travelling Salesman Problem. In this problem, a salesperson travels to a known set of cities represented as nodes. S/he has to visit each city exactly once and return to the starting point. The criterion is to minimize the total travel distance. This problem is known to be NP-hard, which means it cannot be solved using deterministic optimization techniques in polynomial time [7].

Whether someone is interested in solving a path planning problem modeled on a network graph or a more real-world planning problem in 3D, the solution methods, in general, can be summarized and classified into the following three main categories though not all of them address the problem in full generality [9].

- *Roadmap techniques:* roadmap techniques map the geometric space (in any dimension) to a 1D connectivity graph of the free space. The graph can then be searched using any of the local search or network optimization algorithms to find the shortest path. Probabilistic Road Map (PRM), visibility graph, and Voronoi diagram are examples of roadmap techniques. Roadmap techniques have roots in computational geometry[10].

  In PRM, the vertices of the graph are generated randomly in the collision-free space. These vertices are then connected to their k-nearest neighbors to form the edges of a graph such that there will not be any intersections with obstacles [11]. As pointed out in [10], PRM is an effective method in dealing with dynamic path planning. Dynamic path planning problems involve dynamic instead of stationary obstacles and the locations of obstacles could be changed real-time, thus, they are not given a priori. However, Bhattacharya and Gavrilova [10] claim that PRM could hardly meet the optimization criteria of the path planning due to its probabilistic nature. Visibility and Voronoi (also known as retraction) techniques are explained in detail in chapter 4.

- *Motion planning:* motion planning in robotics is a problem similar to routing or path planning. The only difference is that in motion planning, the robot is not a simple point and its configuration and topology should be taken into account while planning for a collision-free path. However, since planning a path for an agent with an arbitrary size and typically complex geometry is quite challenging, robot motion planning introduces the concept of configuration space. Configuration space is a way of representing the workspace by treating the robot as a point, rather than an object with a complex geometry, traveling from the initial point to a final point and modifying the geometry of the obstacles instead to reflect the shape of the robot. Some of the common techniques used widely in robot motion planning are potential fields and exact or approximate cell decomposition.

  In the Potential Field (PF) method, scalar functions similar to electrostatic potentials are assigned to all nodes of the search graph. The potentials assigned to the nodes lying on the obstacles are the highest. Knowing that the constraint is to avoid any collisions, the objective is to find a path with the minimum potential among all. The path can then be generated by following the steepest descent directions of the potential toward the goal [12]. Despite its efficiency in dealing with collisions in real time, the potential field has a major drawback. As stated in [8], there usually could exist local minima at points other than the goal point where the path could be stuck, which causes problems in reaching the goal. The Cell decomposition technique is described in chapter 4.

- *Mathematical programming:* in contrast to the former techniques, mathematical programming does not require a graph of the free space to identify the shortest path. Unlike the other approaches, mathematical programming develops a mathematical (optimization) model of the problem. Like any optimization problem, one needs to define the optimization objective(s) and all applicable constraints to be satisfied. The fundamental criterion of the shortest path problem is obviously to minimize the length of the path while the constraint is often times to avoid interference with obstacles. Solving this problem using deterministic optimization techniques is almost impossible due to the nonlinearity of the objective function (nonlinear Euclidean distances are to be minimized as an objective) and difficulties in modeling the collision avoidance constraints, mathematically. To overcome the problem of modeling the constraints, researchers usually discretize the workspace as a grid and try to drive the number of overlapping cells to zero. Overlapping cells are the cells of the path interfering with the occupied cells in the obstacles. To avoid collisions, the ratio of the overlapping cells over the total number of cells in the workspace is calculated. This ratio is then entered into the objective function as a penalty to be minimized [13]. Often, researchers use heuristics methods to solve this optimization problem since heuristics can result in global optimal solutions. However, heuristic methods result in different solutions each time they are run. In addition to the modeling challenges, defining the design variables of the optimization problem is not quite straightforward. In path planning problems, design variables for the optimization problem are usually the x, y, and z coordinates of the points located in the free space denoting the end points of a line segment since the final path is a piecewise linear path consisting of several line segments. Given this definition of the design variables, the number of variables is not known a priori making the optimization modeling even more difficult.

1.1 Objectives of this Research

The objectives of this research are to efficiently model the free space of the given 2D environment cluttered with arbitrary polygonal obstacles and then find the shortest collision-free path connecting the initial and final points. The outcome of this research will help to expand the solution idea to higher dimensions including 3D and to optimally route cable harnesses in electro-mechanical systems.

The rest of this thesis is organized as follows. In the next chapter, a brief overview of the literature on the path planning problem with the main focus on 2D path planning is presented. In chapter 3, the geometric representation technique chosen in this research is explained in detail. Chapter 4 is allocated to the general intersection detection techniques for path planning problems and focuses on 2D detection techniques. Chapters 5 and 6 deal with the construction of the free space graph and finding the shortest path through searching that graph. In chapter 7 the results of the research followed by the validation and case studies are presented. The main findings from implementing the developed algorithm in this research are also summarized. The conclusions are drawn in chapter 8 and some ideas for moving the research forward are provided as potential future work.

Chapter Two
LITERATURE REVIEW

The Path Planning problem has been widely studied in the literature. Path planning in 2D environments typically involves simplifying the unoccupied space (free space) to a graph of the free space. This graph is later explored using network optimization methods. Extensive research has been done on the representation of this free space. Briefly, some of the approaches to undertake the free space representation and generation include visibility graphs, Voronoi diagrams, sweep volume, wavefront, and so on. In what follows, a brief summary of the previous work done on this topic is provided.

2.1 State of the art in Roadmap techniques

One approach to model the free space is known as roadmap technique[9]. Roadmaps map the free space to a connectivity graph. Visibility graphs and Voronoi diagrams are well-known examples of roadmaps and are explained in detail in chapter 5.

Constructing the visibility graph to model the free space is considered as the very first method in computational geometry to address the shortest path problem in the plane[14]. Visibility graph is an undirected graph of edges connecting every two nodes that are visible to each other, meaning the edge they share does not intersect the interior of any obstacle [14]. The algorithm is computationally expensive since it explores all the vertices of all the obstacles. In fact, the fastest known algorithm to construct the visibility graph developed by Asano et al. [15] has the time complexity of order $O(n^2)$ n being the total number of obstacles' vertices. Should one consider f objects with n_{ave} vertices on average per object, then the complexity is of the order $O(f^2 n_{ave}{}^2)$ Therefore, research efforts have been undertaken to improve the efficiency of the algorithm even further.

Focusing on improving the efficiency of visibility graphs, Rohnert [16] develops an algorithm that computes the shortest path in a Euclidean plane in presence of a set of disjoint convex polygonal obstacles in $O(f^2+n\log n)$ time, f being the number of the obstacles and n the total number of vertices. To better understand the significance of this improvement in the time complexity, one could take a numerical example. Suppose, there exist 10 objects in the workspace with average 4 vertices per object, resulting in total 40 vertices in the plane. Asano's algorithm implemented on this example yield a complexity of $(10*4)^2$ or 1600 while Rohnert's algorithm results in a complexity of $O(10^2+40\log 40)=164$ which is significantly lower.

Instead of generating the entire visibility graph of the workspace, to improve the time complexity of the algorithm, Rohnert generates a part of the graph relevant in finding the path between the start and termination points in $O(n+f^2\log n)$ time. Based on a lemma stated in this article, "the shortest collision free path from point s to t in the plane runs via the edges of the polygonal obstacles and the supporting segments between the pairs of polygons"[16]. Rohnert defines the supporting segment as a line segment of a common tangent of the two polygons lying between the two points of contact of the tangent and the polygon[16]. By this definition and based on the aforementioned lemma, the part of the visibility graph needed to be constructed consists only of the edges of the polygons and the supporting segments rather than all edges connecting the visible nodes. However, if the supporting segment between a pair of polygons intersects the interior of another polygon, the algorithm eliminates that segment from the graph while the segment could still be used to generate the optimal solution. After the construction of the partial visibility graph, Dijkstra’s algorithm is implemented to find the shortest path on the graph. Dijkstra’s algorithm is explained in detail in chapter six. Rohnert uses the Dijkstra’s algorithm developed by Tarjan and Fredman [17] that finds the shortest path in $O(|E| +|V| \log|V|)$ time, $|E|$ being the cardinality of the set of edges and $|V|$ the cardinality of the set of vertices in the graph.

Rohnert’s algorithm works efficiently for planes with convex polygonal obstacles. However, it cannot deal with concave and more complex shapes. In addition, since it eliminates the intersecting supporting segments and only keeps the “useful” ones besides the polygon edges, hence restricting the feasible region, it may not be able to find the global optimal solution.

In an independent study by Welzl [18], the construction of a visibility graph of a set of L nonintersecting line segments is explained and the problem of finding the shortest path between two points of the plane while avoiding intersection with these line segments is addressed. The developed algorithm to construct the visibility graph has an improved time complexity of order $O(L^2)$. The visibility graph is then searched using a standard single source shortest path algorithm of Dijkstra.

Sharir and Schorr investigate the shortest paths in 2D and 3D spaces with polyhedral obstacles [19]. For the 2D space, they develop an algorithm that constructs the visibility graph of the environment with n total number of vertices in $O(n^2 \log n)$ time although they present some special cases for which the time complexity of the construction is of order O(nlogn). Taking the same numerical example, Sharir's algorithm in general case yield a complexity of (40^2*log40) =2563 which is the least efficient algorithm known to construct the visibility graph.

The constructed visibility graph is then explored using Dijkstra's algorithm developed by Aho et.al. [20] in O(n^2) time to find the shortest path. They also address the more complicated 3D shortest path problem. They claim that the shortest path passes through the points lying on the edges of the polyhedral obstacles. They develop a method to find the sequence of those points through which the shortest path passes in doubly exponential time (has the form of a^{b^x}) which is much faster than factorial (O(n!)). Lastly, they show a special case of the 3D shortest path problem along the surface of a convex polyhedron which is solvable by their technique in O(n^3logn).

Visibility graphs are not only constructed to act as the building blocks for the optimization aspect of the path finding problems, but they are deployed in facility location problems as well. Butt and Cavalier in their article [21], propose an algorithm to find an optimal location to place a new facility X in presence of convex polygonal forbidden regions the travel through which (and not along!) is prohibited such that the sum of the distances from facility X to the existing facilities is minimized. They first generate the visibility graph of the existing facilities and the polygonal forbidden regions. After determining the visible nodes, the new facility, X, is introduced and the visible nodes of the predetermined graph with respect to X are found. Then, the Euclidean distance of the facility X to each of the existing facilities is defined and the location of the facility X is determined such that the sum of the distances is minimized. In order to avoid searching the entire environment for the location of X, based on a theorem that states the optimal location of the new facility lies within the convex hull of the existing facilities[21], they only search the region restricted by that convex hull. They also define N regions corresponding to the N existing facilities to simplify the search for the location. With X lying inside each of the different regions, the definition of the objective function will differ. The optimal location of the facility X is the one that guarantees the minimum sum of the distances to the N existing facilities.

In all the aforementioned research works, the planning occurs for an object reduced to the size of a point. However, there are instances (especially in robotics) in which the moving object itself is a polygonal or polyhedral object in 2D or 3D environments respectively. In this case, an approach based on the Minkowski sum is utilized to take the geometry of the moving object into account.

Lozano and Wesley [22] tackle the problem of planning a collision-free path for a moving object of known geometry among polyhedral obstacles using visibility graphs. They start with taking the 2D planning into account and move on to the 3D problem. Since the moving object is no longer a point, construction of the visibility graph becomes a great challenge. Hence, they first come up with a method to transform the object to a reference point. To do so, they grow the obstacles by an offset related to the size of the moving object and shrink the moving object to a reference point. The new obstacles represent the locus of the positions of the reference point that cause a collision with the obstacles[22]. The reference point can be any point of the moving object such as its center or corner points. To find the configuration space of the problem, the authors take into account position as well as the orientation of the object. After determining the configuration space, a visibility graph need be constructed and finally searched for the shortest path.

One of the famous shortest path problems is the Traveling Salesman Problem as briefly mentioned in the previous chapter. This NP-hard problem is of interest to a lot of researchers working on the shortest path problems. Research is still going on to improve the efficiency of the solution for the TSP problem.

Meeran and Shafie in [23] propose an algorithm to solve the TSP in polynomial time using convex hulls generated by Graham's method [14]. The idea behind their method is based upon a proposition by Flood [24]which states that if all the cities in TSP lie on the boundary of their convex hull, the TSP has an optimal solution. The initial sub-tour in this algorithm is the boundary of the convex hull of the cities. They introduce a heuristic rule to group cities into circular neighborhoods, the diameters of which are the edges of the sub-tour convex hull. If a city has no neighborhood, children neighborhoods are created based on the parent neighborhood until all cities are assigned to at least one neighborhood. If a city belongs to more than one neighborhood, the neighborhood that yields the smallest distance to that city is chosen as the main one. In this way, the algorithm inserts all cities on the boundary of the convex hulls of the neighborhoods in order to achieve the optimal path. The order of visiting the nodes is then optimized by the nearest neighbor [23] method. The authors claim that by combining the solutions for the local search in each neighborhood, the algorithm is able to yield the global solution.

The second most common roadmap method of constructing the graph of the collision-free space is using the Voronoi diagram also known as *retraction method* [9].

Voronoi diagram of n vertices partitions a plane or space to n regions. An edge of a Voronoi diagram is equidistant to two vertices. The technique of constructing the Voronoi diagram is explained in chapter 5 in detail. Researchers have attempted to incorporate the Voronoi diagrams in solving the path planning problem during the past decades especially for the cases in which finding the maximum clearance path is the main criterion.

Bhattacharya and Gavrilova[25], tackle the problem of 2D path planning using Voronoi diagrams and develop a shortest path algorithm that works in O(nlogn) time, n being the total number of vertices. They start with creating the Voronoi diagram of the workspace by approximating the obstacles by their boundary points, and dynamically add the start and target points into the diagram. Then, they connect the start and target points to all Voronoi vertices to avoid intersections. Next, they define the minimum clearance (c) from the obstacles and remove all the edges of the Voronoi diagram that result in a clearance less than c. Now the graph is ready to be searched for the shortest path. The search algorithm of their choice is Dijkstra's [26]. However, the solution found might require some smoothing and refinement since the shortest path includes redundant vertices and unnecessary turns.

To achieve both the shortest path and the maximum clearance from the obstacles, researchers use Voronoi diagrams in conjunction with visibility graphs to take advantage of both yielding the shortest path and ensuring a certain amount of clearance from the obstacles.

Wein et.al present an algorithm in their paper [27]to find the shortest path that is both smooth and guarantees a clearance c from the obstacles. They improve the efficiency of their algorithm to a time complexity of O(n^2logn) for total n vertices, over the time-expensive visibility graph construction. The algorithm evolves from a visibility graph to a Voronoi diagram as c grows from 0 to ∞. In the preprocessing phase, they dilate the polygonal obstacles by c using the Minkowski sum of the polygon and a disk of radius c. They then, construct the visibility graph of the dilated obstacles and in case a narrow passage is blocked by two or more dilated obstacles, they find the intersection of the union of dilated obstacles and the Voronoi diagram, hence replacing the blocked portion by a Voronoi edge passing through the narrow passage. Although the clearance of the Voronoi edge from the blocking obstacles is less than c and it may yield sharp turns, to ensure that the path is optimal in terms of its length, this passage is allowed by this algorithm. The graph is later searched by Dijkstra's algorithm to find the shortest path. Despite the proved efficiency of this algorithm, it may not be practical to implement this algorithm on a large scale problem as mentioned in [25].

In another paper by Clarkson [28], a method is proposed to improve the time complexity of the visibility-based shortest path algorithm. The developed speed-up technique works on eliminating some of the unnecessary edges of the visibility graph through generating the Minimum Spanning Tree (MST) of the vertices of the obstacles. The MST of a set of nodes is the minimum length tree that spans all the nodes [14]. The new graph (sub-graph) is a subset of the original visibility graph that need be augmented by the start and end points of the path. To find this augmented subgraph, Clarkson uses the conical Voronoi diagrams of the vertices in his algorithm. He then deploys the algorithm developed by Fredman and Tarjan [17] to find the ε-shortest path. The ε-short path is the path that has a length no longer than (1+ε) times the shortest path between s and t . Clarkson's algorithm is capable of constructing the data structure in O(nlogn) and finding the ε-short path in 2D cases in O(nlogn+n/ε) time, with n being the total number of vertices and ε a given value satisfying $0 \leq \varepsilon \leq \pi$. The algorithm works both on 2D as well as 3D spaces with slight changes in the vertices of the visibility graph of the 3D space.

Roadmap techniques are not limited to the visibility and Voronoi methods. For example, Hershberger and Suri[29] propose a method to solve the shortest path problem in a plane with significant improvement in the time complexity over the previously developed techniques. The proposed technique is capable of finding the optimal solution to the shortest path problem in O(nlogn) time using wavefront propagation technique. Wavefront propagation roughly imitates Dijkstra's algorithm by simulating the propagation of a wave from a source node to other nodes of the shortest path map spreading among the obstacles. The wavefront at time t includes all points of the plane with distance t from the source node[29]. This algorithm has been proved to find the shortest path in $O(n^2)$ time previously, however, the authors of this article propose two speed-up techniques that improve the time complexity of the wavefront propagation up to O(nlogn). The first speed-up implementation corresponds to a quad-tree style subdivision (conforming subdivision) of the plane and the second one approximates the wavefront. Conforming subdivision splits the plane into a linear number of cells using vertical and horizontal edges generating the shortest path map for the wavefront to travel through. By subdivision of the plane, the propagation of the wavefront is guided through the subdivided cells, resulting in expediting the process of finding the shortest path. In each cell, a Voronoi diagram technique is deployed to take care of the collisions and provide the edges of the shortest path map. Vertices of the map are the vertices of the obstacles.

2.2 3D shortest path problem

In addition to the mathematical modeling and graph construction methods, scholars have also studied more applied path planning problems such as pipe routing in ships and chemical process plants, wire and/or cable routing in automobiles and aircrafts, robot motion planning and so forth. In what follows, a brief overview of the state of the art in the applied path planning problems is provided. These problems are mainly in 3D spaces.

Yin et al. [30], solve the 3D pipe routing problem representing the physical obstacles by their vertices and convex hulls in 3D space. They claim that the shortest path for a pipe while avoiding convex obstacles is the path through an obstacle's edges. Then, they use the visibility graph approach to find the candidate edges and nodes of the shortest path.

Cagan and Szykman [31] propose an approach based on Simulated Annealing (SA) to produce non-orthogonal routes for pipes in a 3D environment. Given the locations for a pair of terminals, an initial route, which is the straight line between the two terminals, is chosen. Then, the optimizer based on SA moves the locations of bend points, which are design variables to minimize an objective which consists of the sum of three components: the total length of the route, the number of bends, and the degree of penetration inside obstacles. Weights are used to distribute the importance of the three objectives, and the aim is to drive the third one (obstacles interference) to 0. In [13], Sandurkar and Chen solve a pipe routing problem in 3D space using the tessellated format (triangles and nodes) to represent components in the workspace as obstacles, which enables them to handle both convex and concave objects along with a Genetic Algorithms (GA) that determines angles and lengths of each segment of a single pipe. To detect interference with obstacles, they use an interference checking program, RAPID, developed at the University of North Carolina [32].

Conru and Cutkosky [33] address the cable harness problem by starting with the generation of an initial solution without considering any obstacles. Then, the obstacles are introduced gradually and the path is refined to satisfy collision avoidance constraints. In a Separate study [34], Conru uses a GA technique to find near-optimal solutions for cable harness routing in a 3D environment consisting of nodes. He starts with a random configuration of cable harness and refines it using a GA.

The automotive wire routing and sizing for weight minimization is addressed in [35] using the minimal Steiner tree algorithm and Linear Programming (LP) formulation on a predefined graph. Also, authors of [36] address the problems of wire routing, wire sizing, and consider the allocation of splices in their paper. They use a depth-first (graph traversing) approach to compute the minimal cost path and a two-phase heuristic with a Simulated Annealing (SA) algorithm to tackle the wire sizing problem.

Researchers have also looked into cable harness routing problem. Zhu et al. [37] propose a bi-level optimization approach to find optimal paths for wire harnesses in an aircraft. They assert that since cable harness routing is a multi-destination path finding problem, *simple routing algorithms to find shortest paths between two points do not result in accurate optimal solutions*. They perform a two-step hybrid strategy to tackle this problem. The first step, initialization, generates a preliminary harness configuration using a roadmap technique. The second step deals with the optimization part to refine the preliminary configuration. In the local level of their bi-level optimization method, they use the A* search algorithm to find optimal paths between two end points of a branch. And, in the harness level, which they call global optimization level, they use a Hill Climbing algorithm to come up with an optimal solution for the whole harness. The objective function of this problem is the harness cost which itself is a function of three variables: length of the harness (as summation of the lengths of all bundles in the harness), number of clamps to fix harness on the airframe, and the amount of protecting layers to protect the harness from harsh areas (humid, hot, and vibratory areas). The design variables are the coordination of the clamps and transition points. Also, there are three constraints that need to be satisfied while designing the wire harnesses: minimum bend radius, maximum clamping distance (distance between two adjacent clamps), and minimum fixing distance (distance from the center of harness curve and its fixing structure).

As could be implied from the above listed research articles, to solve the 3D path planning problems, researchers mainly use heuristic techniques. These techniques though capable of yielding the global optimal solution, are approximations and have greater time complexities than exact methods since they search the entire feasible region for an optimal solution.

Although many research works have tackled the path-planning problem and improved the efficiency of the current geometric approaches, some limitations still exist in this field. Chen in his short article [38], after defining the geometric shortest path problem in a cluttered environment, summarizes some of the shortcomings of the current path planning algorithms and the potential for further research in this field. This summary is presented in Table 2.1 below.

Table 2.1 Shortcomings of the Geometric Path Planning Approaches

Aspect of the path planning problem	Limitations
Shortest path in 3D and higher dimensions	Little to no research studies
Multiple criteria path planning	Not addressed using geometric approaches
All-pairs Euclidean shortest paths	Lack of an efficient theoretical solution
Practical applications and geometric setting	Environment-specific rather than generic
Implementation framework	Lack of a general framework to implement the geometric path planning approaches
Computational operations	Complicated rather than simple

In Chen's perspective, problems such as shortest path in 3D and higher dimensions and path planning under multiple criteria (number of turns, angle of turns, etc.) are NP-hard, and finding their exact solutions may be difficult if at all possible. He then claims that there exists little research to show how commonly used geometric techniques (e.g. visibility graphs) can efficiently find the approximate solutions for the aforementioned problems[38]. Another drawback of the current geometric approaches as Chen argues [38] is that these approaches are environment-specific, i.e. their efficiency mainly relies on the properties of the environment. For example, it could be very difficult to implement these approaches in a more complex and real world environments since they include complex-shaped obstacles or obstacles whose shapes/geometry do not remain fixed. He also believes that there still does not exist a general framework to implement these geometric approaches and the user needs to develop the code on his or her own. Hence, the practitioner must first study a great deal of geometric techniques and data structures to be able to program a path planning method. On the other hand, often times the geometric approaches involve too many computational operations and sophisticated geometric procedures (such as visibility graphs, Voronoi diagrams, triangulations, etc.) and/or data structures. Lastly, as a suggestion, Chen proposes that the researchers look into developing more general (rather than problem-specific) yet simple-to-implement geometric algorithms to fulfill the necessity of solving a path planning problem in a more general and even complex geometric setting. From his point of view, the efficiency of this general approach will depend more on the configuration of the input rather than its size.

In addition to Chen's summary of shortcomings, there are limitations corresponding to the current roadmap techniques of solving the shortest path problem. For example, Voronoi diagram despite being efficient in dealing with the collision avoidance aspect of the path planning, yields sub optimal solutions since the path would be longer and with more turns than needed. Also, visibility graph is not computationally efficient since explores all nodes of the environment while in some path planning problems only a portion of the workspace may be involved, hence no need to explore all the vertices of the obstacles by the expense of increasing the computation time.

2.3 Research Questions

Based on the study of the literature and previous research, we propose a new method to tackle the planar path planning in a cluttered environment that has a potential to be implemented in 3D environments as well.

The main research question to be addressed is whether or not there is an efficient way with less time complexity than the visibility graph to preprocess the path planning problem and construct the graph of the free space. The objective is to find multiple collision free paths (if there exists any) forming the graph of the free space in presence of various-shaped stationary and disjoint obstacles in a 2D workspace regardless of the size of the workspace. The next question to be addressed is if it is possible to find the shortest path on the found free space graph using any network optimization algorithm.

Chapter Three
GEOMETRIC REPRESENTATION

Geometric representation of the workspace and the associated data is paramount in planning a collision-free path in a cluttered environment. Since the intersection detection and optimization domains in the path-finding algorithms rely on the geometric data, the entire workspace needs to be well represented.

In the following sections, the types of geometric representations, the advantages of using tessellated formats and the data structures used to represent and manipulate the geometric data in this research are discussed.

3.1 Geometric Representation Schemes

There are various types of geometric representation schemes to create solid models in CAD software packages. However, the two most popular schemes are Constructive Solid Geometry (CSG) and Boundary Representation (B-rep) [39].

The general idea behind the CSG model is that a physical object can be decomposed into a set of primitives. Primitives act as building blocks of a solid model. They are basic shapes that can generate solid models of any physical object using mathematical Boolean operations [39]. The most widely used examples of primitives are rectangular block, cylinder, cone, plane, and sphere.

On the other hand, a B-rep model is built upon the notion that a physical object is surrounded by a finite number of faces. These faces are closed (a continuous region in space without breaks) and orientable (the two sides of the face are distinguishable through the direction of the surface normal). A B-rep model consists of faces, edges, and vertices connected together to shape the object.

By this definition, the representation used in this research fall into B-rep models since we are mainly dealing with the vertices and edges of the objects in the workspace as explained in the upcoming chapters, though a CSG could also generate the model of such a 2D workspace.

For the purpose of this research, the objects of the workspace are first modeled in a CAD software, SolidWorks, with a B-rep scheme. For the 2D workspace, the objects are created as 2D planar surfaces as shown in Figure 3.1. The tessellated format of the solid model along with the VRML file format are used to easily exchange the file between different CAD packages and between CAD packages and other data manipulation software. Tessellated file formats are explained in the next section.

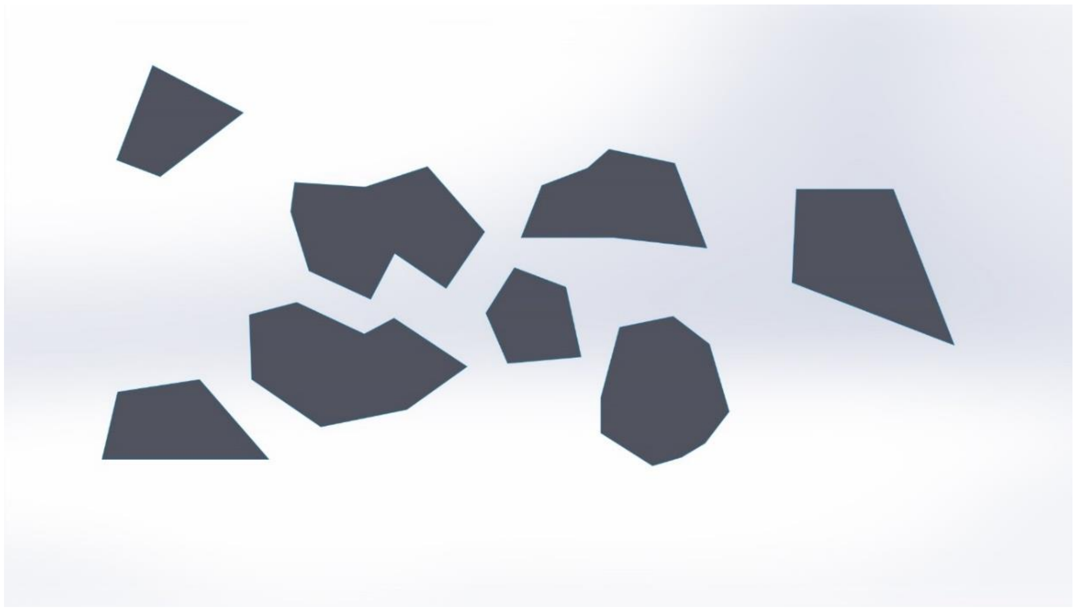

Figure 3.1: Sample Solid Model of a Workspace

3.2 Tessellated Representation

In this research, the tessellated format of all the objects involved in the workspace is used. The 2D planar solid models of the components are created using the STereoLithography (STL) format in SolidWorks®. STL is a standard file format that facilitates data exchange between CAD software and other systems, primarily 3D printers. STL files are developed based on the triangulations of the solid models in order to facilitate the handling of any free-form shapes for the solid model. In addition, the data needs to be extracted from a CAD software to be able to be manipulated in the packaging and routing problem. Since a case study of routing in 3D will be to route cables and harnesses of a vehicle under-hood (previously addressed for the packaging optimization problem) in which the components are tessellated. Hence, to generalize the algorithm we need to use the tessellated format of the objects for consistency. Figure 3.2 below shows the tessellated components of the vehicle under-hood.

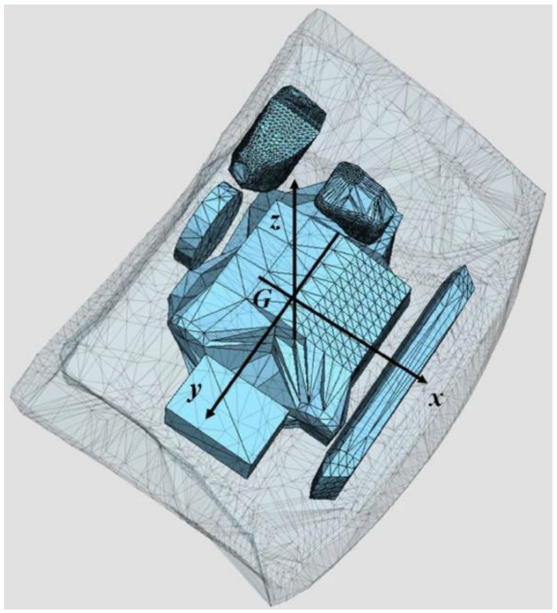

Figure 3.2: Tessellated Under-hood Components

An STL file of a solid model includes the X, Y, and Z coordinates of each triangle's vertices as well as the coordinates of the normal to the surface of that triangle. An edge must be shared by no more than two triangles. STL data can come in two representations: ASCII or binary. Both representations contain same geometric information in accordance with the STL file, though binary format requires less amount of memory to store the data. Nevertheless, ASCII can be read easily since it provides a better visualization of data [40].

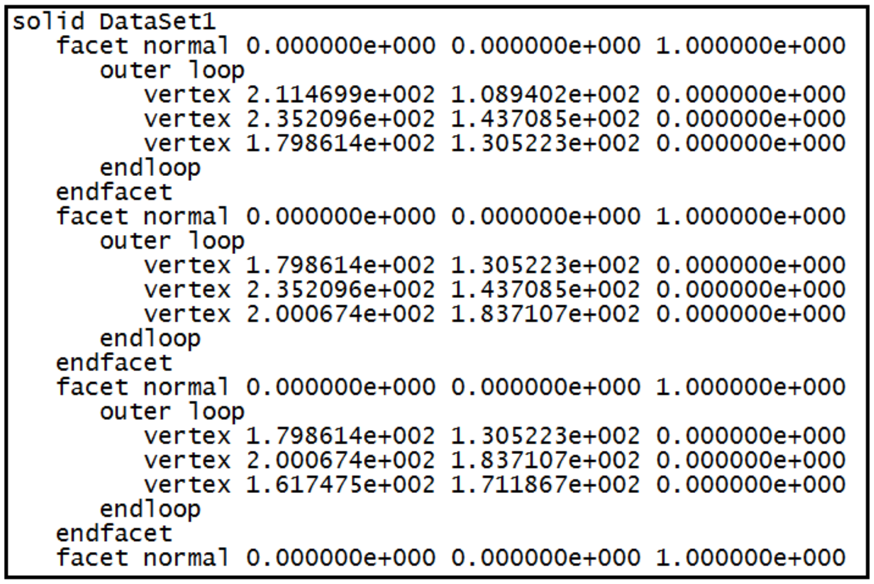

```
solid DataSet1
   facet normal 0.000000e+000 0.000000e+000 1.000000e+000
      outer loop
         vertex 2.114699e+002 1.089402e+002 0.000000e+000
         vertex 2.352096e+002 1.437085e+002 0.000000e+000
         vertex 1.798614e+002 1.305223e+002 0.000000e+000
      endloop
   endfacet
   facet normal 0.000000e+000 0.000000e+000 1.000000e+000
      outer loop
         vertex 1.798614e+002 1.305223e+002 0.000000e+000
         vertex 2.352096e+002 1.437085e+002 0.000000e+000
         vertex 2.000674e+002 1.837107e+002 0.000000e+000
      endloop
   endfacet
   facet normal 0.000000e+000 0.000000e+000 1.000000e+000
      outer loop
         vertex 1.798614e+002 1.305223e+002 0.000000e+000
         vertex 2.000674e+002 1.837107e+002 0.000000e+000
         vertex 1.617475e+002 1.711867e+002 0.000000e+000
      endloop
   endfacet
   facet normal 0.000000e+000 0.000000e+000 1.000000e+000
```

Figure 3.3: Sample STL File of a Workspace in ASCII Format

As can be seen from Figure 3.3, the ASCII file does include coordinates of triangles, 34 in total, and surface normals. However, it is not quite clear which triangle belongs to which object in Figure 3.1. The ASCII STL file of the represented workspace occupies 10 KB of the memory, approximately.

Despite the efficiency of the STL format and its strengths in tessellating solid models, it has some accuracy issues as described in[40]. First, it may be possible that one edge is shared by more than two triangles. This needs to be corrected, since, as mentioned before, each edge should be shared by no more than two triangles. This erroneous situation is shown in Figure 3.4.

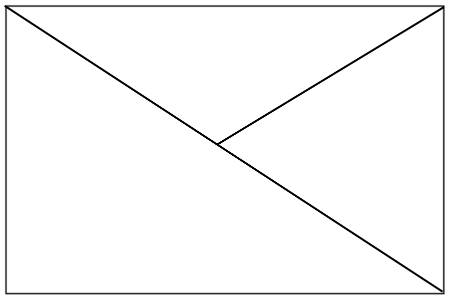
Figure 3.4: Shared edge of a triangulated solid

The second accuracy problem as discussed in [40] occurs in accordance with the round-off errors. This error, which is also called the closure error, appears because of rounding off errors and leads to multiple very close points to be generated, although they are the same point. This could cause a hole inside a tessellated object since the edge that two triangles share is no longer common due to different coordinates of the "common points". This situation can be seen in Figure 3.5.

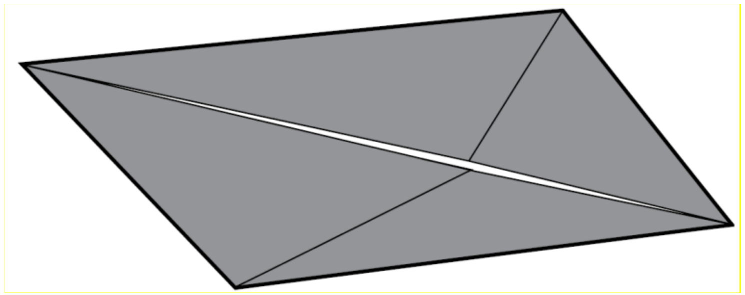
Figure 3.5: Closure Error in an STL Tessellated Solid Model[40]

There are also some other types of errors such as truncation, flipped normal, etc. which are out of the scope of this research and left without further discussion.

Another CAD file format working based on the tessellations is Virtual Reality Modeling Language (VRML). Solid models could be saved and processed as “.wrl”, the associated extension with VRML, either in ASCII or Binary format similar to the STL. A VRML file includes the coordinates of the vertices of the triangles resulting from triangulation of the solid model, same as the STL format, as well as a matrix containing the connectivity information of the vertices. However, the coordinates in a VRML file are grouped together for each object’s solid model and separated from the other objects of the environment, in case there are multiple objects. In addition, VRML contains data fields for color, shininess, and transparency in contrast to STL which only includes the triangles’ coordinate data and surface normal. In order to obtain the surface normal of each triangle in a VRML file, one needs to use the right hand rule and determine the outward pointing normal by the cross product of any two out of the three vectors forming the triangle. In Figure 3.6, an ASCII format of the VRML data corresponding to the workspace of Figure 3.1 is presented.

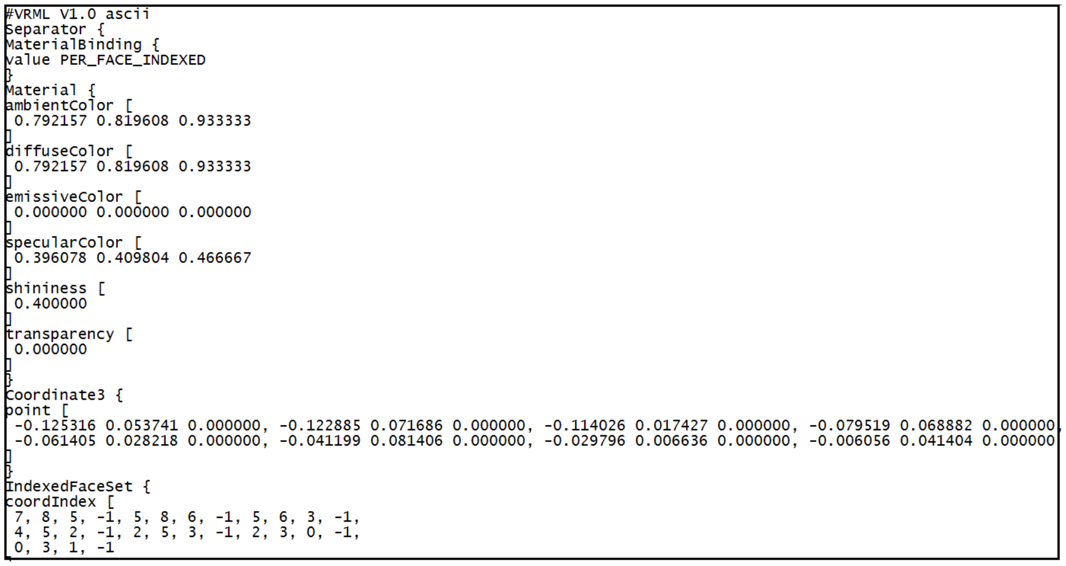

```
#VRML V1.0 ascii
Separator {
MaterialBinding {
value PER_FACE_INDEXED
}
Material {
ambientColor [
 0.792157 0.819608 0.933333
]
diffuseColor [
 0.792157 0.819608 0.933333
]
emissiveColor [
 0.000000 0.000000 0.000000
]
specularColor [
 0.396078 0.409804 0.466667
]
shininess [
 0.400000
]
transparency [
 0.000000
]
}
Coordinate3 {
point [
 -0.125316 0.053741 0.000000, -0.122885 0.071686 0.000000, -0.114026 0.017427 0.000000, -0.079519 0.068882 0.000000,
 -0.061405 0.028218 0.000000, -0.041199 0.081406 0.000000, -0.029796 0.006636 0.000000, -0.006056 0.041404 0.000000
]
}
IndexedFaceSet {
coordIndex [
 7, 8, 5, -1, 5, 8, 6, -1, 5, 6, 3, -1,
 4, 5, 2, -1, 2, 5, 3, -1, 2, 3, 0, -1,
 0, 3, 1, -1
```

Figure 3.6: Sample VRML File of a Workspace in ASCII Format

Figure 3.6 includes the coordinate data for one of the objects in the workspace shown in Figure 3.1.

Both VRML and STL could generate ASCII as well as Binary formats of the geometric data associated with the solid model. However, the ASCII format is more human-readable and the flow of information can be more easily understood. Hence, we use the ASCII format in all the CAD data analysis of this research.

A comparison of Figure 3.3 and Figure 3.6 shows that the VRML file is more organized in terms of the data for each object. It explicitly shows which vertices of an object are connected to each other and the coordinates of the vertices are not repeated for each relevant triangle. Furthermore, VRML is efficient and more practical in data exchange over the web [41] which makes it a better option for collaborative design projects. Besides, VRML format occupies less storage. For example, the VRML format of the workspace of Figure 3.1 only takes 6KB whereas its STL counterpart takes approximately 10KB. Hence, as the scale of the problem becomes larger there will be more difficulties in storing data as STL. Above all, the VRML format does not result in the closure or other types of errors challenge the STL format. Considering the advantages of VRML over STL, all CAD data in this research is saved and processed as .wrl files.

After creating the solid model of the workspace and generating the corresponding geometric data, the VRML data needs to be imported to the main program for manipulations. We use MATLAB to program the algorithm and find the safe path since it could deal with matrices and vectors efficiently.

The geometric data in .wrl format is thus imported into the MATLAB code and all the vertices and faces are read using a function listed in Appendix A. After the data is read, a matrix that includes the number of elements of the workspace, the coordinates of the vertices and the connecting edges is generated. This matrix is further used for the intersection check, graph generation, and pathfinding processes that are explained in the upcoming chapters. The tessellated workspace of Figure 3.1 is plotted using the aforementioned matrix of geometric data imported in MATLAB and depicted in Figure 3.7.

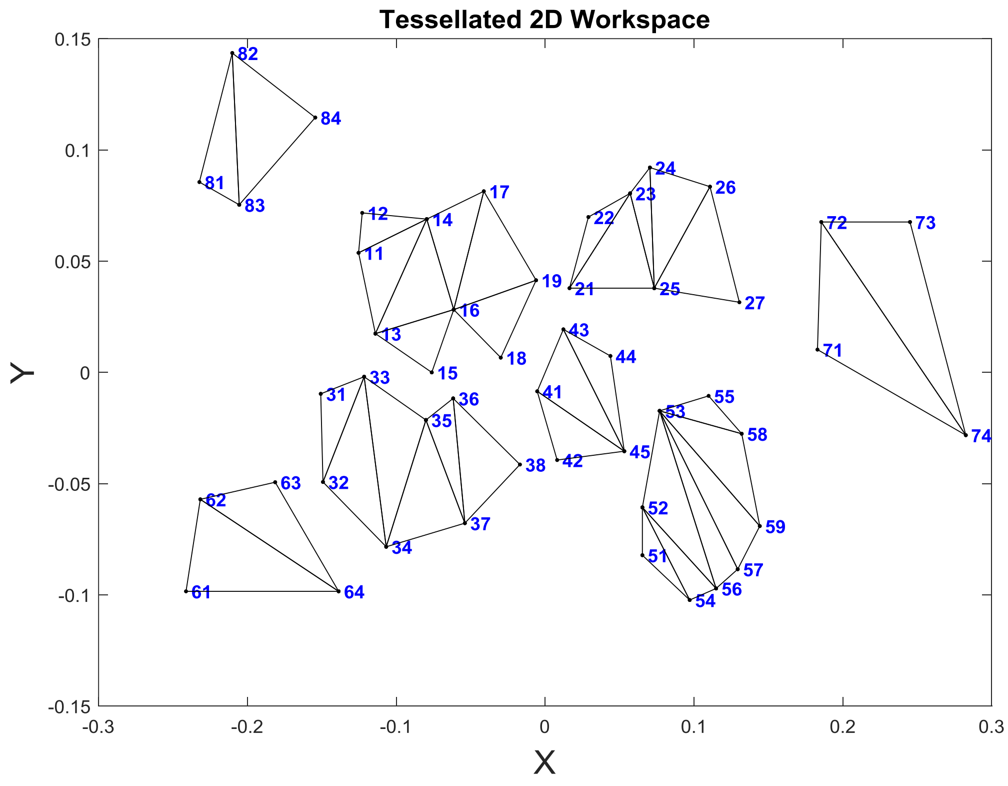

Figure 3.7: Sample Tessellated 2D Workspace Imported in MATLAB

This figure shows eight planar objects scattered in the workspace. The objects have convex as well as non-convex shapes that could be easily handled with tessellations. The triangles in each object represent the tessellations performed on the solid model. In addition, each vertex is numbered. These numbers are unique IDs assigned to each vertex to identify them. If there are no more than 10 objects in the workspace, the first digit of each node ID shows the corresponding object to which the vertex belongs. The rest of the digits show the vertex index in that object, which is generated by the VRML file automatically. For example, node 54 in Figure 3.7 corresponds to vertex number 4 of object 5. However, this numbering does not work in the case where there are more than 10 objects. For example, suppose the ID of a node is 2045. This ID could be interpreted both as node 45 of object 20 and node 5 of object 204. Hence, to distinguish between these IDs, a new node numbering system is proposed for the workspaces containing more than 10 objects. In this case, the object number is multiplied by 1000 (or any big number) and the node number is added to it. By this numbering system, node 45 of object 20 has ID of 20045 while node 5 of object 204 has the ID of 204005, which are unique.

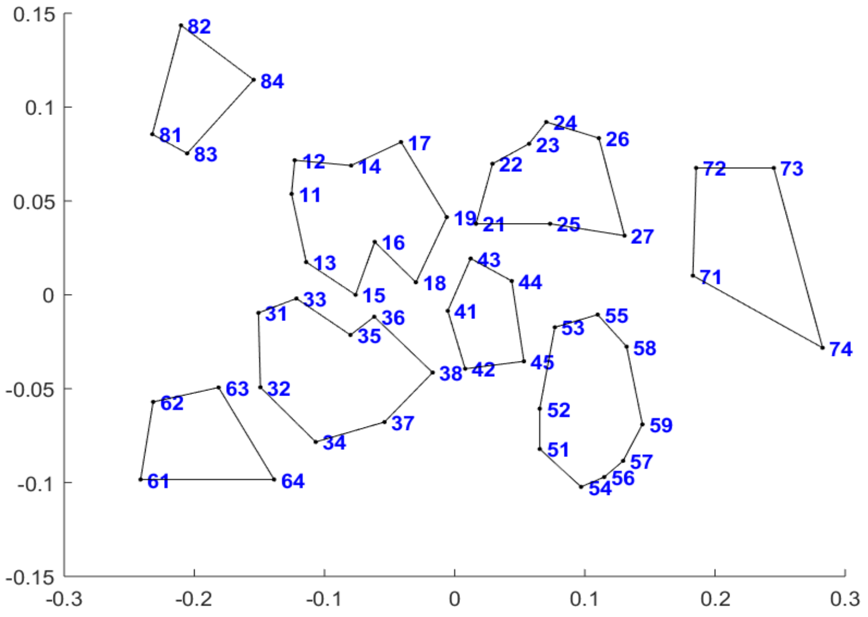

Figure 3.8: Planar Workspace after the Elimination of the Interior Edges

For the planar (2D) path planning, there is no need to include the interior edges caused by the tessellation of the workspace since the path is not allowed to pass through those edges. Hence, the interior edges of the tessellated surfaces are excluded in this research. However, for the 3D path planning, there is no restriction on passing through the interior edges of the outer surfaces of an obstacle as long as it does not intersect the interior of the obstacle. A sample resulting workspace after the elimination of the interior edges is shown in Figure 3.8. One should note that keeping the interior edges does not interfere with the process of finding the shortest path following the proposed algorithm in this research except that it occupies memory and may slow down the computations slightly.

The next section of this chapter is allocated to the data structures used in the MATLAB program for this research.

3.3 Data Structures

Data structures are important when it comes to storing, organizing, and processing data. Choosing the correct data structure leads to less memory storage and shorter run-times of a code.

Since the coordinates of the vertices are real numbers, the primary data type would be in the form of double, which could deal with larger floating points. The composite data structures for storing and implementation used in this research are as the follows:

- Array:

Arrays are one of the basic data structures in every programming language. An array could store vector data of any primitive structures. Matrices could be created by combining multiple arrays. In fact, arrays are one-dimensional matrices. On the other hand, there are cell arrays that could contain multiple matrices or any other type of data in each of their cells. Cell arrays, as well as typical arrays in general, can have more than two dimensions which are called multidimensional arrays [42]. The first and second dimensions are associated with the row and column number and usually, the third dimension is referred to as *page* [42]. Figure 3.9 shows an example of a multidimensional cell array. Note that in each cell, different types of data could be stored, whereas a matrix can only contain the same type of data. Additionally, data in each cell could have a different size, while matrices only contain same size data. For example, cell (1,1,1) in Figure 3.9 is a 2x2 matrix while cell (2,2,1) is a 1x1 matrix.

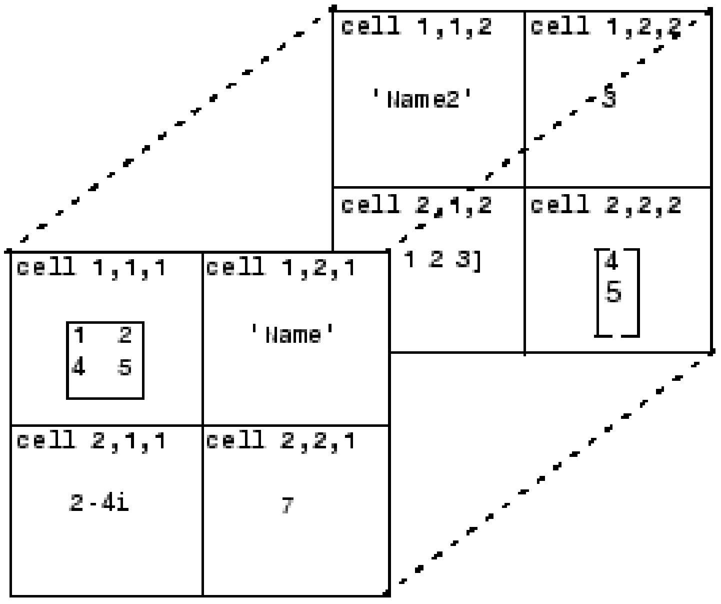

Figure 3.9: Multidimensional Cell Array[42]

In this research, the geometric data read from a VRML file is stored in an n by 2 cell, n being the number of components in the workspace. The cell includes both the coordinate data and link data. For example, row i and column one of this cell corresponds to the coordinate data for the vertices of the object i while the second column of the same row includes the connectivity data indicating the links which connect pairs of vertices of object i.

Another important type of arrays which is used extensively in this research is the dynamic array. A dynamic array is a variable-size array used whenever predefining an array is not possible or the array size is not known a priori. For example, in creating a path consisting of multiple connected points and line segments, the number of points may not be known in the beginning assuming that a path is created by putting the points alongside each other. In this case, defining the path as a dynamic array would be helpful in creating the path by adding a point at each iteration until reaching the goal point.

- Record or struct

A struct is a set of fields similar to cell except a struct could contain both numeric and character or string type data while cell could only store data of the same type.

- Graph

This data structure is critical in any routing problem. Since 2D problems mainly work with graphs and there typically exists a graphical model of the workspace which is searched for the safe shortest path, the graph data structure needs to be defined and created correctly. This graph includes the start and end node and the connectivity nodes and edges between them.

The data structure used in different parts of this research is explained in more detail as different parts of the algorithm are discussed.

After representing the workspace geometrically and building the foundation of the pathfinding method, the intersection detection and development of the free-space graph used for calculating the shortest path is built upon this foundation and further discussed in the upcoming chapters.

Chapter Four
INTERSECTION DETECTION

Generic path planning problems involve a planar (2D) or spatial (3D) workspace occupied by certain (or even uncertain) number of objects. Such problems cannot be treated as network or graph optimization problems since there does not exist a predefined graph or network of nodes to search for the shortest path between a pair of nodes, instead, a workspace containing multiple objects is given. Hence, care must be taken while planning a path to ensure its safety. Safety of the path is defined by a metric related to the avoidance of intersections with the interior of the objects called obstacles. Before avoiding such probable collisions, one has to detect the possibility of the intersection. In this chapter, the intersection detection technique utilized in this research is explained in detail.

As the shortest path between any two points is simply the straight line connecting them, we need to check if that line intersects with the interior of any of the obstacles. If there is no intersection, the straight line is the shortest path. Otherwise, the path must be re-routed until a new collision-free shortest path is identified.

4.1 State-of-the-art in Interference Detection

Interference detection is a common problem in any path or motion planning problem and it could be seen as the bottleneck of the path-planning problem. Once one guarantees the path is collision-free, the shortest path could be found using any optimization algorithm developed for this purpose.

Interference detection or collision avoidance occurs inevitably in robot motion planning problems. Robotics researchers, mostly model the collision avoidance constraints as forbidden regions of the workspace [22]. In other words, they take the components of a 2D or 3D workspace and model the obstacles as areas of 2D or volumes of the 3D workspace where the path is not allowed to go through.

Sandurkar and Chen[13] solve a pipe routing problem in 3D space using Genetic Algorithms (GA) that determines angles and lengths of each segment of a single pipe. To detect interference with obstacles in the environment, they use an interference-checking library, RAPID, developed at the University of North Carolina [32]. This library is capable of detecting collisions in large environments containing unstructured objects.

4.2 Bi-level Collision Detector

In this research, we develop a bi-level collision detection algorithm that checks for intersections between a line specified by the start and end points of the path and the objects of the 2D workspace modeled as polygons.

The first level or the boundary check level of this algorithm checks if a polygonal obstacle is within the boundary limits of the line connecting the start and end points of the path and filters the out-of-bound obstacles out. The obstacles could have any convex or nonconvex shapes since the workspace representation is based on the tessellations which are capable of handling any free-form solid model through triangulations.

The first step in the boundary check is to rotate the coordinate system of the workspace about Z axis and with respect to the line such that the new X-axis lies on the start-end line and translate the origin onto the start point of the line. Later on, it is shown how this coordinate transformation helps to simplify the computations for intersection detection. By rotating the coordinate system about the Z-axis (out of the x-y plane of the

2D representation) by the line angle, the coordinates of all vertices of the objects are also rotated by the same angle of rotation and translated by the same amount the origin is translated.

In order to perform the coordinate transformation, the homogenous coordinate system is required to make the matrix multiplications possible. The homogeneous coordinate system is the augmented array or matrix of the original coordinates. Augmentation adds a fourth coordinate to a 3D coordinate system. For example, consider point P as defined by its coordinates P = [X_p Y_p Z_p]. The augmented coordinates of P are P_{aug} = [X_p Y_p Z_p h]. For simplicity, h is often set to one.

Now that the coordinates are altered to the homogeneous coordinates, the translation is performed by multiplying the augmented coordinates of the point by the translation matrix defined as Eq(4.1).

$$T_T = \begin{bmatrix} 1 & 0 & 0 & 0 \\ 0 & 1 & 0 & 0 \\ 0 & 0 & 1 & 0 \\ \Delta X & \Delta Y & \Delta Z & 1 \end{bmatrix} \tag{4.1}$$

Where:

ΔX , ΔY , ΔZ : are the magnitudes of translations along the X, Y, and Z axes, respectively.

A similar strategy is used to come up with the rotation matrix given by Eq.(4.2) to rotate the coordinate system about the Z axis. Note that for consistency, this matrix is also defined through the augmented coordinate system.

$$T_R = \begin{bmatrix} \cos\theta & -\sin\theta & 0 & 0 \\ \sin\theta & \cos\theta & 0 & 0 \\ 0 & 0 & 1 & 0 \\ 0 & 0 & 0 & 1 \end{bmatrix} \tag{4.2}$$

Where:

θ: Angle of rotation, which is equal to the slope of the line

To transform any vector using the translation and rotation defined above, one only needs to multiply the augmented vector by the translation matrix (T_T) followed by the rotation matrix (T_R) as needed. Hence, the resulting vector after transformation can be calculated using Eq.(4.3).

$$V_{new} = V_{aug} * T_T * T_R \tag{4.3}$$

Figure 4.1 depicts an example of the workspace in Figure 3.1 (top) and its transformed version (bottom). Note that the straight line becomes horizontal after transformation. The coordinate system is transformed by 20.9735 deg, which is the angle between the straight line and X-axis.

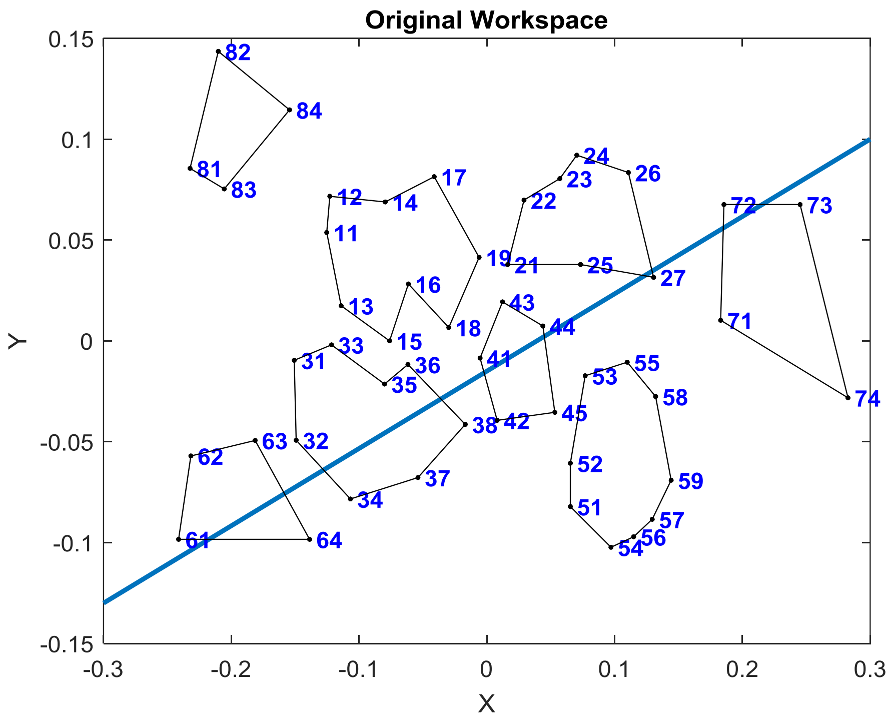

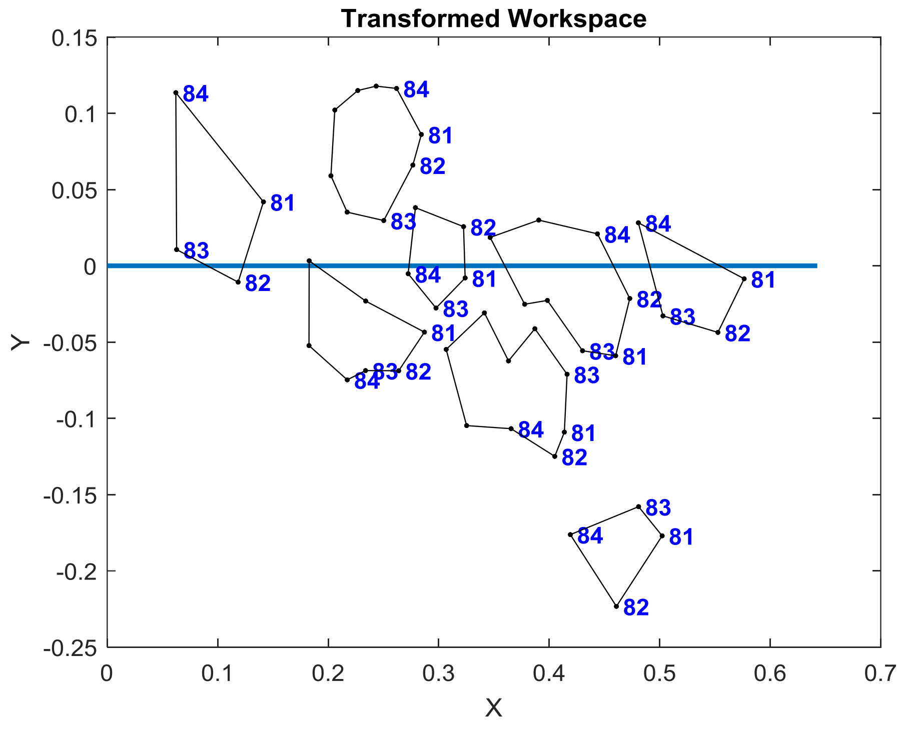

Figure 4.1: Transformation of the Coordinate System

After coordinate transformation, the next step is to check whether the polygonal obstacle's coordinates are within the limits of the coordinates of the straight line connecting the two points, or now the X-axis. To simplify checking of this criterion and to avoid looping over all coordinates of each polygon's vertices, which could be computationally expensive, we only consider the Minimum Bounding Box (MBB) of each polygon. The minimum bounding box of a polygon is the smallest rectangular box or envelope that contains the polygon. Extreme points of the polygon usually determine the MBB (i.e. maximum and minimum values of X and Y coordinates in 2D and also Z coordinate for a block in 3D). Figure 4.2 shows an example of an MBB for a polygon.

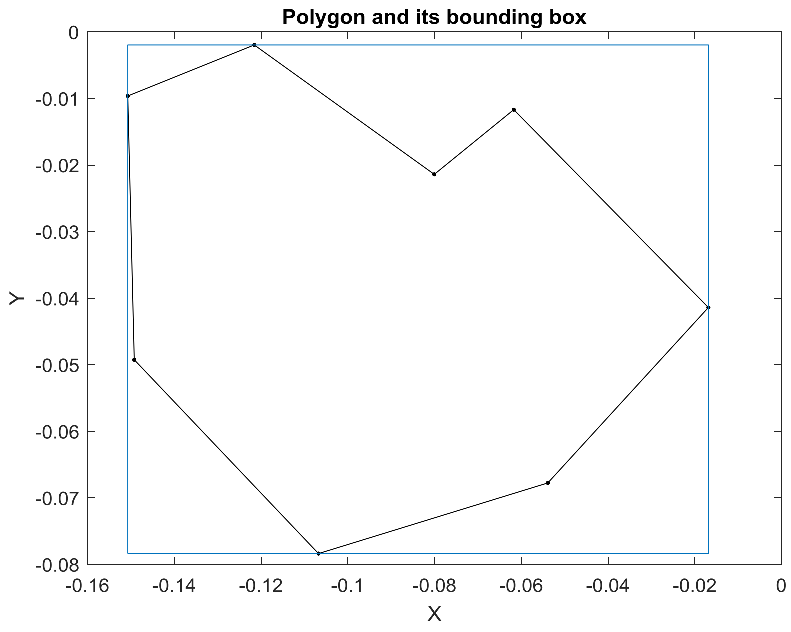

Figure 4.2: Minimum Bounding Box (MBB) of a Polygon

After creating the MBB, the algorithm compares the extreme X coordinate values to those of the line's. The comparison is made such that if either the minimum X of the MBB is greater than the line's maximum X coordinate or the maximum of the MBB is less than the line’s minimum X coordinate then the polygon is out of the line’s range and there is no probability of having interference.

If the X coordinates of the polygon’s MBB are within the range of X coordinates of the line, there could be a possibility of collision. Hence, further investigation is needed to determine the intersection. If the polygon, whose MBB is in the range of the line’s minimum and maximum coordinates, lies on either side of the line within the line’s X values, there will not be any chance of having a collision. This condition is demonstrated in Figure 4.3.

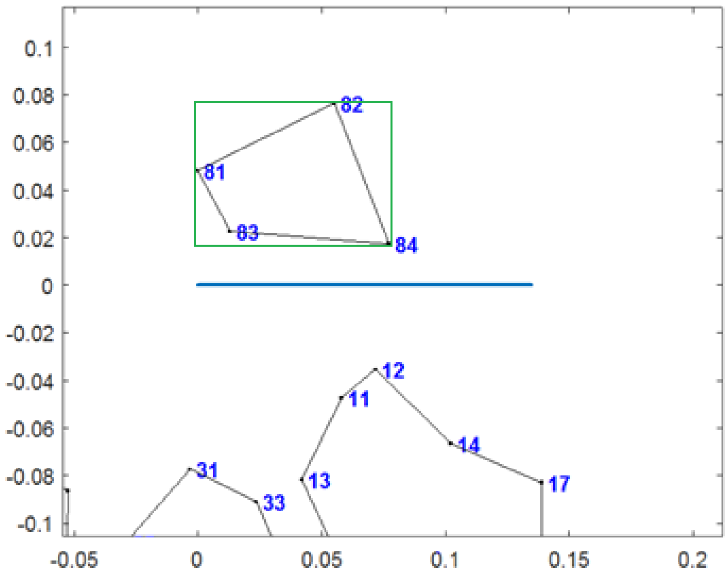

Figure 4.3: Example of a Polygon Lying at One Side of the Line

Therefore, checking if the polygon is within the X coordinate range of the line is not sufficient to ensure the possibility of collision. To check whether the polygon intersects the line or not, we need to also check the Y coordinates of the MBB. Since after rotation, the X-axis of the coordinate system lies on the line, any point on the line must have zero Y coordinate, and any point not lying on the line either has a negative or positive Y coordinate value, depending on which side of the line the point is located. Applying this fact to the collision detector helps to determine the intersections. In more details, if the polygon intersects the line, there exists at least one vertex on the other side of the line, which makes the sign of the related Y coordinate opposite to the sign of the Y coordinates of other vertices. Figure 4.4 shows an example of a collision between a line and a polygon determined using the sign of the Y coordinate of the vertices.

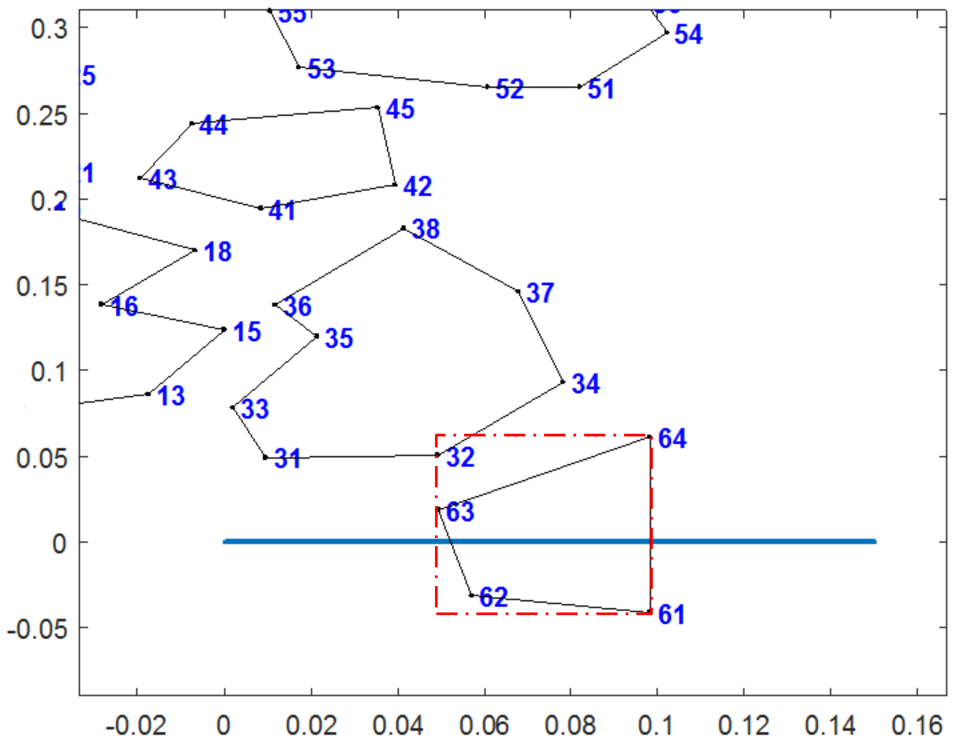

Figure 4.4: Example of an Intersecting Polygon

As shown in the Figure 4.4 (transformed coordinates) nodes 61 and 62 lie below the abscissa line while nodes 63 and 63 are above that line. In addition, Table 4.1 includes the values of Y coordinates of the vertices of object 6 before and after transformation. As obvious from this table, there exist both positive and negative values of Y coordinates after transformation.

Table 4.1: Y-Coordinate Values of Object 6

Node ID	Y before transformation	Y after transformation
61	-0.0983890000000000	-0.0412660000000000
62	-0.0570530000000000	-0.0316530000000000
63	-0.0493630000000000	0.0186540000000000
64	-0.0983890000000000	0.0612720000000000

Checking the signs of all Y coordinate values of vertices of a polygon could be tedious especially if the polygon has a large number of vertices. To avoid over-computing for collision check, the bi-level collision detector we develop in this research only checks the signs of the minimum and maximum Y coordinates of the MBB. Hence, if the multiplication of the two min/max Y coordinates is positive, all vertices lie on one side of the line and there is no collision. Otherwise, there is at least one vertex in the other side of the line, which could cause an intersection between the line and polygon. In Figure 4.5, a flowchart of the boundary check within the bi-level collision detector is shown.

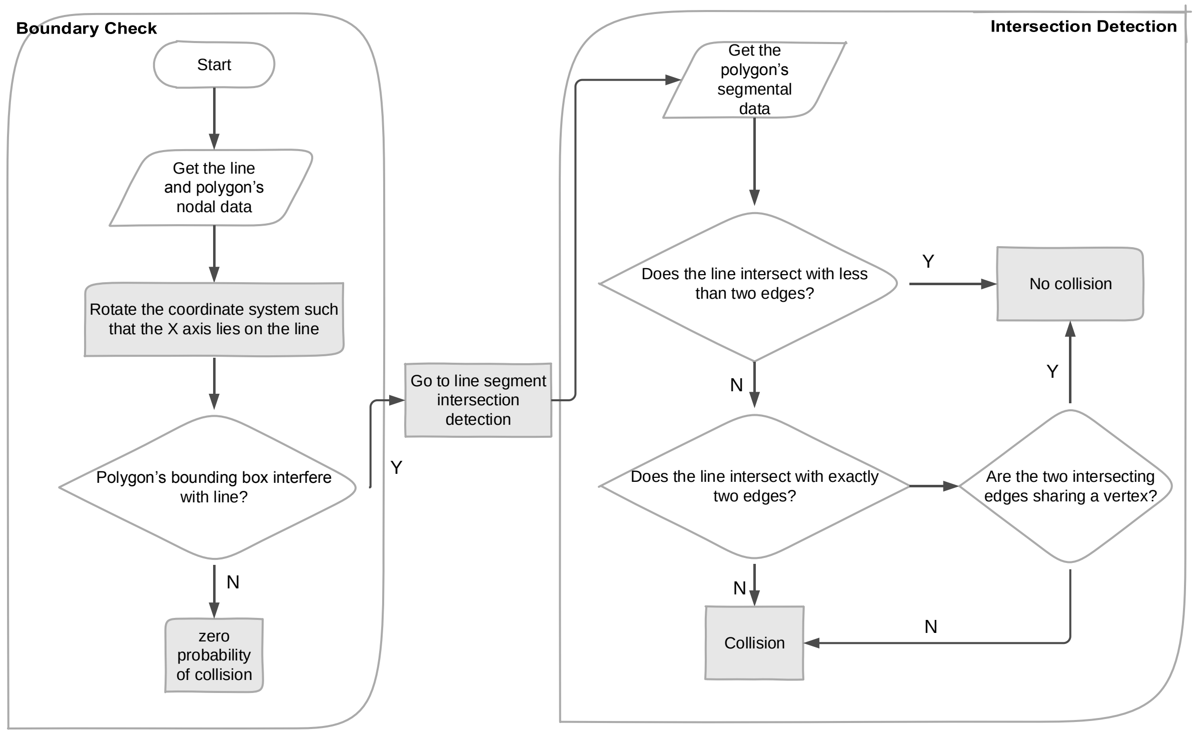
Boundary Check
Start
Get the line and polygon's nodal data
Rotate the coordinate system such that the X axis lies on the line
Polygon's bounding box interfere with line?
N
zero probability of collision
Y
Go to line segment intersection detection
Intersection Detection
Get the polygon's segmental data
Does the line intersect with less than two edges?
Y
No collision
N
Does the line intersect with exactly two edges?
Are the two intersecting edges sharing a vertex?
Y
N
Collision
N

Figure 4.5: Flowchart of the Bi-level Collision Detector Algorithm

Although this algorithm works efficiently in detecting the possibility of collision, it cannot determine explicitly if there exists any intersection since it only checks if the MBB of a polygon lies within the line range. However, detecting the intersection is more than checking the boundaries of a polygon. For example, the object of Figure 4.6 has no intersection with the line; however, running the boundary check results in reporting a collision since the X coordinates of the MBB shown in red dashed lines are interfering with the line and there exist vertices on both sides of the line. Instances like Figure 4.6 most likely occur when a nonconvex polygon is involved or one of the end points of the line touches an edge of the polygon at a point other than a vertex. To detect intersections more exactly and explicitly, especially for cases similar to Figure 4.6 we use a line segment intersection check. Thus, based on the flowchart of Figure 4.5, after determining the possibility of collision, the problem enters the second level of the collision detector where the polygon edges are checked for intersections with the line.

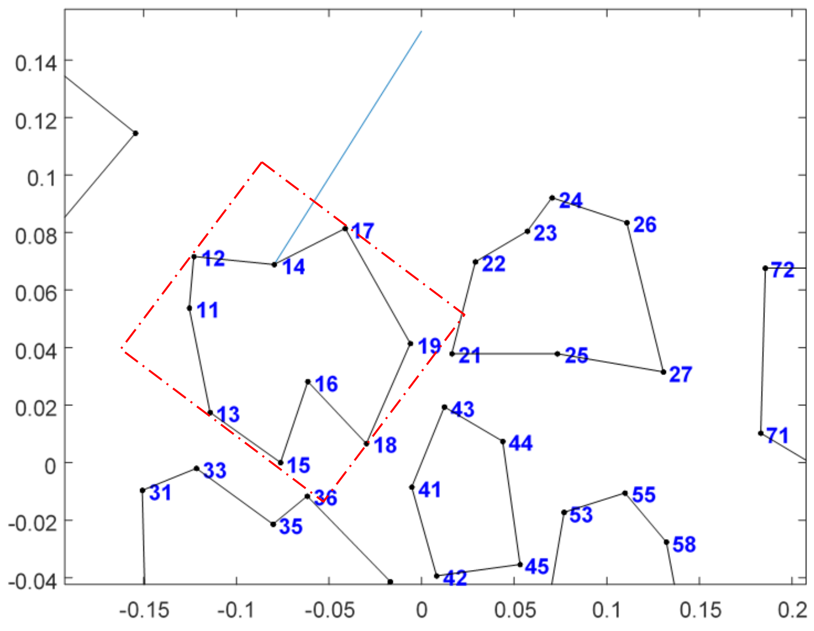

Figure 4.6: Non-intersecting Polygon with Collision Possibility

Before explaining the segment intersection detector, it is necessary to know the basic definition of intersection. The first phase of the collision detector, boundary check, mainly works with the coordinates of the extreme points or vertices of the polygon’s MBB and does nothing with the polygon’s edges. However, the second phase, intersection check, deals with the segments or edges of a polygon and checks if any segment intersects with the line.

A line segment is a line which has two fixed endpoints. A polygon, as defined by O’Rourke[14], is “a region of the plane bounded by a finite number of line segments”.

Thus, a polygon could be specified by its line segments, and in order to check if a polygon intersects a line, one can check each of its segments.

The algorithm developed works based on a line segment intersection detection process. It identifies a set of line segments corresponding to a known polygon and checks which segment intersects the line. If the two line segments are defined by Eq. (4.4), their intersection point can be determined using Eq. (4.5).

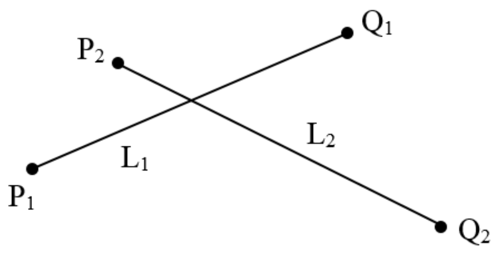

$$P_1 = \begin{pmatrix} X_{P_1} \\ Y_{P_1} \end{pmatrix} \quad Q_1 = \begin{pmatrix} X_{Q_1} \\ Y_{Q_1} \end{pmatrix}$$

$$P_2 = \begin{pmatrix} X_{P_2} \\ Y_{P_2} \end{pmatrix} \quad Q_2 = \begin{pmatrix} X_{Q_2} \\ Y_{Q_2} \end{pmatrix}$$

$$\begin{aligned} L_1 &= (1-\lambda)P_1 + \lambda Q_1 \\ L_2 &= (1-\mu)P_2 + \mu Q_2 \end{aligned} \qquad (4.4)$$

Where λ and μ are unit-less coefficients such that $0 \le \lambda, \mu \le 1$. To determine the intersection point, one needs to set the above equations equal:

$$\begin{aligned} (1-\lambda)X_{P_1} + \lambda X_{Q_1} &= (1-\mu)X_{P_2} + \mu X_{Q_2} \\ (1-\lambda)Y_{P_1} + \lambda Y_{Q_1} &= (1-\mu)Y_{P_2} + \mu Y_{Q_2} \end{aligned} \qquad (4.5)$$

Solving these equations gives the expressions of Eq.(4.6) for λ and μ.

$$\lambda = \frac{\begin{vmatrix} X_{P_2} - X_{P_1} & X_{P_2} - X_{Q_2} \\ Y_{P_2} - Y_{P_1} & Y_{P_2} - Y_{Q_2} \end{vmatrix}}{\begin{vmatrix} X_{Q_1} - X_{P_1} & X_{P_2} - X_{Q_2} \\ Y_{Q_1} - Y_{P_1} & Y_{P_2} - Y_{Q_2} \end{vmatrix}}, \quad \mu = \frac{\begin{vmatrix} X_{Q_1} - X_{P_1} & X_{P_2} - X_{P_1} \\ Y_{Q_1} - Y_{P_1} & Y_{P_2} - Y_{P_1} \end{vmatrix}}{\begin{vmatrix} X_{Q_1} - X_{P_1} & X_{P_2} - X_{Q_2} \\ Y_{Q_1} - Y_{P_1} & Y_{P_2} - Y_{Q_2} \end{vmatrix}} \qquad (4.6)$$

If the calculated λ and μ are real numbers between 0 and 1, the two line segments intersect. If the denominators of Eq.(4.6) are zero, the two line segments become parallel, and if both the numerator and denominator of the expressions are equal to zero, the two line segments have infinitely many intersection points or they coincide.

In view of the intersection, it is important to note that only in case of a line passing through a polygon we do encounter an intersection. In other words, for an intersection to happen there needs to be at least two intersections at different points. All examples shown in Figure 4.7 are examples of non-intersecting obstacles while Figure 4.8 shows two examples of a complete intersection.

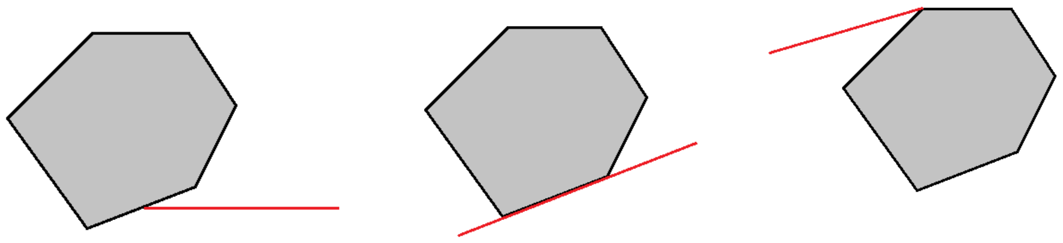

Figure 4.7: Non-intersecting Obstacles

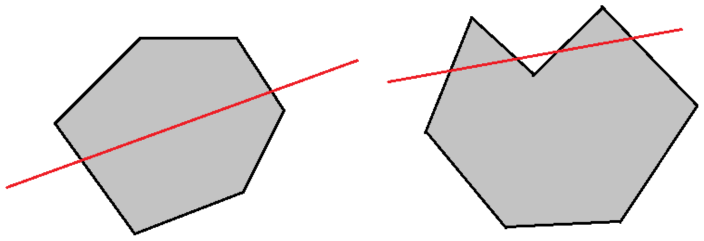

Figure 4.8: Intersecting Obstacle

The flowchart of Figure 4.5 shows the second level of the collision detector. As shown in the flowchart, after the boundaries of an object are checked and the collision potential is determined, the object's segments are further investigated to prove or disprove the existence of an intersection.

We program this collision detector algorithm in MATLAB as a function to check for intersections. Once the function is called, it takes the start and end points in the form of L=[X_s Y_s Z_s; X_e Y_e Z_e] where X_s, Y_s, Z_s, X_e, Y_e, and Z_e are the X, Y, and Z coordinates of the start and end points, respectively, as well as the workspace data as inputs. The workspace data includes the number of objects in the environment, the coordinates of their vertices, and the connectivity data of objects' vertices (edges). After getting the input data, the inclination of the line is computed using the coordinate values of its end points and the coordinate system is rotated about the Z-axis by the calculated angle of line folloed by a translation to the start point of the line. Then the data is passed to the boundary check level. All the objects of the workspace are checked by their MBB boundaries so that some obstacles are filtered out and the secondary level intersection check is limited to the obstacles with the potential for collision. This speeds up the process of intersection detection by only focusing on a portion interfering with the line's MBB. Once the boundaries of all the objects are checked, the potential colliding objects are passed to the second level of the collision detector to prove or disprove intersection.

The line segment intersection detector at the second level, takes two sets of line segments as inputs. The input should be two matrices, XY1 and XY2, corresponding to the two sets of line segments. Each matrix is Nx4 with N being the number of line segments and each row in the form of [X_1 Y_1 X_2 Y_2] where (X_1 Y_1) specifies the start and (X_2 Y_2) specifies the end point of the line segment. Since we need to check intersection of a line and a polygon, the first matrix associated with the line has a size of 1x4 while the second matrix or the set of line segments for the polygonal obstacle has a size of N_sx4 with N_s being the number of edges in the obstacle. After checking for segment-segment intersections, the function outputs a 1xN_s adjacency matrix which indicates the segments in the obstacle that intersect with the line, and two 1xN_s intersection matrices that include the X and Y coordinates of the intersection point(s). Since a complete intersection happens when a line intersects an object at (at least) two distinct points on the object's boundary, if the number of intersection points is greater than two, an intersection between the line and the object is guaranteed to happen. This situation can be seen in Figure 4.8. Normally, if the number of intersection points is greater than 2 the object is non-convex as in Figure 4.8 right. If there are exactly two intersection points, they must have different coordinates in order for an intersection to exist, otherwise, there is no intersection. For example, in Figure 4.7 the middle and right figures show intersections at more than two points. In the figure on the right, the line intersects two of the polygon's edges. However, since the intersections overlap at a vertex resulting in equal coordinates for the intersection points, this situation is not considered as a complete intersection because the line does not pass through or intersect the interior of the polygon. Note that the middle figure shows an intersection situation in which a line segment intersects a polygon at more than two points the coordinates of which are distinct. However, this object would be filtered out by the first level of the collision detector since it lies completely on one side of the line (it only touches the boundary and does not intersect the interior of the object) so there is no need for further investigation of the coordinates of the intersection points. The MATLAB code for bi-level collision detector along with the line segment intersection check is included in Appendix B of this thesis.

Table 4.2 includes some test cases of intersections in the workspace shown in Figure 3.1 with different start and termination points. None of the first three cases could be considered as an intersecting condition.

Table 4.2: Different Cases of Intersections in a Planar Workspace

Workspace Representation	**Line Coordinates**	**Intersecting Objects**
1. 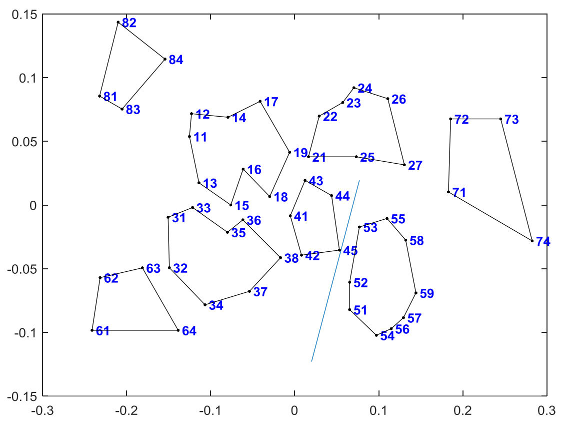	$\begin{bmatrix} 0.076939 & 0.019347 & 0 \\ 0.020000 & -0.12300 & 0 \end{bmatrix}$ Line touching an object at a vertex	[] No intersection
2. 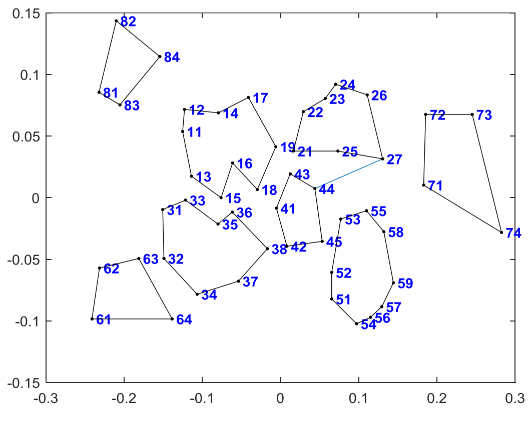	$\begin{bmatrix} 0.043853 & 0.007384 & 0 \\ 0.130513 & 0.031514 & 0 \end{bmatrix}$ Line touching two polygons at two vertices	[] Touching two vertices. Intersecting the line segments [25 57] and [26 27] of object 2 and [43 44] and [45 44] of object 4 at two points with the same coordinates

3. 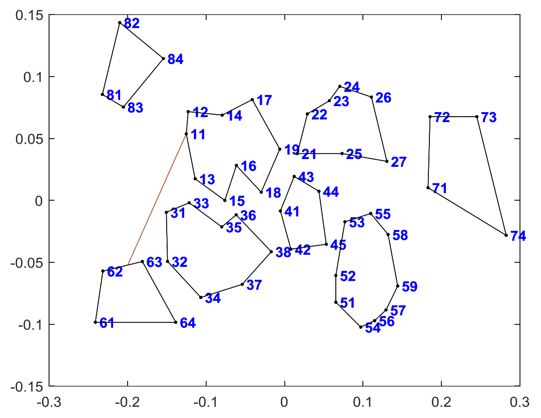	$\begin{bmatrix} -0.125316 & 0.053741 & 0 \\ -0.200000 & -0.05230 & 0 \end{bmatrix}$	[] Touching vertex 11 of object 1 and intersecting it at two points with the same coordinates, intersecting object 6 at one mid-edge point (edge [62 63])
4. 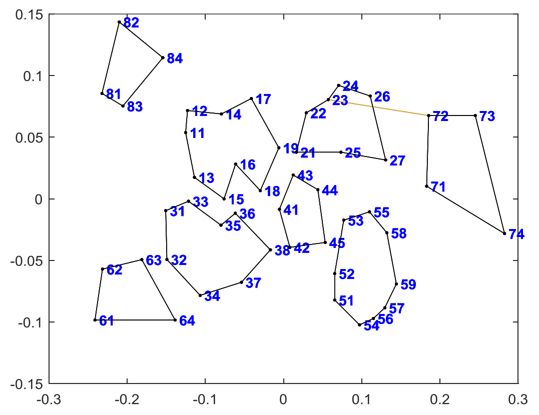	$\begin{bmatrix} 0.185547 & 0.067594 & 0 \\ 0.057125 & 0.080472 & 0 \end{bmatrix}$	[2] Intersecting object 2 at three points, the two of which have the same coordinates at vertex 23.
5. 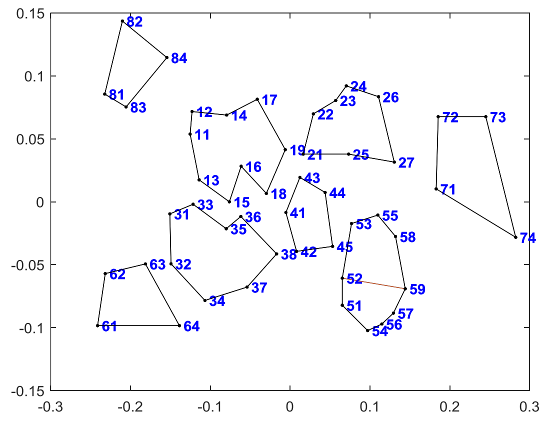	$\begin{bmatrix} 0.065349 & -0.060658 & 0 \\ 0.144232 & -0.069069 & 0 \end{bmatrix}$	[5] Intersecting object 5 at 4 points with two different coordinates at vertices 52 and 59.

6. 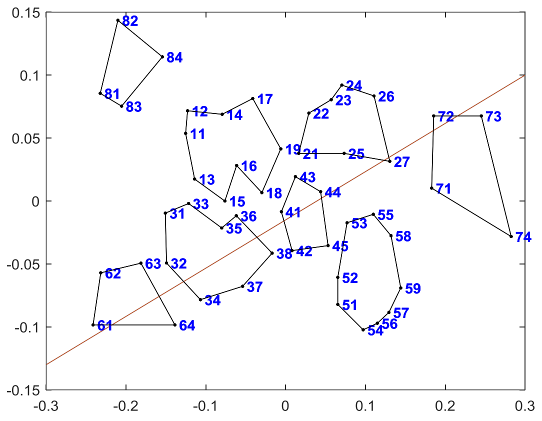	$\begin{bmatrix} 0.3 & 0.1 & 0 \\ -0.3 & -0.13 & 0 \end{bmatrix}$	[2,3,4,6,7] Intersecting objects 2,3,3,6, and 7 at two points with different coordinates.

In the next chapter, the collision-free graph of the environment is derived from the obstacles intersecting with the line connecting the start and termination points of the path. This graph is later used in chapter 6 to optimize the length of the path using a network optimization approach.

Chapter Five
DEVELOPMENT OF THE FREE-SPACE GRAPH

Path finding in an environment is usually coupled with avoiding possible interferences with scattered obstacles, as pointed out in the previous chapter. After detecting such possible interferences, an approach must be taken to avoid the collisions. One method of avoiding collision is to identify the regions of the potential intersections and mark them as forbidden zones or to define an inclusive graph of the unoccupied space known as the free space graph in literature. The free space graph is a graph whose edges do not intersect the interior of any obstacles and its vertices are the obstacles' vertices. Such a graph would automatically handle the collision avoidance problem and all paths found on it will be collision-free. Construction of the free space graph builds up the geometric data structure needed for the optimization of the path. Hence, the continuous problem of path finding in the 2D (or 3D) environment would be converted into a discrete problem of searching a graph for the optimal, often times shortest, path between two nodes of the graph.

In computational geometry, there are some methods of generating collision-free graphs in a cluttered workspace to circumvent the intersection problem. These methods fall into the category of roadmap techniques. The two most common techniques of graph generation as noted in chapter 2 are visibility graphs and Voronoi diagrams. In addition to the roadmap techniques, researchers employ cell decompositions to address the problem of robot motion planning. In the following sections, we elaborate on these graph generation techniques. Then, we elucidate the approach we develop to undertake the problem of generating the free space graph.

5.1 Existing Techniques

In this section, the current available techniques for constructing the graph of the free space for planar path planning problems are explained and their limitations are discussed.

5.1.1 Visibility Graph

Generating the visibility graph of a cluttered 2D or 3D environment is among the very first approaches to undertake in the path planning problem. According to Welzl [18], the bottleneck in solving the shortest path problems in 2D is the construction of the visibility graphs. Once the visibility graph is known in a workspace, the shortest path can be computed using single-source shortest path algorithms such as Dijkstra's [18]. The graph search methods such as Dijkstra's are described in the next chapter.

Visibility graph is an undirected graph of edges connecting every two nodes that are visible to each other. In computational geometry, two nodes see each other if and only if the edge they share does not intersect the interior of any obstacle [14]. Nodes that can see each other are visible nodes and the segment they share is called the visibility edge. The edges of the polygonal obstacle are all visibility edges by definition. Figure 5.1 indicates an example of a visibility graph. Note in this figure line segments 14,16,17, 34,37,36, and all edges of the two polygons (12,13,23,56,67,47, and 45) are all visibility edges.

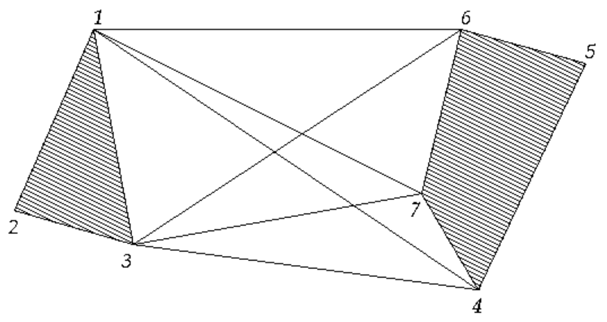

Figure 5.1: Sample Visibility Graph

Visibility graphs are widely used in the path planning problem to capture the free space. In fact, once the visibility graph of the vertices of the polygonal obstacles is at hand, the shortest path could be determined as a sub-path of the graph [14]. However, as mentioned in chapter 2, the construction of the visibility graph is computationally expensive and even the fastest known algorithm to do so takes O(n^2) time with n being the total number of polygons' vertices. This is because the construction of the visibility graph requires the information of the entire workspace. Furthermore, some planning cases include nonconvex obstacles i.e. polygonal or polyhedral obstacles with at least one concave vertex. The concave vertices are also called reflex points or vertices[14]. Creating the visibility graph of environments containing nonconvex obstacles results in including unnecessary edges since as noted by Wein et.al. [27], the visibility edges corresponding to reflex vertices are never used in a shortest path. The reason why these edges are excluded is because based on the triangle inequality these edges will lengthen the path if being included. For example, in visibility graph of Figure 5.2, edges 12-26, 13-26, and 14-26 cannot be used in a shortest path since they are considered as dead ends and a path ending up at vertex 26 has no way out but to go to a convex vertex, hence lengthening the path.

For instance, in Figure 5.2 if edge 13-26 is used, the path should go to either vertex 25 or 21 using edges 26-25 or 26-21, respectively, while based on triangle inequality edges 13-25 or 13-21 results in a shorter path.

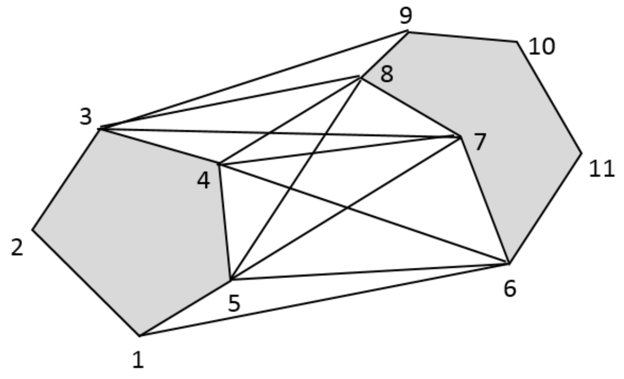

Figure 5.2: Visibility Graph of a Nonconvex Polygon

5.1.2 Voronoi Diagram

The Voronoi region of a point *p*, V(*p*), on a plane, is the set of all points that are closer to *p* than any other specified points or sites [14]. With that being said, the Voronoi diagram of a set of n disjoint planar polygons, which builds the foundation for the shortest path problem, divides the plane into n maximal clearance connected cells[27]. Points lying in each cell are closer to the polygon corresponding to that cell than other polygons in the plane. This means an edge of a Voronoi diagram is equidistant to two vertices or polygon edges while any Voronoi vertex is equidistant to vertices or edges of at least three polygons. Because a Voronoi region is created by the intersection of half-planes, it is a convex polygonal region [43]. Figure 5.3 illustrates a Voronoi diagram of four obstacles in the plane.

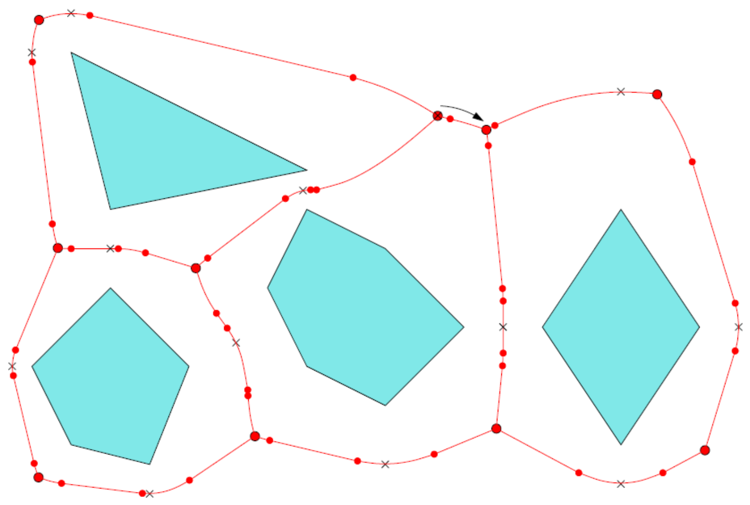

Figure 5.3: Example of a Voronoi Diagram of Four Obstacles[27]

Voronoi diagrams are utilized in path planning problems to avoid collisions through proximity detection. Since points on a Voronoi edge are equidistant to two polygons, the edges yield the maximum distance to the two nearest polygons, resulting in the Voronoi diagram generating the maximum clearance path [43].

Since the Voronoi diagram maximizes the obstacle clearance, it does not necessarily result in an optimal path [10]. The path may require unnecessary turns and long lengths only due to the locations of obstacles and workspace configuration. Hence, a path found using a Voronoi diagram may not be optimal and requires further smoothing and refinement to shorten its length.

In addition, although it is a somewhat straightforward process to generate a Voronoi diagram for a set of sites when it comes to construction of the Voronoi diagram for a number of polygonal obstacles, the complexity and computation time of the algorithm rises. Because of this level of complexity and time, often the obstacles are approximated with their extreme points and the approximate Voronoi diagram is generated for those points[44], [10]. In general, the construction of a Voronoi diagram for path planning among polygonal obstacles requires the proximity information of the entire workspace.

Both construction of, and search in, a Voronoi diagram are faster than a visibility graph [10]. In fact, even the fastest developed algorithm for constructing a visibility graph [45] that takes O(n^2) is much slower than constructing the Voronoi diagram for the same environment which takes O($n$log$n$) time [10].

Despite the efficiency and versatility [10] of the Voronoi diagram in addressing the path planning problem, it does not guarantee the optimality of the final solution. Besides, the approximation of the obstacles by points is challenging and it often affects the final solution. Last but not the least, similarly to a visibility graph, the Voronoi diagram also requires the proximity information of the whole workspace, which may not seem effective and fast when only a portion of the workspace may be involved in the path planning.

5.1.3 Cell Decomposition

Cell decomposition is among the first methods developed to tackle the problem of motion planning [14]. Similar to visibility and Voronoi techniques, cell decomposition also has its origin in computational geometry. In this method, the free space is partitioned into a finite number of non-overlapping cells. To determine a collision-free path between the start and end points using cell decomposition, one requires to first identify the cells containing the start and end points. These cells are then connected using a sequence of connected cells. Decomposition could be either exact or approximate. Approximate decomposition is a recursive process of breaking down the free space into rectangular cells until each cell is entirely inside an obstacle or in the free space. Recursion terminates when a pre-defined accuracy of decomposition is achieved. Exact cell decomposition uses trapezoidal and triangular cells and is often faster; nevertheless, the solution is not optimal. However, upon increasing the accuracy of the approximate cell decomposition(decreasing the cell size), near-optimal solutions are achievable at the cost of longer computation time [10].

In all the aforementioned roadmap techniques, the entire environment's information is required to be able to construct a graph of the workspace. Nevertheless, there might be cases in which a portion of the environment comprised of a subset of obstacles is involved in the path-finding problem. Thus, restricting the construction and search processes to that specific portion should help to simplify the problem by eliminating the complexities and speeding up the path-planning algorithm.

Based on this, we propose a method to capture the free space graph using the convex hulls of the intersecting obstacles that are detected from employing the bi-level intersection detector. In the next section, the details of this method are provided.

5.2 Proposed Approach: Planning based on the convex hulls of the obstacles

In order to speed up the path-planning algorithm, simplify the complexities that lie in roadmap techniques, and to come up with an optimal rather than near-optimal solution to the 2D path-planning problem, we underlie our technique based on the notion of convex hulls of the obstacles. Convex hulls have properties that are important in finding the shortest path. For example, in [23] the authors claim that the shortest path in the TSP problem passes through the convex hull of the cities. Also, as pointed out by Wein [27], the shortest paths in a cluttered environment are tangent to the obstacles (the proof of which is simple using the triangle inequality). Since by definition the convex hull of an object is the smallest enclosure containing the object, hence including tangent edges to the obstacles, it could be used to determine the shortest path. Based upon these properties of the convex hulls, we develop an efficient algorithm to find the free space graph of the environment.

In our proposed approach, instead of capturing the free space using the information from the entire workspace, we limit our scope to that portion of the workspace interfering with the shortest straight line connecting the start and end points. Since the straight line is the shortest path between two points regardless of colliding the obstacles, it is set as the reference line of our algorithm. The closer the router moves towards the reference line, the shorter the path is to reach the goal. Hence, instead of planning the path as far as possible from the obstacles, unlike the Voronoi diagrams, we attempt to keep it close to the obstacles such that it touches them but not intersect their interior. Consequently, the obstacles detected to be intersecting, using the bi-level intersection detector, are the foundations of this approach. In the next section, the construction of the free space graph based on convex hulls is explained.

5.2.1 Free space graph formation

Suppose we denote the workspace by W, since we are looking at solving the problem in a 2D environment, we know that:

$$W \subseteq \mathbb{R}^2$$

Now, suppose there are n polygonal obstacles, P_i , (i = 1, 2, …, n) scattered in the workspace. The geometry and location of each of the obstacles are known and they are all stationary and disjoint. In addition, the coordinates of the start and end points of the path of interest are given. The problem is to construct the free space defined as Eq.(5.1) in the form of a graph.

$$C_{free} = W \setminus \bigcup_{i=1}^{n} P_i \tag{5.1}$$

In Eq.(5.1) C_{free} denotes the free space as a subset of the workspace which could be generated by subtracting the union of all occupied spaces by the obstacles from the workspace. The graph G to be constructed from the free space is defined as follows by its set of vertices (V) and edges (E).

$$G \subseteq C_{free}\,, \quad G = \{V, E\} \tag{5.2}$$

Now, we need to find this graph such that its edges do not intersect the interior of any of the obstacles. To find this graph means to determine its vertices and edges.

Assuming there is only one obstacle in the workspace, one needs to determine if the path connecting the start (A) and termination (B) points intersects the interior of the obstacle. By definition, the convex hull of a set of points is the smallest convex set containing all points. The convex hull of two points, by this definition, is the line connecting the points. Thus, we confirm the intersection between a line segment (AB) and a polygon (P) if the condition below holds:

$$Conv(A, B) \cap P \subset int(P) \cup \partial(P) \tag{5.3}$$

Where Conv(A,B) is the convex hull of the two points A and B, P is the polygonal obstacle in the workspace, $P \subset W$, int(P) denotes the interior of the polygon P, and $\partial(P)$ is the boundary of the polygon P as could be seen in Figure 5.4.

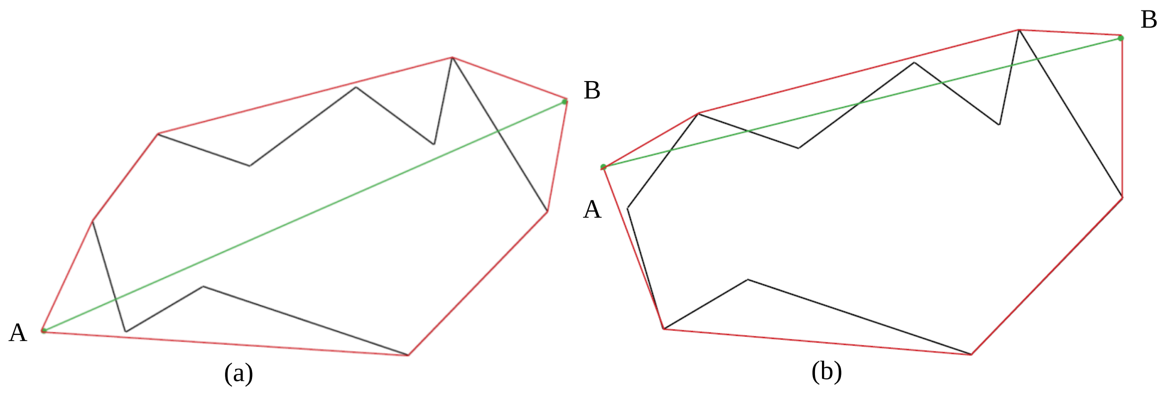

Figure 5.4: Line segment and polygon intersection

The intersection of a line segment with a polygon can be either a line segment itself (as in Figure 5.4(a)) or a set of disjoint line segments (Figure 5.4(b)), depending on the obstacle being convex or concave. In either case, the intersection would be a subset of the polygon which is equal to the union of the interior of the polygon and its boundary shown in Eq.(5.3).

Now that the intersection between a line segment and a polygon is defined, we should find a way to move the line segment such that it does not intersect with the interior of the polygon anymore, hence defining a collision free path between the points A and B.

We propose that if one considers the convex hull of the line segment AB and the polygon P shown in Figure 5.4 in red, this convex hull only intersects with the boundary of P, hence avoiding its interior and there is no more chance of collision between a path formed by this convex hull and the polygonal obstacle. This condition is shown in the equation below.

$$Conv(A, B, P) \cap P \subset \partial(P) \tag{5.4}$$

Thus, if we define a graph from the free space based upon the convex hull of the start and end points of the path (A and B) and the obstacle(s) that collide with it, the above condition holds. Therefore, this graph would not be in the occupied space though it will touch some of the edges or vertices of the obstacle(s) which is not considered as an intersection. As a result, the graph G = {V, E} of the free space can be defined as follows:

$$v_i \in V \Leftrightarrow v_i \in \partial Conv(A, B, P), \;\; \exists e_{ij} \in E \tag{5.5}$$

$$e_{ij} \in E \Leftrightarrow e_{ij} \subset \partial Conv(A, B, P), \;\; e_{ij} \cap P \subset \partial P \tag{5.6}$$

In other words, any edge in the boundary of the convex hull of the start and end points of the path and polygon P is an edge in graph G if and only if (iff) it does not intersect with the interior of the polygon. And any vertex in the same convex hull is a vertex of graph G iff there is an edge corresponding to that vertex in the set E of the edges of the graph defined in Eq.(5.6).

Using the convex hulls is advantageous in the sense that no matter how many concave vertices a polygon has, the convex hull can find a graph containing edges in the free space that do not include the unnecessary edges corresponding to a reflex vertex. However, in the visibility graph or Voronoi diagram, each vertex is treated separately, independent of being convex or reflex, resulting in redundant edges in the graph.

If there is more than one obstacle, after the bi-level collision detector identifies the intersecting obstacles, the convex hull of the start and end points and the intersecting obstacles must be created to construct the free space graph using them. This approach considers all intersecting obstacles and creates every convex hull by a start point and the next immediate intersecting obstacle. It should be noted that the intersecting obstacles are ordered based on the distance from the start point of the path. Thus, the closest intersecting obstacle to the start point is called the first obstacle and the furthest obstacle is called the last.

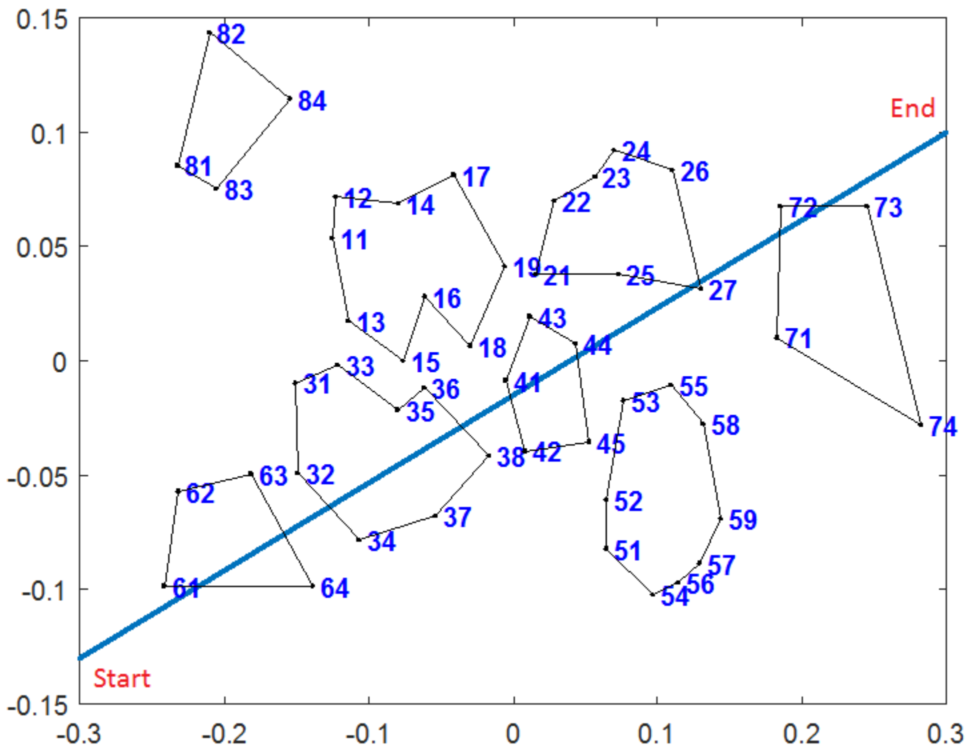

Figure 5.5: Ordering the Intersecting Obstacles

For example in Figure 5.5 above, the order of the intersecting obstacles based on the distance from the start point would be 6, 3, 4, 2, 7 since obstacle 6 is the closest and 7 is the furthest.

Suppose the number of intersecting obstacles is m. Starting from the start point of the path, the first convex hull is formed by the start point and the closest obstacle to it. In case of Figure 5.5, the start point shown in red and obstacle number 6 create the first convex hull. To create the convex hull at step *i*, a new start point and an obstacle are required. However, the end point of the path is not updated and remains the same for all iterations. The start point to create convex hull *i* is defined by the extreme points of the convex hull at step *i-1*. The extreme points of the convex hulls are the points that have the maximum distance from the reference line which is the line connecting the start and end points of the path regardless of it intersecting any obstacles (reference line of Figure 5.5 is shown in blue). Typically, there exists at least two of these extreme points in each convex hull, one for each side of the reference line. However, only the two extreme points on each side of the reference line that are the first points of contact to the obstacle are considered to update the start point at each step. For example, in Figure 5.6 the extreme points of the convex hull in green are 73 and 74 although all points lying on the line segment 74-71 have equal distances from the reference line.

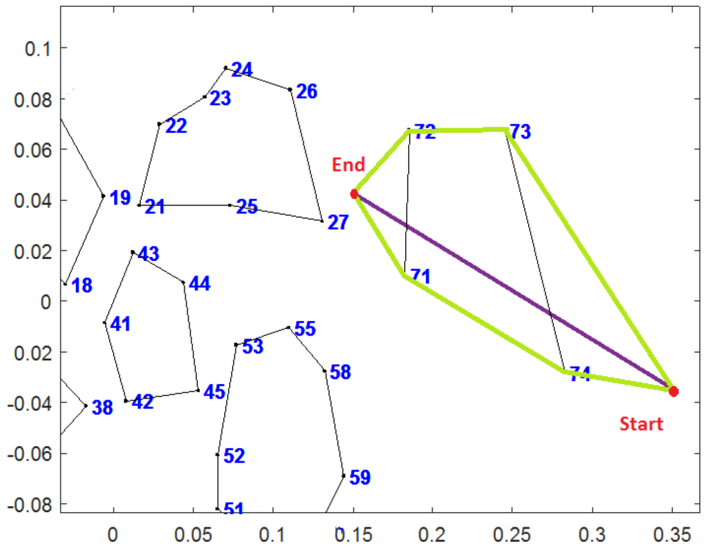

Figure 5.6: Extreme Points of a Convex Hull

Extreme points on obstacles are chosen to ensure that the edges do not intersect the interior of the obstacle itself by having the maximum distance from the reference line. At each step of this approach, two convex hulls are created corresponding to the two extreme points, except at the first and last step. At the last step, the convex hull of the last intersecting obstacle and the end point of the path is created. Hence, for *m* intersecting obstacles *2(m-1) +2* or *2m* convex hulls will be created. Figure 5.7 depicts a schematic of creating the convex hulls for 4 intersecting obstacles. Note that a total of 8 convex hulls are created in this example.

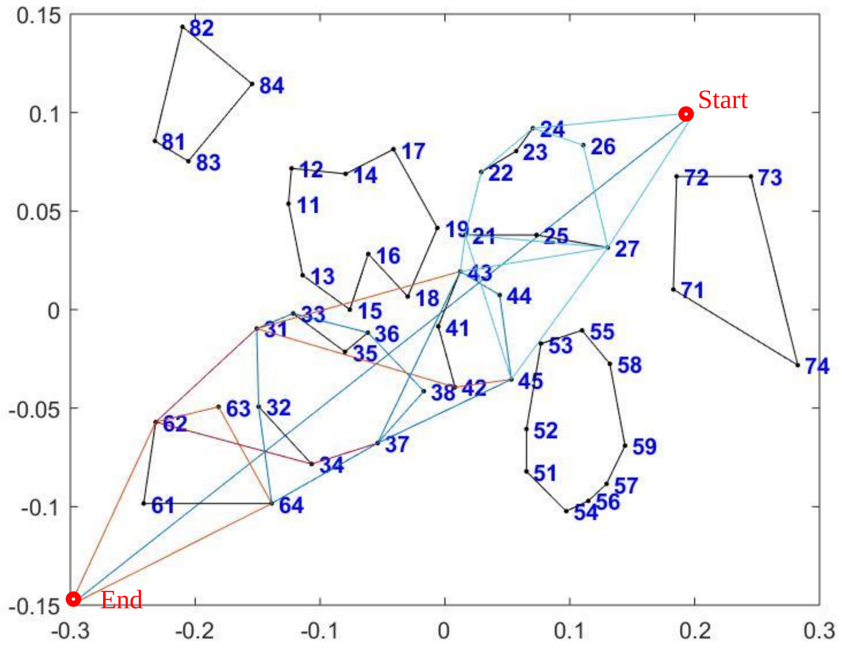

Figure 5.7: Schematic of the First Iteration in Construction of the Free Space Graph

An edge of the convex hull is added to the graph provided it does not intersect any obstacles. Otherwise, the process of convex hull generation is performed recursively, with the new reference line being the edge that has an intersection until the edge is collision free and could be added to the graph. For example, in Figure 5.7 edges 62-34, 31-42, 31-43, 37-43, and 45-21 indicate intersections with obstacles and need be re-routed using the same approach recursively until all edges all collision free. On the other hand, edges such as 62-31, 37-45, and all others are collision free and added to the set of edges of the free space graph. The flowchart of this process is shown in Figure **5.9**. The process is similar to breaking down a line into two segments and then four and so on until all the collision free edges and a set of piecewise linear routes connecting the two points are created. It is worth noting that using this technique, for *m* intersecting obstacles, *4(m-1)+4* or *4m* edges in total would be added to the set of edges of the free space graph. Shown below is the free space graph of the workspace of Figure 5.5.

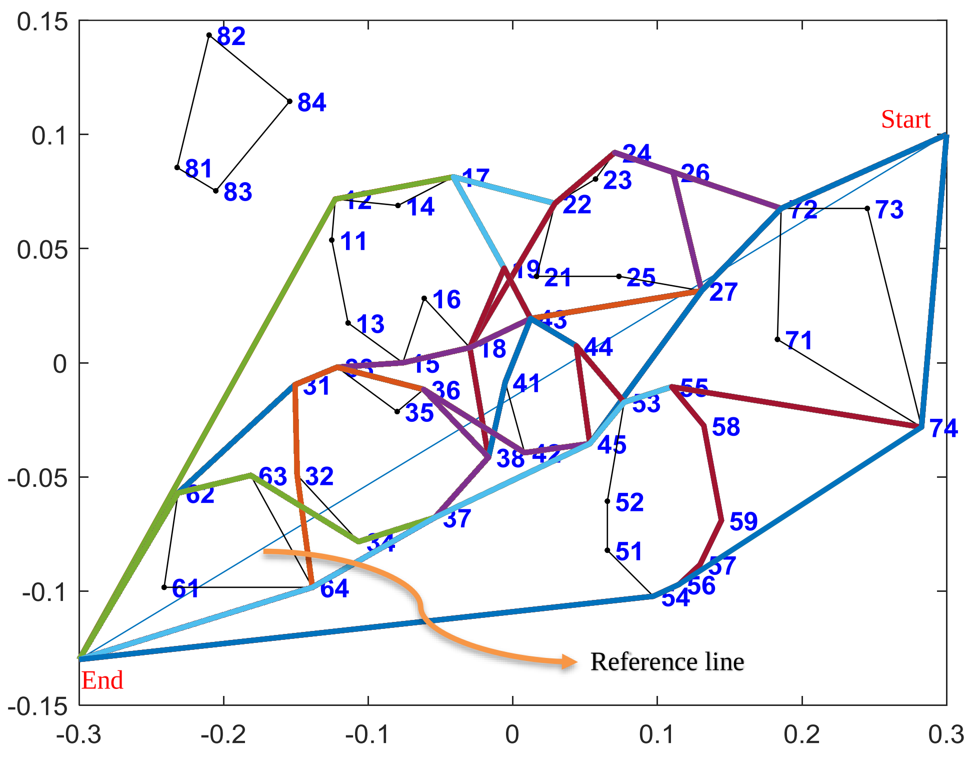

Figure 5.8: Free Space Graph of The Figure 5.5 Workspace

This approach can be applied to any pairs of points in the workspace and the result is an undirected graph of all collision free paths. After the graph is generated, any of the network optimization algorithms can be implemented to optimize the path for different optimization criteria, the most common of which is to find the shortest path. Network optimization and solution of the shortest path problem are discussed in the next chapter.

It is worth noting that since this graph highly depends on the start and end nodes, different graphs would be constructed for different pairs of nodes and there does not exist a unique graph of the entire workspace unlike visibility and Voronoi; therefore, limiting the search to a portion of the workspace which expedites the search for the shortest path.

In addition, the final solution will be the optimal path and there is no need to approximate the obstacles and other elements of the workspace to come up with a solution. In Table 5.1, the free space graphs of the sample workspaces from Table 4.2 in chapter 3 are constructed using the proposed technique. The time complexity of this algorithm is derived in chapter 7.

Note that in cases 1 to 3 of Table 5.1, since the straight line connecting the start and end points of the path does not intersect any obstacle, the shortest path between the two points is the line itself and so is the free space graph of the workspace.

In case 4, the straight line connecting the start and end points passes through obstacle number 5. Hence, a convex hull containing this obstacle is generated and the free space graph is extracted from that convex hull. Since the path has end points lying on the obstacle and only intersects that obstacle, the edges of the graph are the edges of the 5th obstacle.

In case 5, the path has intersection with obstacles 1, 2, 3, 4, 5, 6, and 7. Thus, the required convex hulls are formed and the edges of the free space graph are extracted. One should note that in the beginning, only obstacles number 6, 3, 4, 2, and 7 intersect with the straight line connecting the start and end point. However, as the path is re-routed to avoid collisions, it encounters new obstacles on the way and the resulting collisions need be avoided by creating new convex hulls containing new intersecting obstacles.

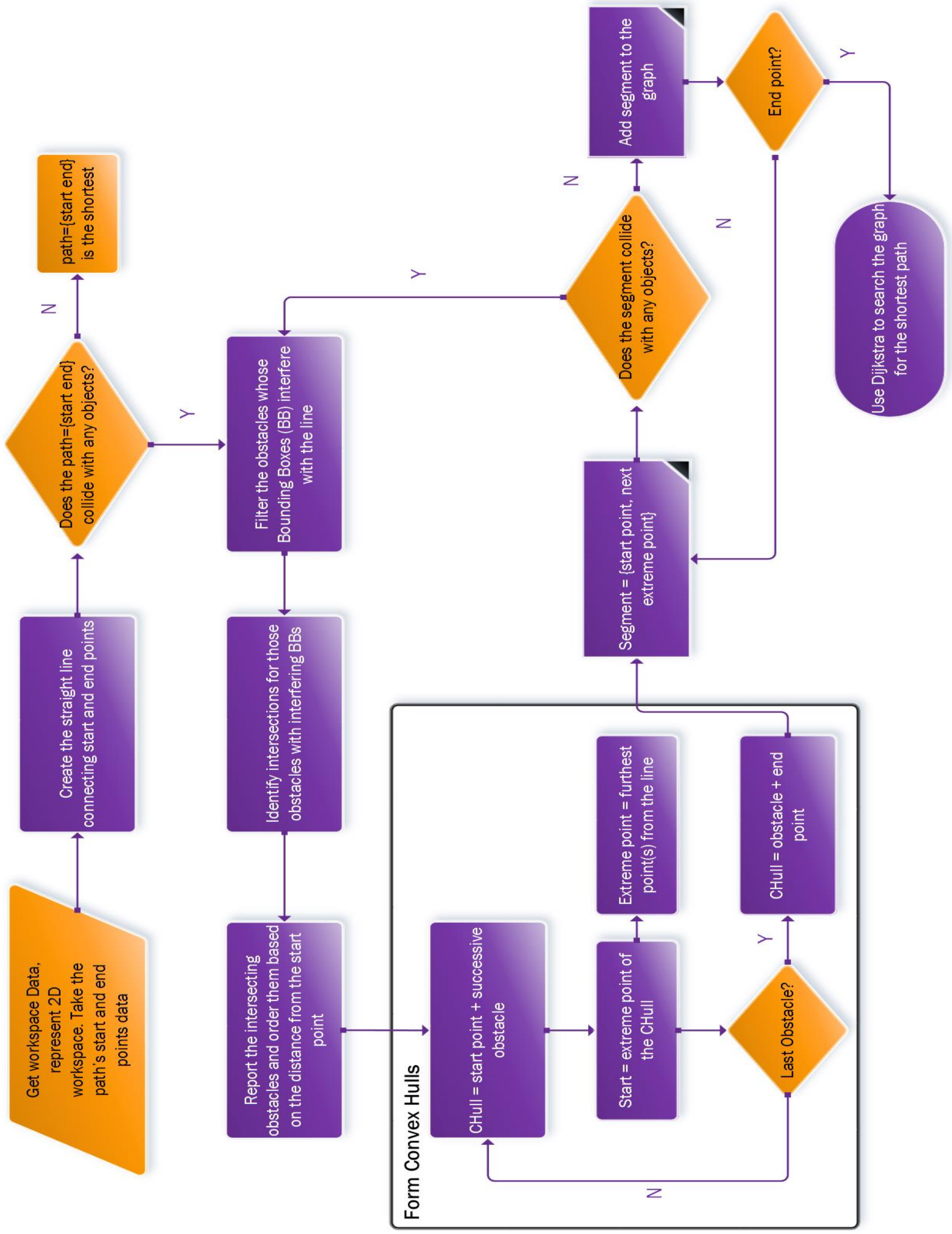
Get workspace Data, represent 2D workspace. Take the path's start and end points data
Create the straight line connecting start and end points
Does the path={start end} collide with any objects?
N
path={start end} is the shortest
Y
Filter the obstacles whose Bounding Boxes (BB) interfere with the line
Identify intersections for those obstacles with interfering BBs
Report the intersecting obstacles and order them based on the distance from the start point
Form Convex Hulls
CHull = start point + successive obstacle
Start = extreme point of the CHull
Extreme point = furthest point(s) from the line
Last Obstacle?
Y
N
CHull = obstacle + end point
Segment = {start point, next extreme point}
Does the segment collide with any objects?
Y
N
Add segment to the graph
End point?
N
Y
Use Dijkstra to search the graph for the shortest path

Figure 5.9: Flowchart of the free-space graph construction

Table 5.1: free-space Graphs of Different Sample Workspaces

Workspace Representation	Line Coordinates	Free-space graph
1. 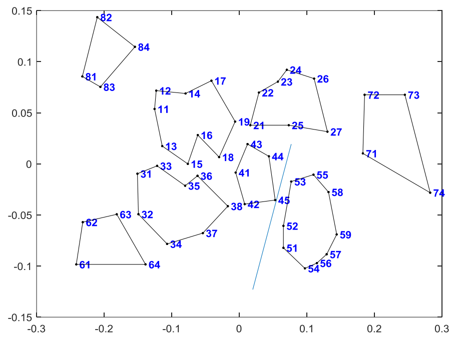	$\begin{bmatrix} 0.076939 & 0.019347 & 0 \\ 0.020000 & -0.12300 & 0 \end{bmatrix}$	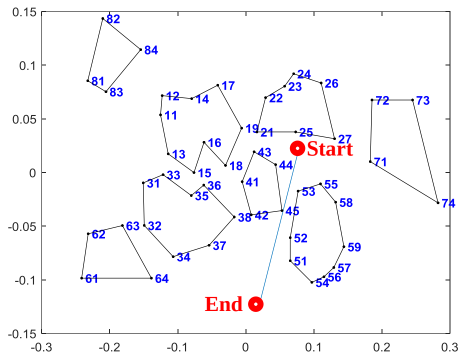
2. 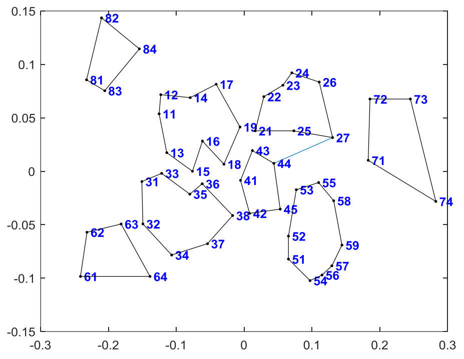	$\begin{bmatrix} 0.043853 & 0.007384 & 0 \\ 0.130513 & 0.031514 & 0 \end{bmatrix}$	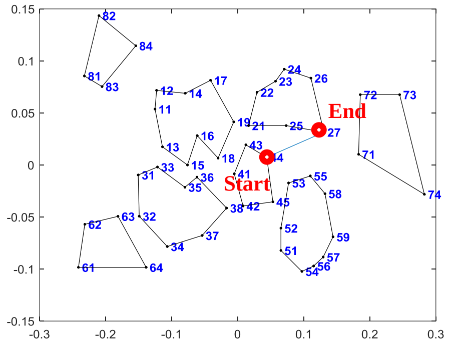
3. 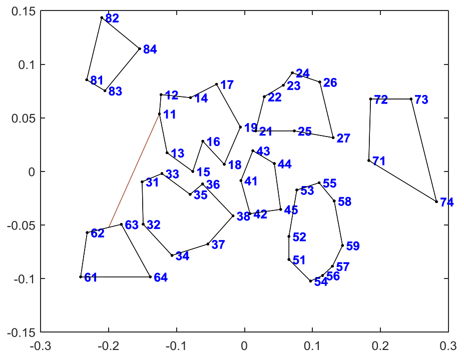	$\begin{bmatrix} -0.125316 & 0.053741 & 0 \\ -0.200000 & -0.05230 & 0 \end{bmatrix}$	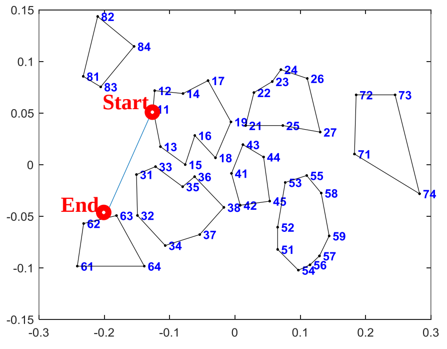

4. 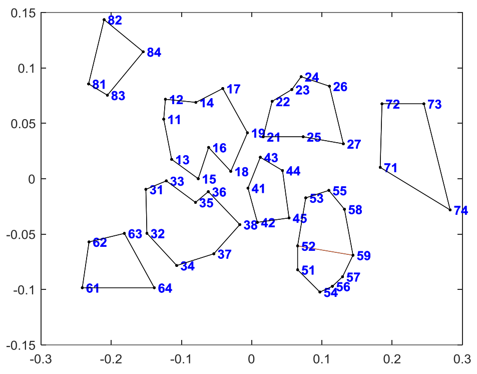	$\begin{bmatrix} 0.065349 & -0.060658 & 0 \\ 0.144232 & -0.069069 & 0 \end{bmatrix}$	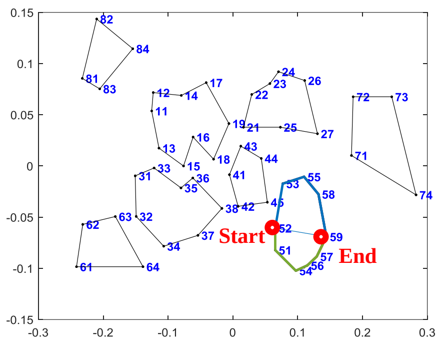
5. 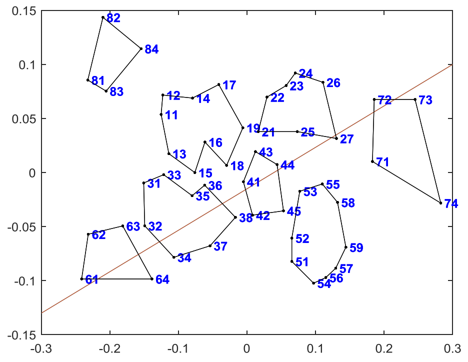	$\begin{bmatrix} 0.3 & 0.1 & 0 \\ -0.3 & -0.13 & 0 \end{bmatrix}$	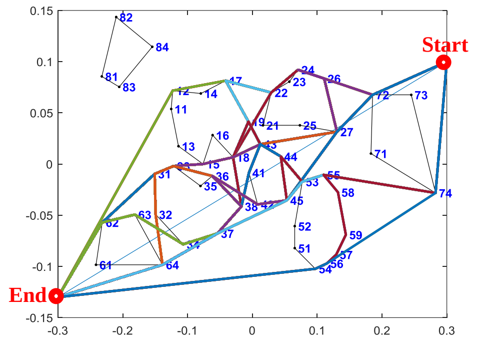

5.2.2 Backtracking

In some cases, after having progressed somewhat in the search for the free space, an intermediary start point may lie inside the convex hull of that point and obstacle resulting in the intermediary start point being excluded from the convex hull. This situation can be seen in Figure 5.10. In this example, the algorithm progressed from start point to node 31, which is the extreme point of the convex hull formed by the start point and the nest immediate intersecting obstacle, obstacle 3. Next, connecting node 31 to the end point, obstacle 2 was intersected. Construction of the convex hull of node 31 and obstacle number 2 resulted in one segment being defined from points 31 to 23. Now point 23 is a new start point, and the algorithm attempts to construct the convex hull of node 23 and obstacle 3 since the connecting node 23 to the end node, the path intersects obstacle 2. It is at this point that node 23 lies inside the convex hull (shown in red dashed lines in Figure 5.10) formed by object 3, and node 23 cannot be considered as a vertex in the free space graph. To solve this problem and find a path from this node to the end point, we propose a backtracking approach: As the algorithm comes across a start point lying inside the convex hull (e.g. node 23) formed between it and the next obstacle, it backtracks a step and finds the previous node (node 31 in this example) that shares an edge with the current node (node 23). The algorithm replaces the current node with the previous node and creates the convex hull of this new start point and the obstacle. For example, in Figure 5.10 the predecessor of node 23 is node 31and the convex hull is created using node 31 and obstacle 3.

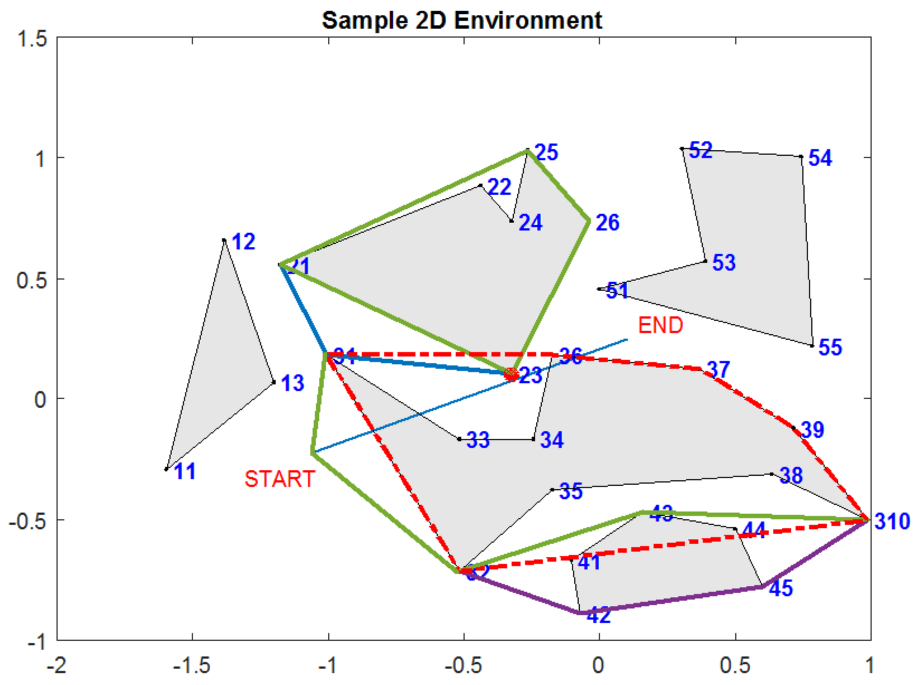

Figure 5.10: Start Point (23) Lying inside the Convex Hull

After the convex hull is created, the successor node of the start point is identified (e.g. node 36) and set as the successor node of the original start node (e.g. node 23). Hence, a successor will be determined for the node that lies inside the convex hull while previously this node could be deemed as a dead end and there was no way from that node to the end point of the path. The construction of the free space graph is continued from the new start point until it finds all safe routes to the end point.

Backtracking of Figure 5.10 works in such a way that node 23 would be connected to node 36 which is connected to node 31 in the convex hull. The resulting graph of the free space is shown in Figure 5.11.

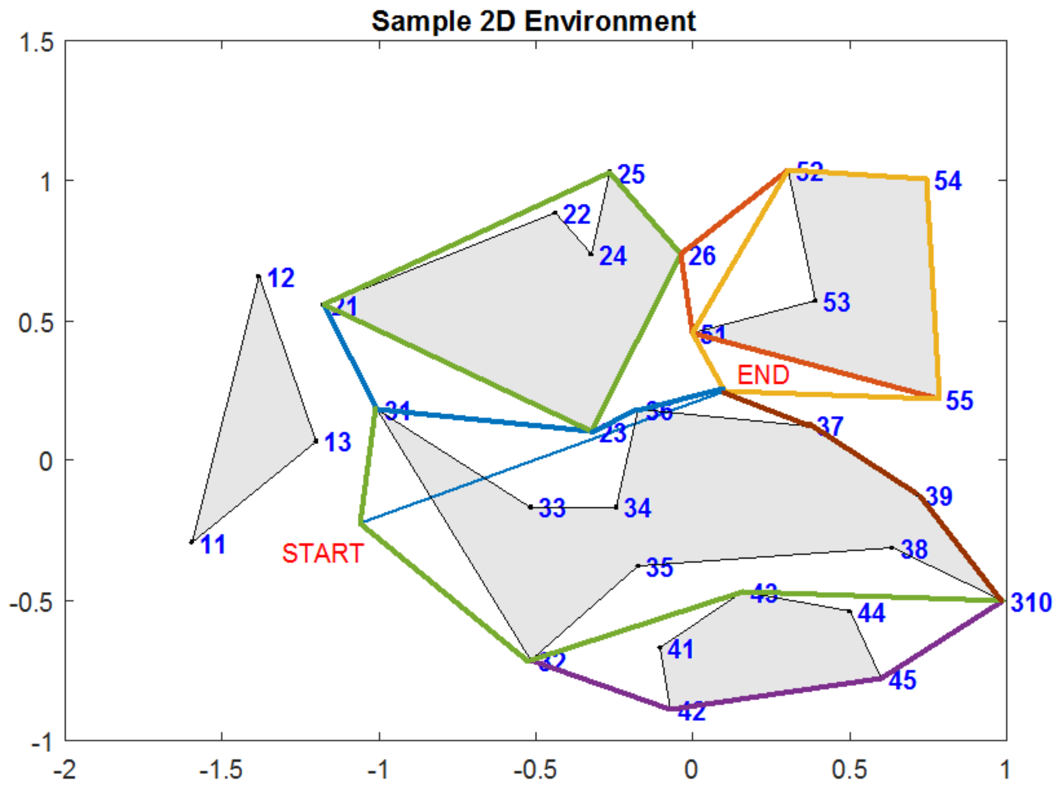

Figure 5.11: Free Space Graph Using Backtracking

Chapter Six
PATH OPTIMIZATION

The objective of most of the path-planning problems is to optimize (minimize or maximize) a criterion or some criteria. The most common objective in path planning problems is to minimize the length of the path while other objectives such as minimizing the number of turns in the path are also considered.

For the planar path planning problem of this research, since the obstacles are disjoint, there always exists a path between the start and end points and the objective is to minimize the total length of the path. After finding the graph of the collision free space, the shortest path between the start and end points on the graph can be found through using a graph search technique known as network optimization problems.

6.1 Formulation of the network optimization problem

The most fundamental part of any optimization problem is the mathematical model. Shortest path optimization problems are often modeled as network flow optimization mathematically. Since the graph is constructed, one only needs to optimize or search this graph for the optimal solution.

Suppose graph G is given by the set of its vertices and edges; G= {V, E}. The shortest path must be found between nodes i and j of this graph where i,j ϵ V, i$\neq$j. Thus, the optimization is to minimize the total length of the piecewise linear path between i and j or:

$$min \sum_{(i,j)\in G} C_{ij}X_{ij}$$

Where:

C_{ij} is the cost of travel from node i to node j which is the L_2 norm or the Euclidean distance between the two nodes. Since the coordinates of all the vertices are known, this Euclidean distance is simply computable. And, X_{ij} are the decision variables such that:

$$X_{ij} = \begin{cases} 1 & if\, e_{ij}\ is\ in\ the\ path \\ 0 & otherwise \end{cases}$$

The decision variables could be either 1 or 0 depending on the edge being selected as part of the path or not. By this definition, the only constraint is:

$$\sum_{\{j:(i,j)\in G\}} X_{ij} - \sum_{\{i:(i,j)\in G\}} X_{ji} = \begin{cases} 1 & i = 1 \\ 0 & i \neq 1, m \\ -1 & i = m \end{cases}$$

This constraint ensures that the first and the last nodes are not connected to other nodes. In other words, the difference between the outflow and inflow of the first and the last nodes is one meaning these nodes are definitely in the path and there is no node before/after the first/last node. The mathematical model of the shortest path problem is summarized as below.

Table 6.1: Mathematical Model of the Network Optimization Problem

$$min \sum_{(i,j)\in G} C_{ij}X_{ij}$$

Subject to : $\sum_{\{j:(i,j)\in G\}} X_{ij} - \sum_{\{i:(i,j)\in G\}} X_{ji} = \begin{cases} 1 & i = 1 \\ 0 & i \neq 1, m \\ -1 & i = m \end{cases}$

Where: $X_{ij} = \begin{cases} 1 & if\, e_{ij}\ is\ in\ the\ path \\ 0 & otherwise \end{cases}$

There are different network optimization methods to solve the above shortest path problem such as branch-and-bound, Dijkstra, A*, dynamic programming, etc. In this chapter, two of the most commonly used local search algorithms are described: Dijkstra and A*. Both algorithms work with predefined graphs. We use the free space graph constructed in the previous chapter as the input to the search algorithm.

6.2 Dijkstra's Shortest Path Algorithm

Dijkstra is an algorithm developed by Edsger Dijkstra [26] to find the shortest path from a single source to one or all other nodes of a given weighted graph consists of a finite number of nodes. The weights are non-negative numbers assigned to each edge of the graph. For instance, weights can be the lengths of the edges of the graph or the Euclidean distance between the two adjacent nodes of the graph connected by an edge. It is important to note that the source node is single but the destination can be any or all other nodes of the graph.

Dijkstra's algorithm constitutes a tree of edges, which link the start point to the end point in several steps. In the beginning, all nodes are divided into two sets a set of visited (or predecessor[46]) and a set of unvisited (or successor[46]) nodes. Hence, initially, all nodes belong to the set of unvisited nodes except the source node. In addition, a tentative cost of ∞ is assigned to each edge, which is updated later on. Starting from the start point, at each step, the algorithm explores all the adjacent unvisited nodes, excludes them from the set of unvisited nodes, and updates their cost by their distance from the start point. It then adds the node with the smallest cost to the path and sets its cost to permanent. This node designates the current node for the next iteration. This process is repeated iteratively until it eventually reaches the goal node. A pseudo code of this algorithm written by Sniedovich [46] is as shown in Table 6.2.

Table 6.2: Dijkstra's algorithm pseudo code

```
Initialization:

    $j = 1$; $F(1) = 0$; $F(i) = \infty$, $i \in \{2 . . . , n\}$; $U = V$
Iteration:

    While ($j \neq n$ and $F(j) < \infty$) Do:
        Update U : $U = U\backslash\{j\}$
        Update F : $F(i) = \min\{F(i), F(j) + D(j, i)\}$, $i \in A(j) \cap U$
        Update j : $j = \operatorname{argmin}\{F(i) : i \in U\}$
    End while
```

F(j) is the cost function associated with node j which is the distance from node one to node j. U is the set of unvisited nodes which is equal to the set of vertices of the graph in the initialization since no vertices have been explored yet. Also, A(j) is the set of adjacent nodes, successors of node j. In the initialization stage, the current node j is set as the first node, which is the start point of the path, and its corresponding cost by definition is zero. Also, as mentioned previously, the tentative cost associated with all other edges is initially set to ∞ which is updated in the next iterations of the algorithm. At each iteration, the set of unvisited nodes, the tentative cost associated with the adjacent unvisited nodes of node j, and the current node (j) are updated until the target node is achieved. The cost of the node i (immediate successor of node j) at each iteration is updated if and only if the sum of the distance from the previous node(j) to node i and cost of the previous node are less than the current tentative cost. The cost of a node will be set to a permanent value if the node is visited and there does not exist a smaller cost associated with that node. Figure 6.1 shown below includes an example [47] of finding the shortest path on a graph of five vertices.

This example is from Dr. Angelia Nedich's lecture notes on "Operations Research Methods".

a) Given the graph b) Initialization

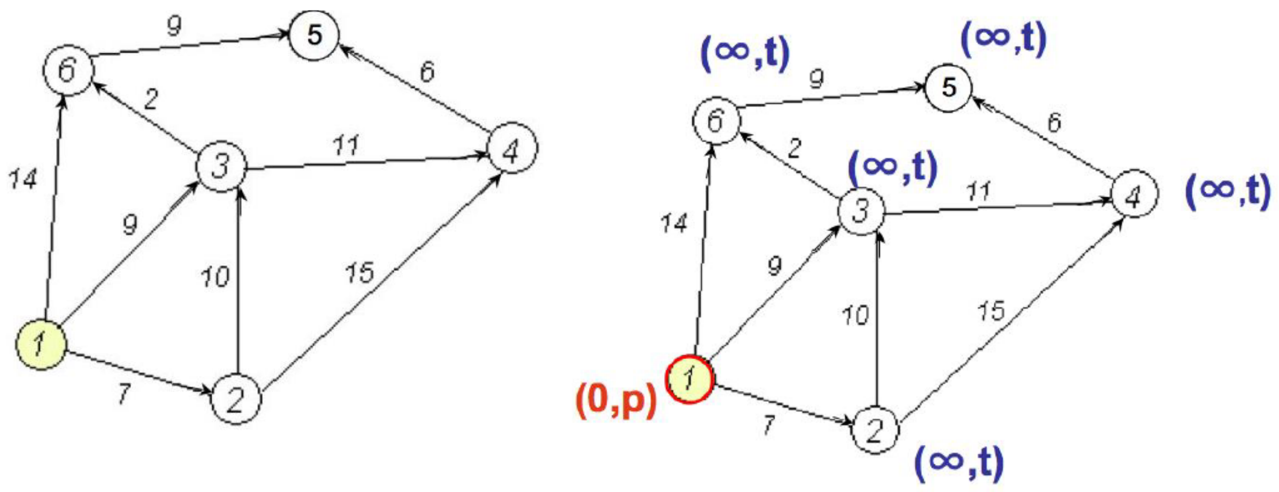

Figure 6.1: Dijkstra's Initialization

Figure 6.1a shows the given graph of five vertices with known costs on the edges (length of each edge). The goal is to find the shortest path from node 1 to node 5. Figure 6.1b depicts the initialization step of the Dijkstra's algorithm. Note that in the initialization all the costs to reach the unvisited nodes are tentative, designated by t, while node 1 has a permanent cost of zero, designated by (0,p).

The first iteration of the Dijkstra is shown in Figure 6.2. In this iteration, nodes 2,3, and 6 that are adjacent to node 1 and are all unvisited are explored. Note that the costs associated with these nodes (cost of travel from node 1 to these nodes) are updated since at node 2: $0+7 < \infty$, at node 3: $0+9 < \infty$, and at node 6: $0+14 < \infty$. However, only the cost of node 2 is permanent and the rest are still tentative because node 2 has the minimum cost and is picked to be included in the shortest path. Hence, the current node is updated to be node 2.

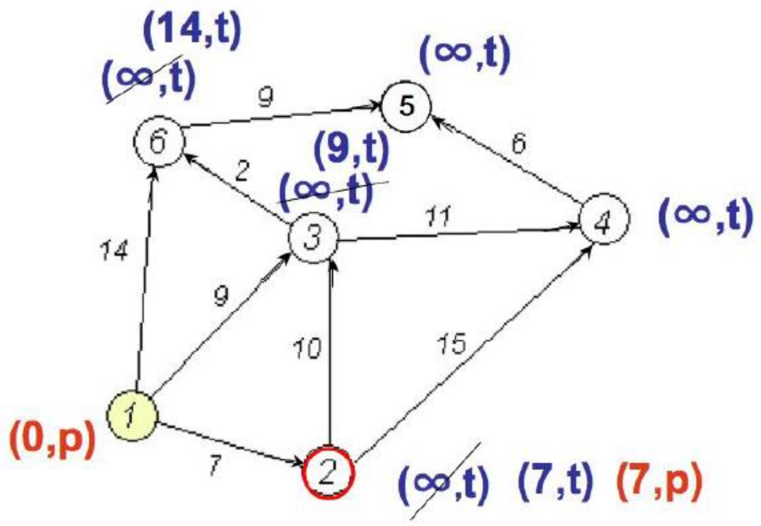

Figure 6.2: Dijkstra's First Iteration

By updating the current starting node to node 2, the algorithm continues on exploring the adjacent unvisited nodes of node 2 which are 3 and 4. The second iteration of Dijkstra for this graph is shown in Figure 6.3.

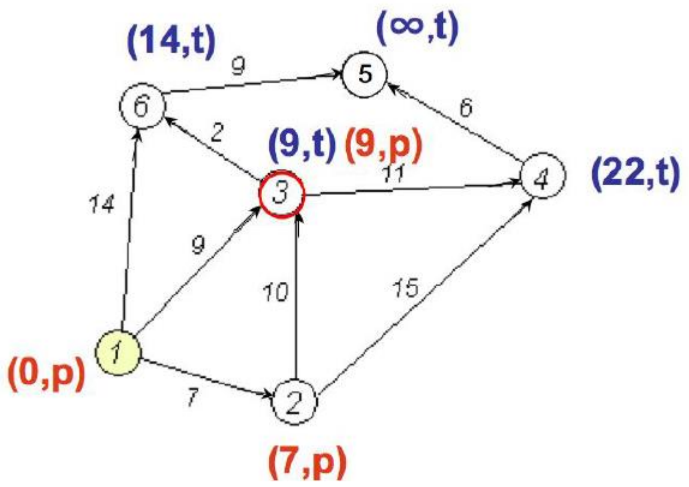

Figure 6.3: Dijkstra's Second Iteration

In the second iteration, cost of travel to nodes 3 and 4 are updated in the same way as the first iteration. Node 3 is chosen, for its minimum cost, as the next node to update the current node; hence, its cost becomes permanent. To determine the cost to reach node 3, the cost of travel from 1-2 and 2-3 or 7+10 is compared to its current tentative cost (9) updated at the first iteration and since 9<17, the new cost is set to 9. Therefore, node 3 is added to the path and replaces node 2. Thus, so far the leg 1-3 of the piecewise linear shortest path is created.

In the third iteration, the adjacent nodes of node 3 are explored, nodes 4 and 6. The costs of travel to these nodes from node 3 are updated since at node 4: 9+11 < 22, and at node 6: 9+2 < 14. Node 6 is added to the path because of its minimum cost. The third iteration of the algorithm is shown in Figure 6.4.

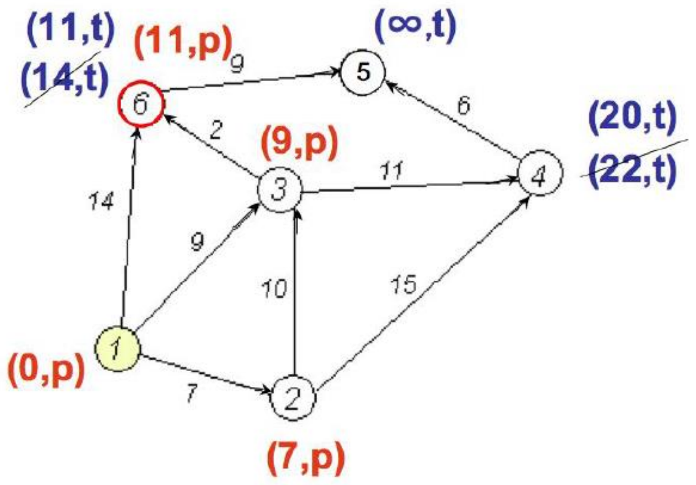

Figure 6.4: Dijkstra’s Third Iteration

At this iteration, node 6 is updated to be the current node only to be adjacent to node 5. Hence, at the fourth iteration, the cost of travel to node 5 from node 6 is updated due to 11+9 < ∞. Now that it reaches the goal node, node 5, the algorithm stops exploring the rest of the nodes. The shortest path is {1-3-6-5} with the length of 20 shown in Figure 6.5. Note that at the end all costs are permanent.

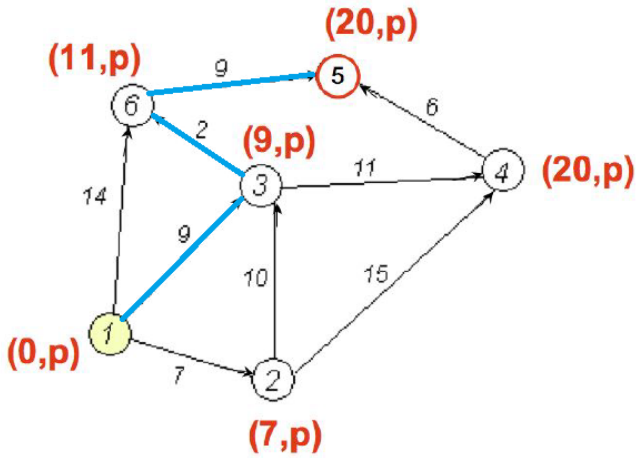

Figure 6.5: Dijkstra's Shortest Path Solution

In this research, the classical Dijkstra's shortest path algorithm is implemented on the graph constructed in the previous chapter. The classical Dijkstra has a time complexity of O(n^2) with n being the number of vertices in the graph. However, researchers recently have made attempts to improve the time complexity of the algorithm. For example, Fredman and Tarjan [17] introduce a new data structure to implement heaps or priority queues in Dijkstra that improves the time complexity of the algorithm up to O(nlogn+e), n being the number of vertices and e the number of edges. Heap, as defined by Fredman and Tarjan [17], is a data structure that contains a set of items each having a key (real value) and is subjected to operations such as insertion (inserts a new item in the heap), find (return an item of minimum key), and delete (deletes an item of minimum key from the heap). Heaps work the same way as tree data structures; there exist a root node and the children nodes branch out from it. Heaps are used in network optimization problems to speed up the search algorithm [17].

The major advantage of Dijkstra besides its simple implementation is that it is capable of finding the exact optimal solution to the shortest path problem once given a graph [46]. Figure 6.6 shows the output of a sample implementation of classical Dijkstra on a random graph. For this research, we use the Dijkstra's MATLAB library written by Joseph Kirk at MathWorks.

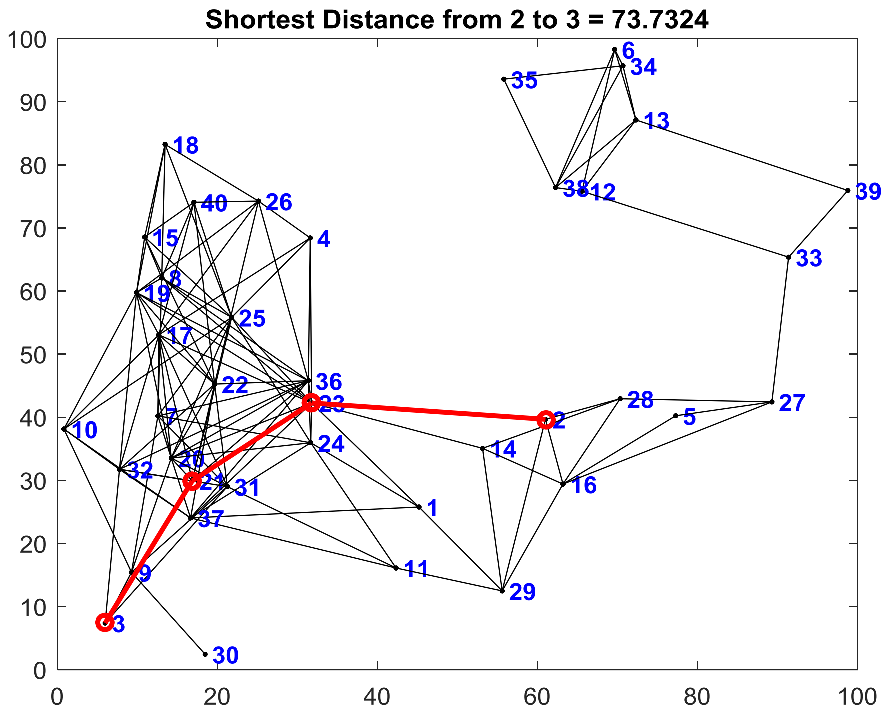

Figure 6.6: Shortest Path Found on a Graph Using Dijkstra

6.3 A* Search Algorithm

A* is another search algorithm that works fairly similar to Dijkstra's. Except, A* keeps track of both visited and unvisited nodes of the graph and unlike Dijkstra that only cares about the start point and calculates the distances from the start node, A* keeps an eye on the distance to the end node as well. In fact, a cost function is defined as Eq.(1) consisting of two terms; the first term is associated with the distance between the start and the current node, while the second term denotes a heuristic estimation of the cost or distance from the currently visited node to the end node. The objective is to minimize this cost function.

$$f(n) = g(n) + h(n) \tag{1}$$

Often, the determination of the heuristic cost is complicated and it may end up with a sub-optimal solution if the heuristic cost is not well defined. Due to the difficulties in defining the heuristic term of the A*, we choose Dijkstra's search algorithm to apply to the free space graph constructed previously. Dijkstra is both simpler in implementation and results in the exact optimal solution.

Figure 6.7 below is a schematic of the steps in our algorithm to find the shortest path using the convex hulls of the intersecting obstacles and Dijkstra's search algorithm followed by Figure 6.8 showing the shortest path on the free space graph of Figure 5.8.

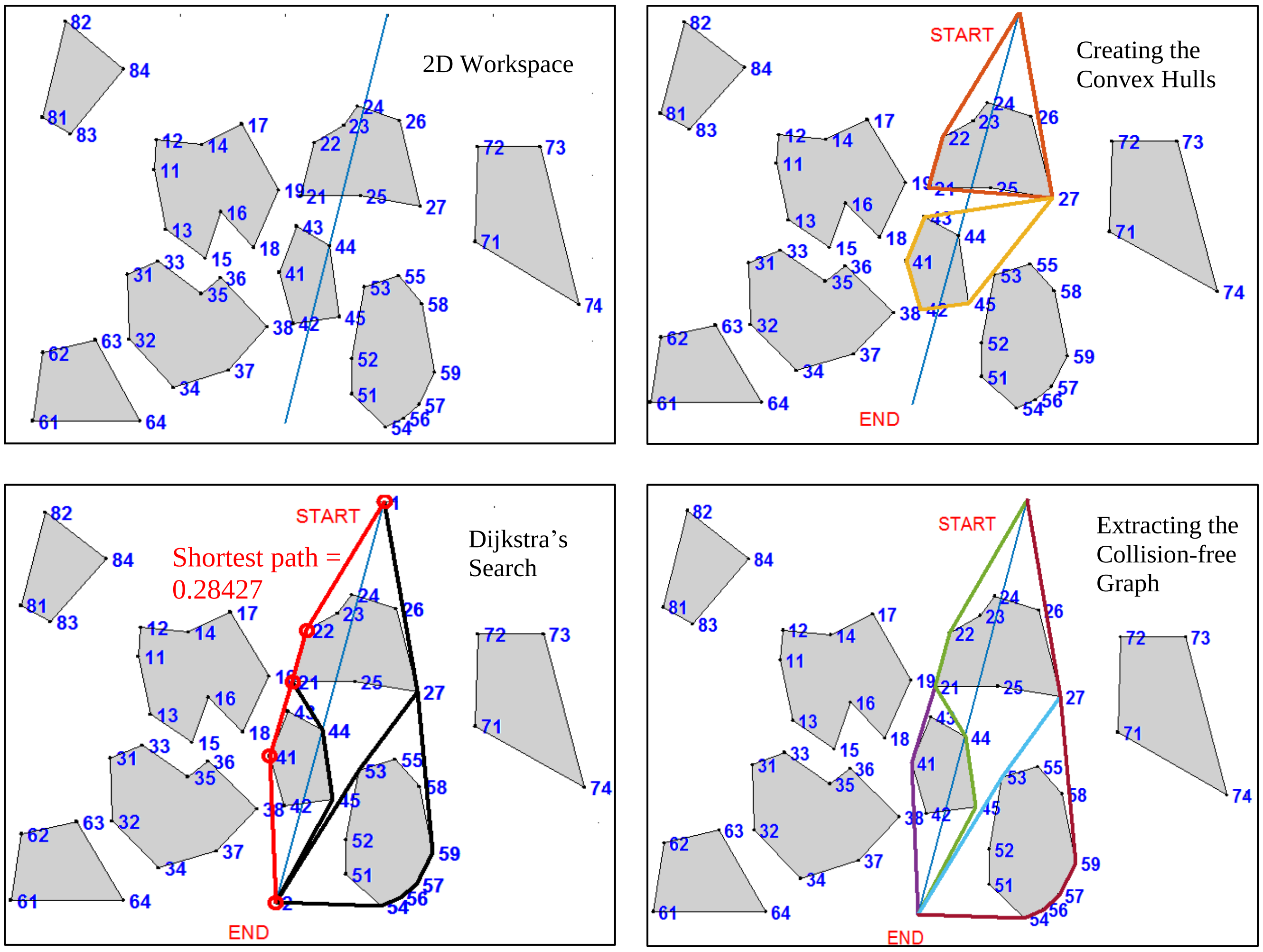
2D Workspace
Creating the Convex Hulls
START
END
Dijkstra's Search
Shortest path = 0.28427
Extracting the Collision-free Graph

Figure 6.7: Finding the Shortest Path

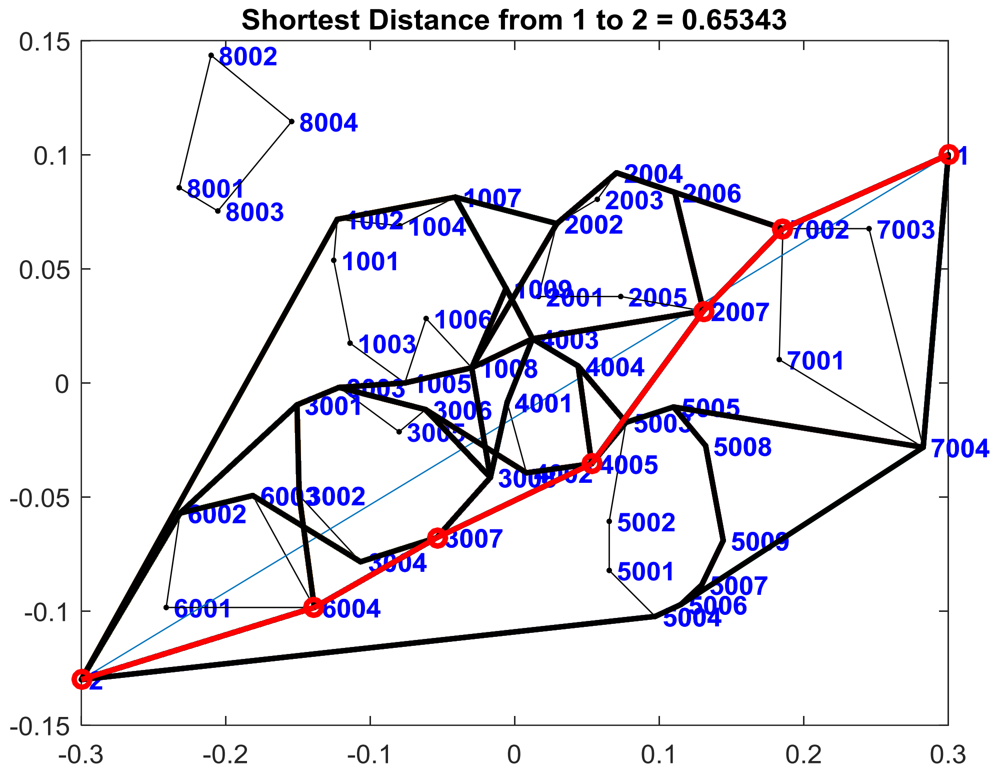

Figure 6.8: Shortest Path on the graph of Figure 5.8

Chapter Seven
VALIDATION AND TIME COMPLEXITY OF THE ALGORITHM

In this chapter, the efficiency of the developed algorithm to construct the free space graph in solving the planar shortest path problem in presence of free form polygonal obstacles is investigated and a comparison between this algorithm and previously developed techniques of solving the same problem is made. The comparison is based upon the preprocessing phase of the shortest path algorithm, which is the construction of the roadmap. Since the Voronoi diagram leads to a longer path, the comparison is limited to visibility-based algorithms that are more efficient in finding the shortest path. In Table 7.1 the complexity of the efficient visibility-based path planning algorithms is shown for n number of vertices and f number of obstacles. As can be seen from this table, the fastest algorithm to develop the visibility graph has a time complexity of $O(n^2)$.

Table 7.1: Time Complexity of the Roadmap Algorithms

Algorithm	**Assumptions**	**Time complexity**
Asano [15]**1985,**	Visibility	$O(n^2)$
Welzl [18]**,1985**	Visibility	$O(n^2)$
Lee, 1985	Visibility	$O(n^2 \log n)$
Rohnert[16]**,1986**	Partial visibility graph	$O(n+f^2 \log n)$
Sharir and Schorr[19]**,1986**	Visibility	$O(n^2 \log n)$
Wein[27]**, 2005**	Visibility-Voronoi	$O(n^2 \log n)$

In the following section, the complexity of the algorithm developed in this research to come up with the free space graph is derived. Since the construction of the free space graph is a preliminary basis for the path planning and provides the means for the optimization/search algorithm, we call this phase of the path planning the preprocessing phase. By this definition, the post-processing is allocated to the implementation of the shortest path algorithm to search for the optimal (often times shortest) route.

7.1 Time Complexity of the C-Hull Based Roadmap

To determine the time complexity of the graph generation technique, we need to first find the complexity of creating the convex hulls (C-hull). Because the complexity of determining the line segment intersection is polynomial, O(n) (because one line segment is checked with all n line segments of all obstacles, in the worst case), the dominant algorithm in determining the complexity of the preprocessing phase is the generation of the convex hulls. Hence, it suffices to determine the complexity of the C-hull generation. The C-hull formation algorithm used in this research is known as Graham's C-hull technique and has a time complexity of O(nlogn) for n vertices, as mentioned in the literature [14]. Hence, in the worst case, if all the f obstacles of the workspace are intersecting the route, the complexity of forming the C-hulls will be O(nlog(n/f)) with n being the total number of vertices. This complexity is the complexity of the graph construction in the worst case since graph construction is nothing but generating the C-hulls. As for f obstacles, 4f C-hulls are generated (as explained in chapter 5), assuming the maximum number of vertices in each obstacle is n_{max}, the algorithm computes the total 4f number of C-hulls in $O(4f(n_{max})\log(n_{max}))$ time in the worst case, using Graham's technique. Since the total number of vertices is designated by n, n is equal to f* n_{max} by this notation, hence yielding the time complexity of O(nlog(n/f)) for the preprocessing.

The post-processing phase of the algorithm is to find the shortest path on the graph constructed in the preprocessing. The Dijkstra algorithm used in this research is a classical Dijkstra that has a complexity of $O(n^2)$ although using the heap based Dijkstra or A* algorithm would result in a faster search-for-the-shortest-paths process.

A comparison of the preprocessing complexity of the algorithm developed in this research and the previous methods show an improvement in the time complexity of the preprocessing of the planar shortest path due to restricting the construction of the free space graph to a portion of the plane rather than generating the graph of the entire workspace. This results in a smaller graph, thus, simplifies and speeds up the search for the shortest path on this smaller graph.

7.2 Validation

This algorithm is tested on different planar workspaces with a variety of obstacles from one to 50 obstacles. The obstacles can have any arbitrary shapes thanks to the tessellated geometric representation of the workspace that is capable of handling any free form surfaces and solid models. The results are shown in Appendix A. The tests have been made based upon the number of obstacles, total number of vertices, average number of vertices per obstacle, number of reflex vertices, and the density of the workspace determined by the clearance between the obstacles. In all cases, the algorithm is able to find the shortest path, though an increase in the number of intersecting obstacles and/or the average vertices per obstacle, and density of the workspace obviously slows down the computation by adding complexities to the problem. The complexity of the algorithm does not depend on the number of obstacles in the workspace, in general, despite its dependence on the number of intersecting obstacles. Also, the number of reflex vertices does not affect the computational time since the C-hulls do not include any reflex vertex and in the construction of the C-hulls, all vertices are treated the same way no matter they are convex or reflex.

This algorithm is simple and robust since the C-hulls can be generated repeatedly and recursively for any types and sizes of the workspace.

Chapter Eight
CONCLUSIONS AND FUTURE WORK

In this research, the problem of constructing a collision free graph (free space graph) of a cluttered 2D environment and planning the shortest path between any arbitrary pairs of nodes in that graph has been studied and the results are presented. The developed algorithm could be applied to any planar environments with scattered free form (both convex and concave) obstacles. Since the obstacles are tessellated in a CAD software, they can have any shapes and their shapes can be simply processed through the program.

The preliminaries of the algorithm consist of reading the tessellated geometries in a VRML format and storing the data of the coordinates of the vertices and connectivities (edges that connect two vertices of an obstacle). The preprocessing of the algorithm is about constructing the free space graph based upon the result of the line segment intersection check and formation of the C-hulls of the intersecting obstacles (detected using the bi-level collision detector). The preprocessing algorithm is proved to have a time complexity of order $O(n\log(n/f))$ with n being the total number of vertices in the workspace and f the number of obstacles directly in the path. Instead of studying the entire workspace, we restrict the graph construction and search to a portion of it including the reference line and the interfering obstacles. The post-processing of the algorithm is allocated to finding the shortest path on the graph between the two specified nodes using the classical Dijkstra's shortest path algorithm in $O(n^2)$ time. Further improvements can be made to the algorithm through the implementation of a more efficient search algorithm such as heap-based

Dijkstra or A*. The classical Dijkstra is used in this research for its simplicity of implementation, which is slightly compromised by its speed of computation.

This algorithm is capable of finding the shortest path between two nodes on any planar workspace with any number of free form obstacles and vertices. We claim that the developed algorithm could be applied to 3D spatial workspaces as well though with a greater time complexity. This will be further investigated in a separate research work.

Despite the improvements in the efficiency of the developed algorithm by focusing on a portion of the workspace limited by the reference line and the intersecting obstacles, it highly depends on the start and end points of the path. Hence, changing the start and end points of the path results in a different free space graph while the visibility graph constructs a single constant roadmap of the entire workspace. Having the roadmap of the entire workspace has an advantage of being able to route the shortest path between any two nodes of the graph. However, in the C-hull based path planning, if the shortest path between different pairs of nodes is desired, the corresponding free space graph must be calculated one at a time and the resultant graph would be the union of these subgraphs. For example, consider the planar workspace shown in Figure 8.1. If the shortest path between both pairs of nodes (61, 73) and (82, 53) are required, the algorithm first constructs the free space graph between the two nodes 61 and 73 (Shown in Figure 8.2) and then 82 and 53 (Figure 8.3). Then, the edges of the free space graph for the pair of (82, 53) not included in the graph of (61, 73) are added to the latter graph and the shortest path between the two nodes can be found using single source Dijkstra's algorithm. The resultant union of the two graphs is shown in Figure 8.4.

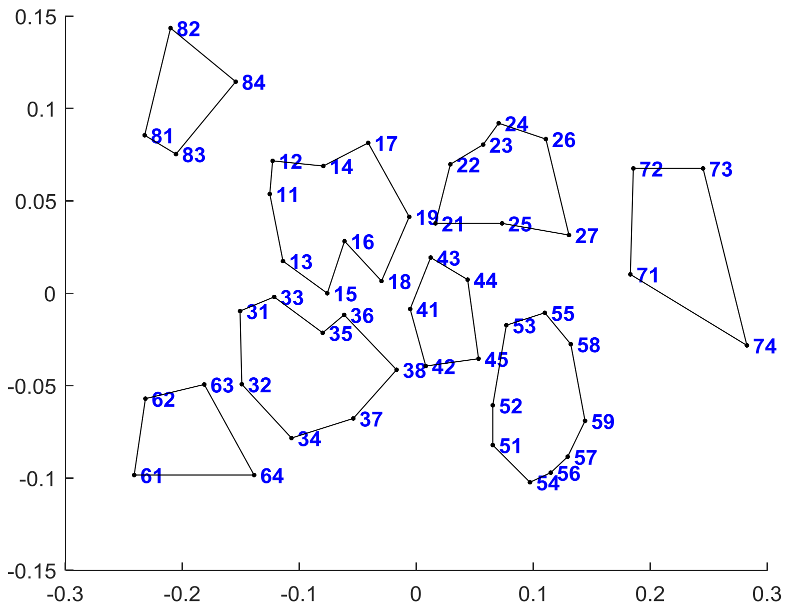

Figure 8.1: Sample Planar Workspace

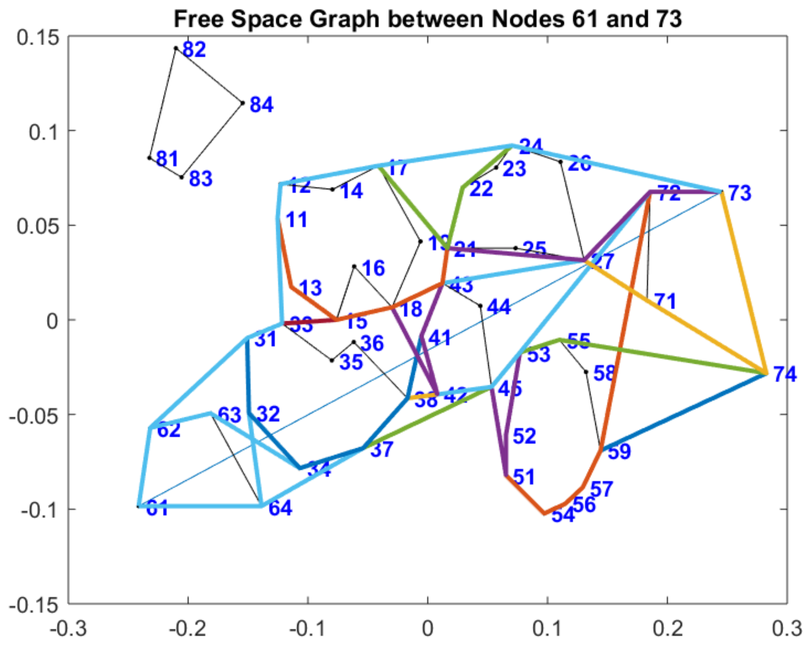

Figure 8.2: Free Space Graph for Pair (61, 73)

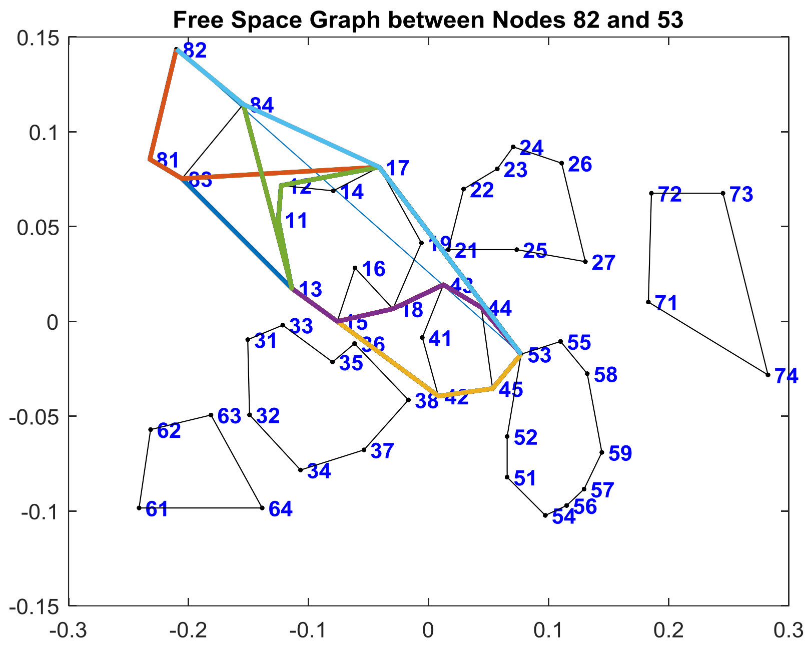

Figure 8.3: Free Space Graph for Pair (82, 53)

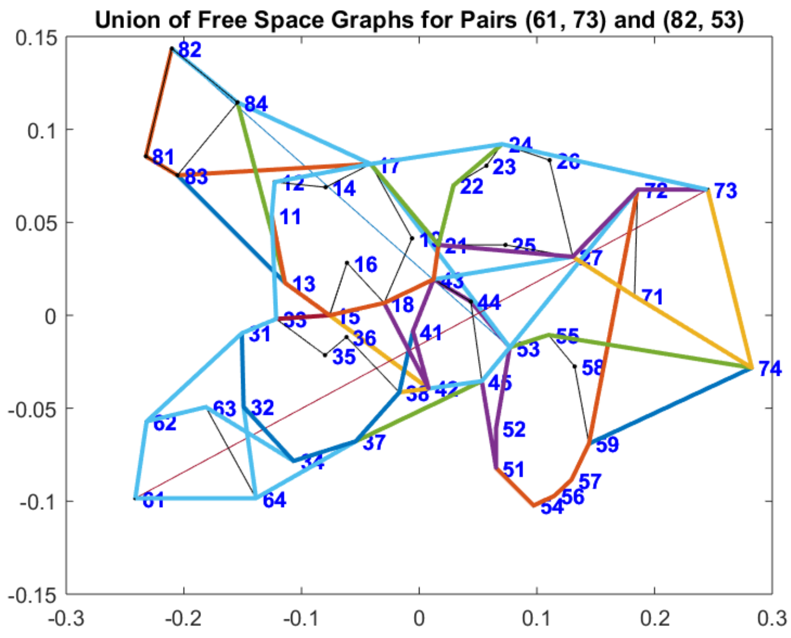

Figure 8.4: Superposition of Tow Free Space Graphs for Pairs (61, 73) and (82, 53)

It should be pointed out that since Dijkstra is capable of finding the shortest path from a single source to all other nodes of the graph, the free space graph of the entire workspace must be constructed with the aforementioned one-at-a-time graph construction technique. Otherwise, Dijkstra will not be able to find the shortest path to all the other nodes since there may not exist any link to some nodes using the C-hull based graph construction approach. Even if the free space of the entire workspace is desired, the algorithm is still more efficient than visibility for its time complexity is less than the fastest visibility. The reason why the time complexity of the C-hull based graph construction is less is because some of the edges that are constructed using the visibility graph are eliminated in this approach and only the edges included in the C-hulls will be added to the set of the edges of the free space graph. A byproduct of using C-hulls in the construction of the free space graph is to end up with a fewer number of turns in the piecewise linear path based on the triangle inequality.

8.1 Future Work

Further research can be conducted to investigate the sensitivity of the shortest path found using the proposed method with respect to small changes in the configuration of the workspace. For example, one could determine how the length of the path would change by moving one of the intersecting obstacles by a certain amount in a specified direction or changing the size of the aforementioned obstacle.

Also, one could take the geometry of the path into account. For instance, if the router is a robot with a given geometry and topology or a cable, hose, or pipe with a given diameter rather than a point, the path may differ since the clearance between some of the obstacles may not allow the router to pass through some of the narrow spaces between the obstacles. A solution to routing a polygonal agent in a cluttered environment may be to offset the obstacles using the Minkowski sum of the agent's geometry and the obstacles and route a single point in the offset environment instead.

There are also some other special cases that need to be considered while a path is being planned. For example, suppose the closest object to the start point of the path is as shown in Figure 8.5. As can be seen in this figure, the second closest intersecting object is larger than the first one. Using the algorithm presented in this study, the resulting free space graph is included in the same figure.

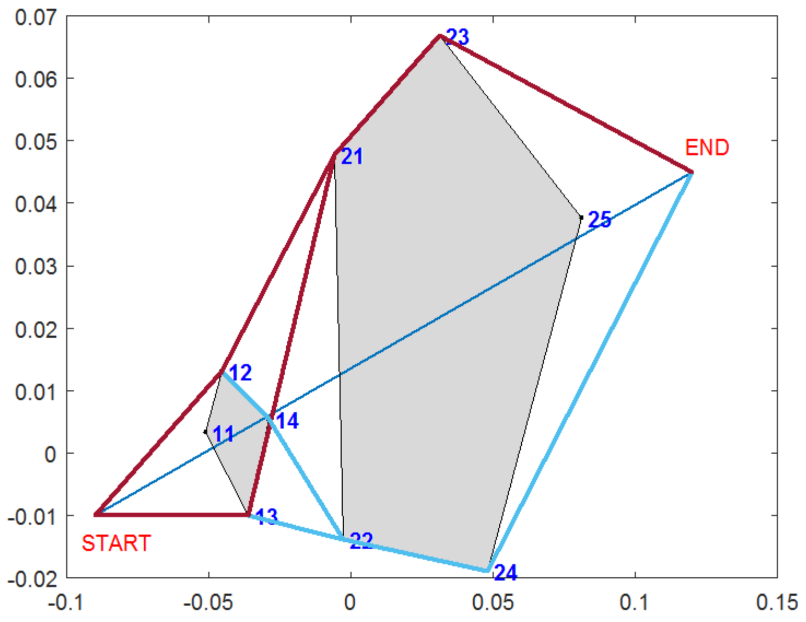

Figure 8.5: Special case with larger object after the closest intersecting object

Although this graph can be used to find the shortest path using Dijkstra's algorithm, it does not indeed include the edges that result in a shorter path. In other words, we suggest that one should consider generating the convex hull of the start point and the larger object rather than the smaller though closer object. This is because the convex hull with the larger object also includes the entire (or parts of the) smaller intersecting object; hence, overcoming the problem of interfering with this object. The free space graph using the convex hull of the larger intersecting object is created for this example and shown in Figure 8.6. In addition, based on the triangle inequality, this convex hull will result in shorter paths from the start to the end point. For example, in Figure 8.6 an edge from the start point of the path to node 21 is created which is shorter than the sum of Start-12 and 12-21 edges based on the triangle inequality.

After the free space graph is generated the Dijkstra's algorithm is implemented to find the shortest path on it from the start node to the end node. The results of Dijkstra on both graphs is compared in Figure 8.7. As can be seen from this figure, the graph generated using the convex hull of the larger object yields a shorter path.

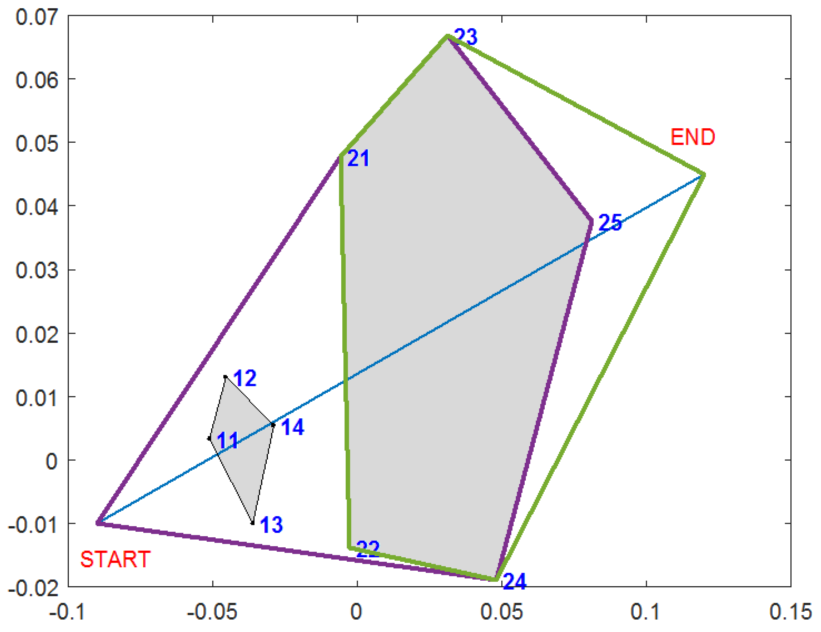

Figure 8.6: Free space graph using the convex hull of the larger intersecting object

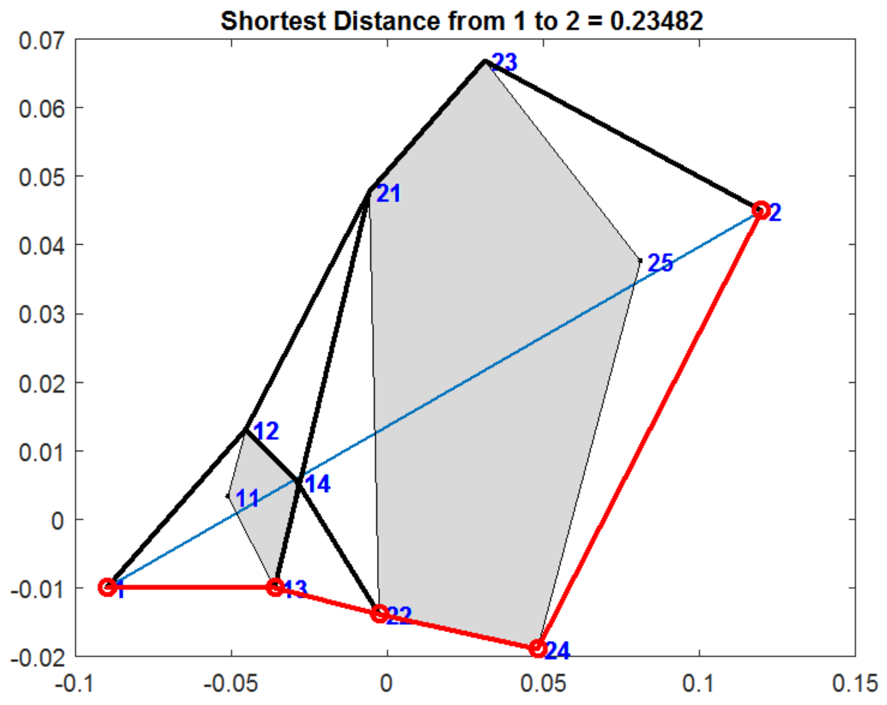

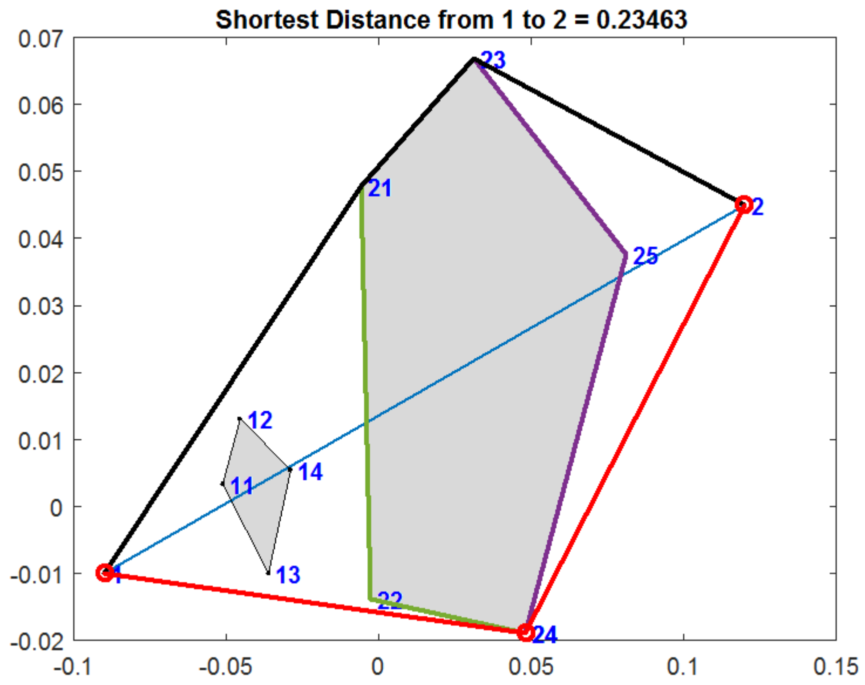

Figure 8.7: Comparison of the results of the shortest path for the two free space graphs

Based on this brief analysis, we propose that in future the size of the intersecting objects with respect to each other and their distances to the start point of the path be considered in generating the convex hulls.

In addition, other criteria could be added to the objective function of the optimization problem including minimizing the number of links or maximizing the clearance from the obstacles.

After solving the simple planar path planning problem, one will be able to plan multi-source multi-destination paths. This research also establishes the basis for the path-planning problem in a 3D environment including routing for more real-life path planning applications such as cable harnesses in electromechanical systems, autonomous vehicles' routing, pipe routing in chemical process plants, etc.

APPENDIX A

In this appendix, the results of different test cases using the C-hull based path planning method are presented. The tests are done on planar workspaces. At each test, the number of objects is increased although it does not affect the path length or computation time. However, increasing the number of intersecting obstacles does affect both the optimal solution and computation time.

First trial: effects of increasing both the number of objects and the number of intersecting obstacles on the path length and the computation time.

1. # objects = 1

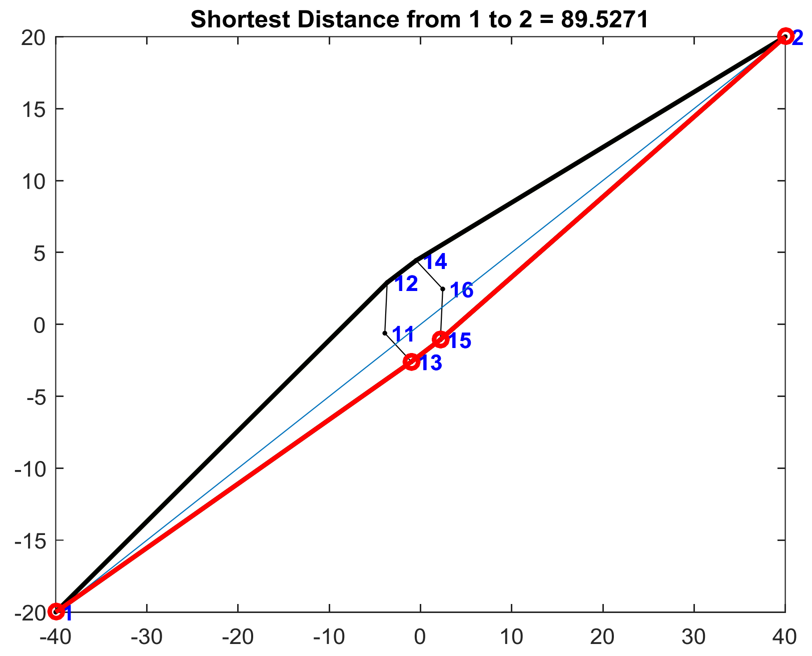

2. # objects = 4

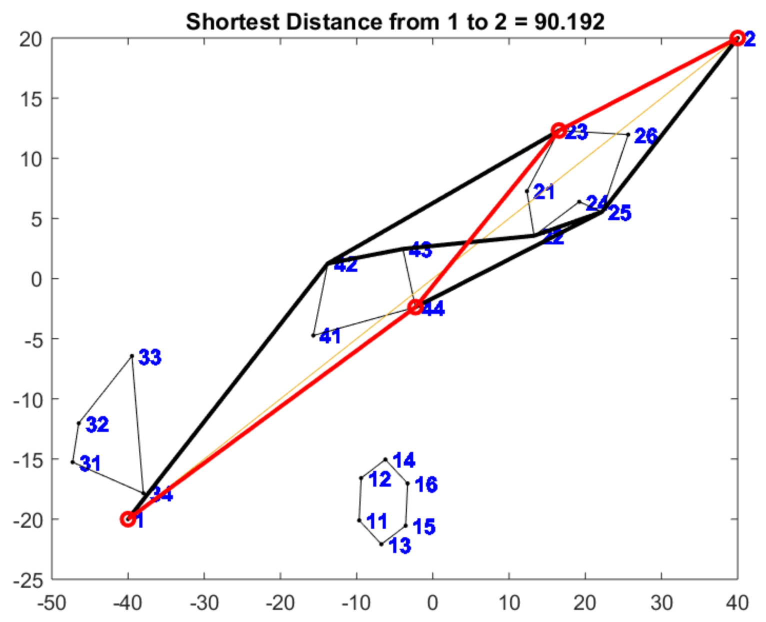

3. # objects = 8

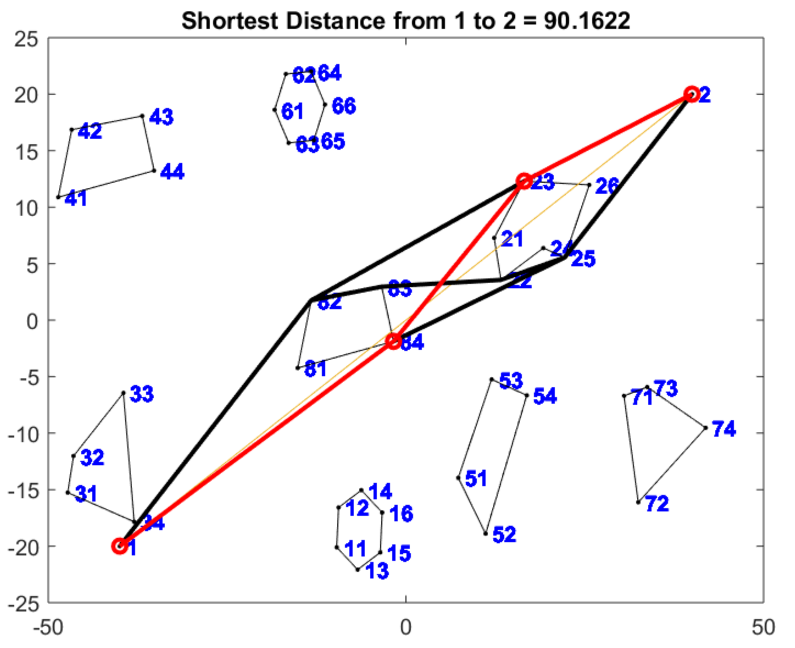

4. # objects =10

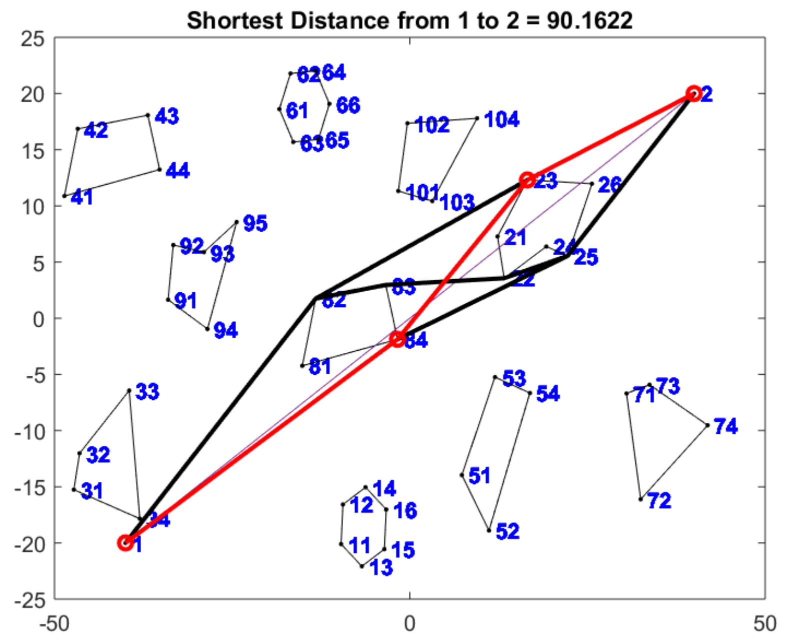

5. # objects =12

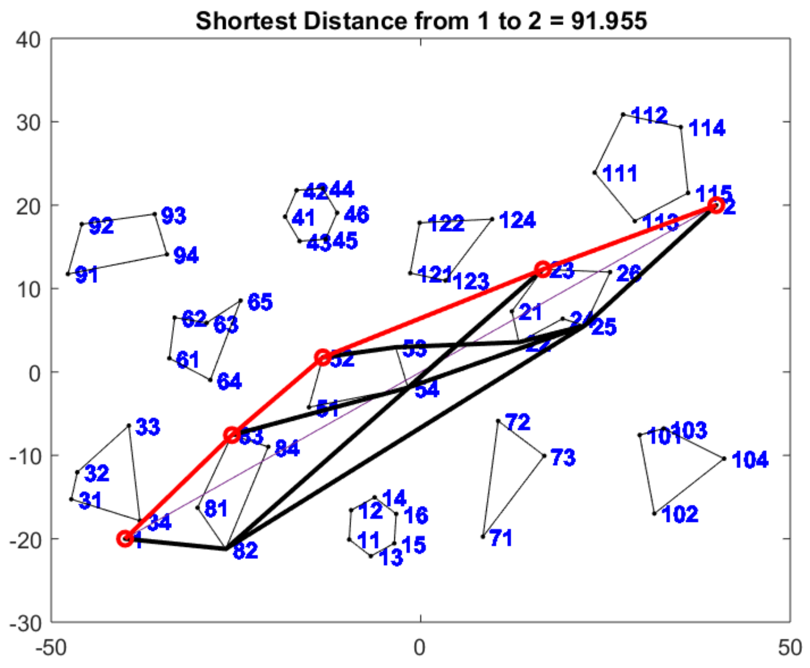

6. # objects =15

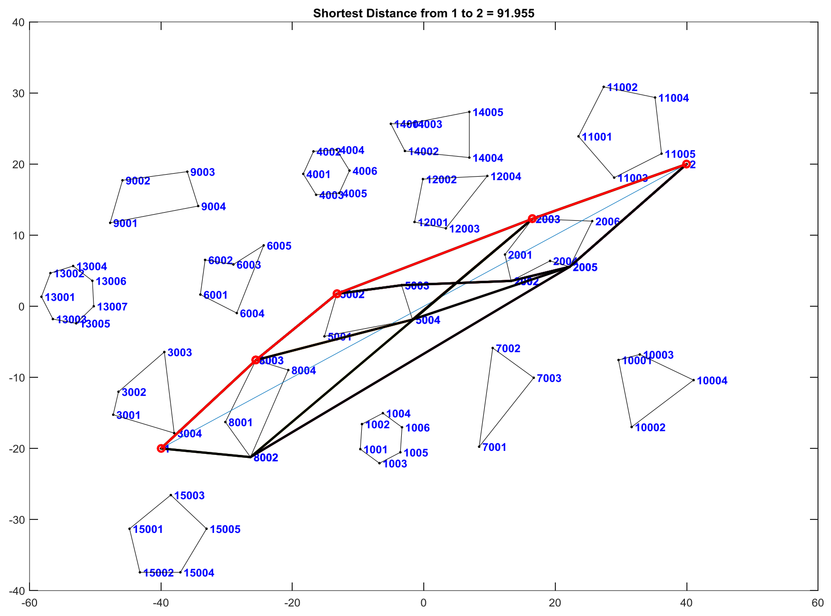

7. # objects =18

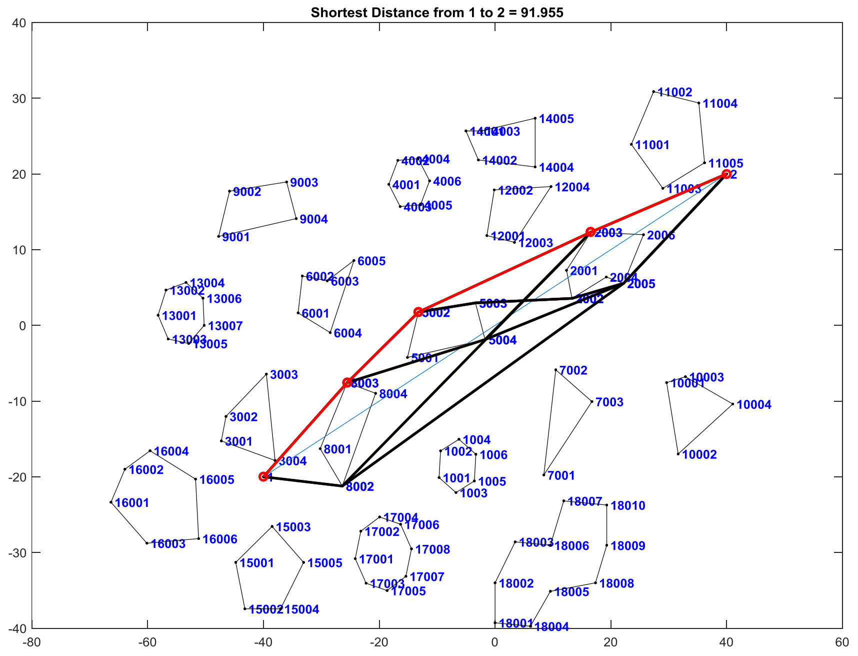

8. # objects =20

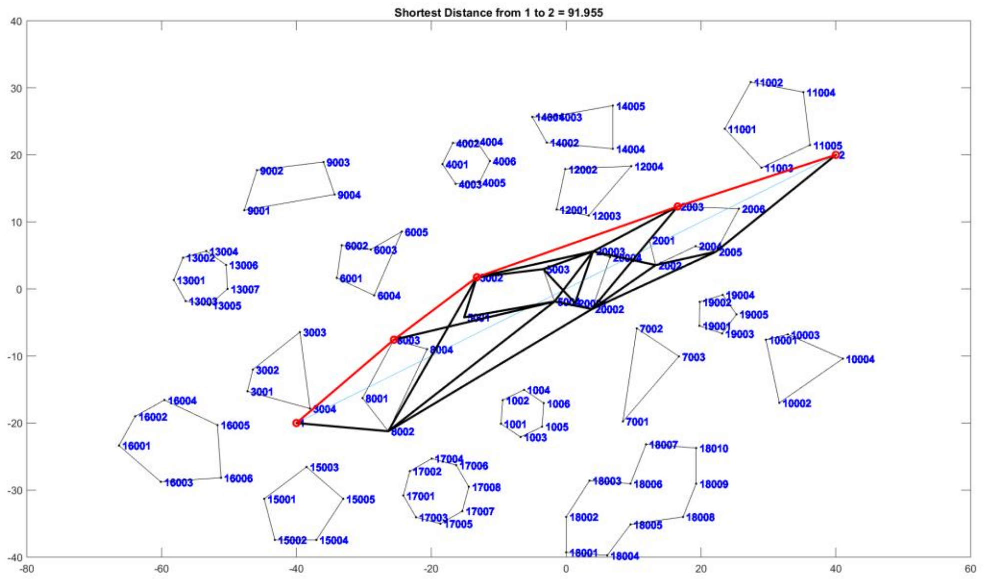

9. # objects =25

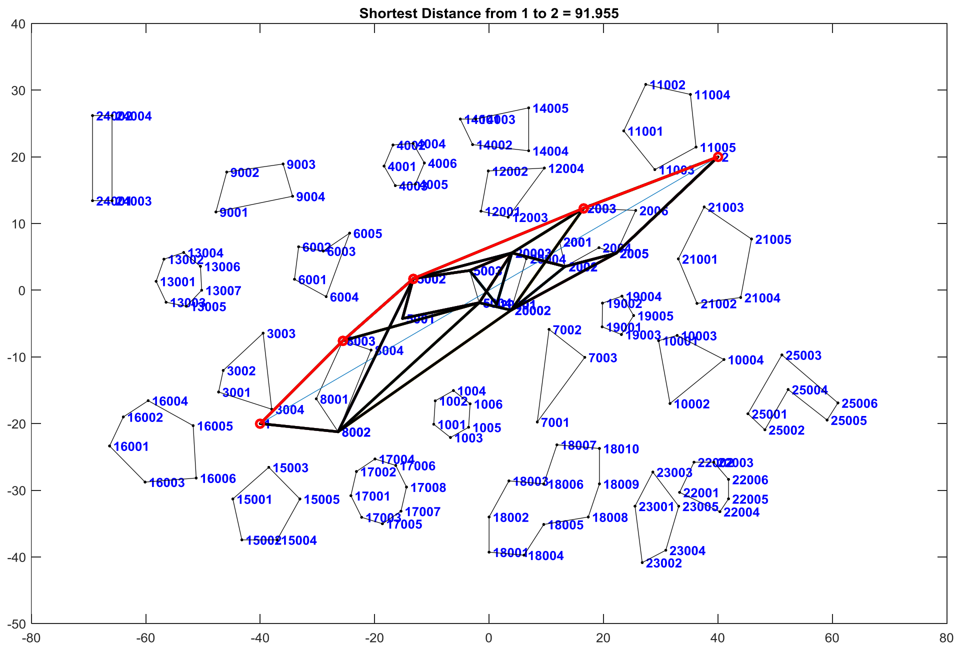

10. # objects =30

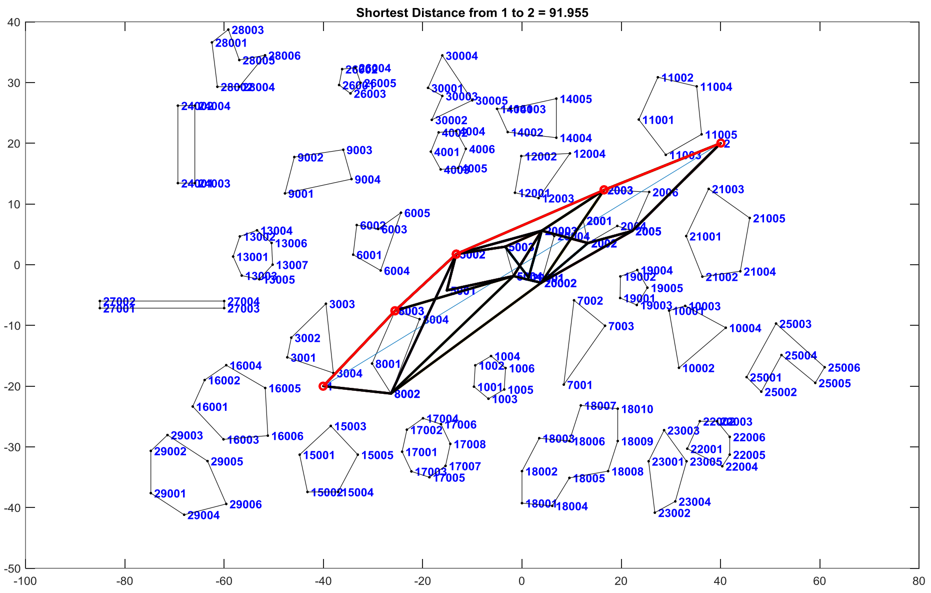

11. # objects =34

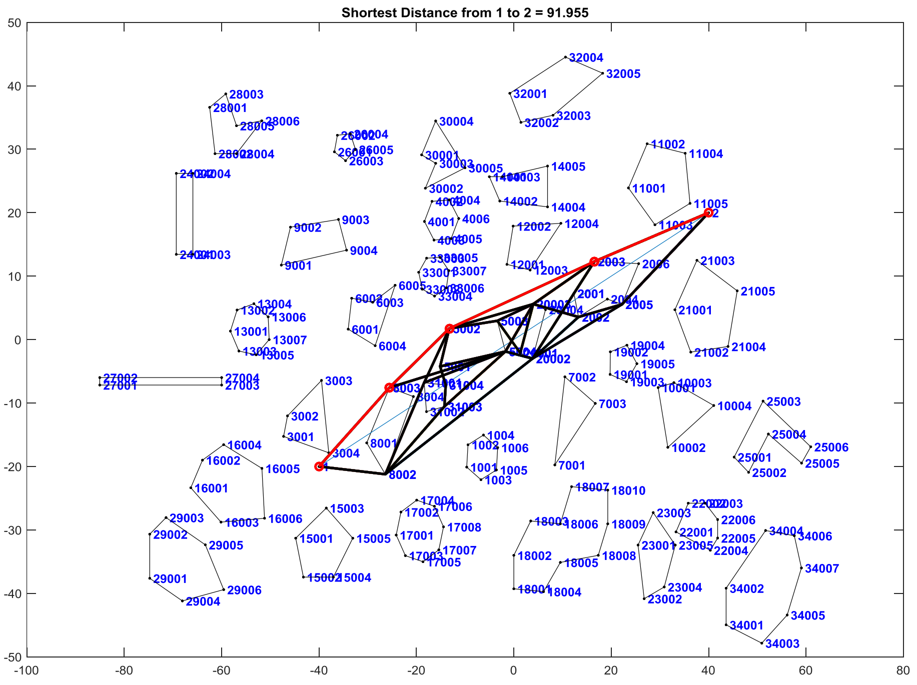

12. # objects =37

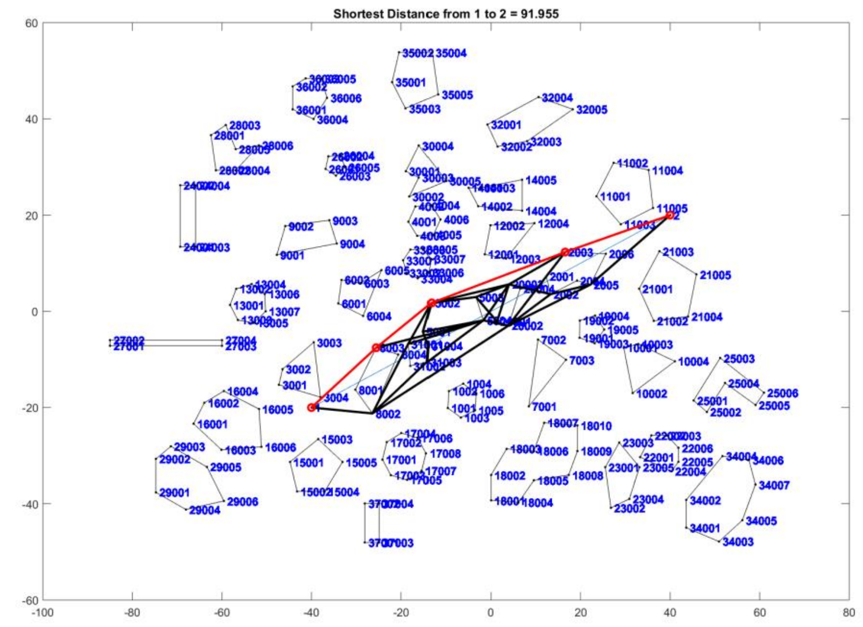

13. # objects =40

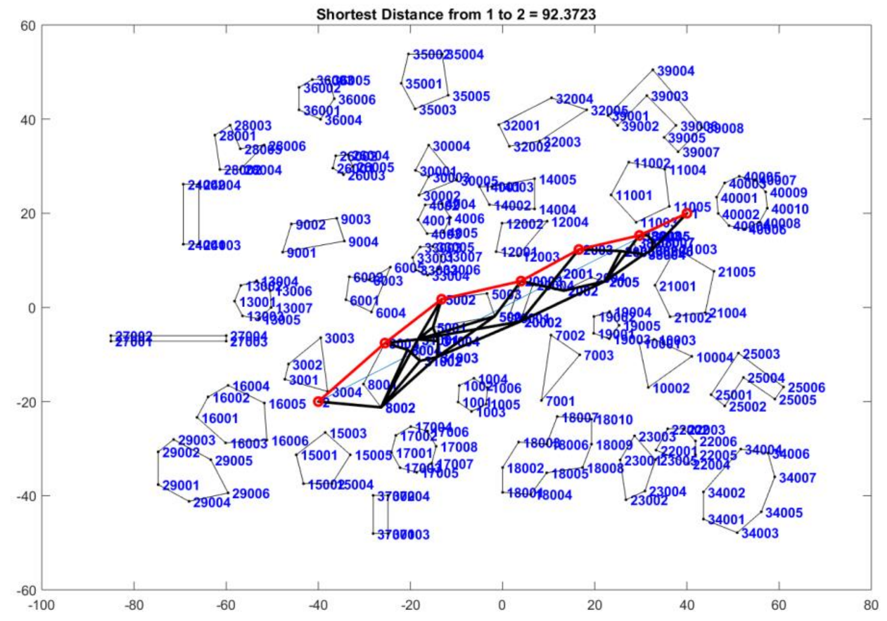

14. # objects =43

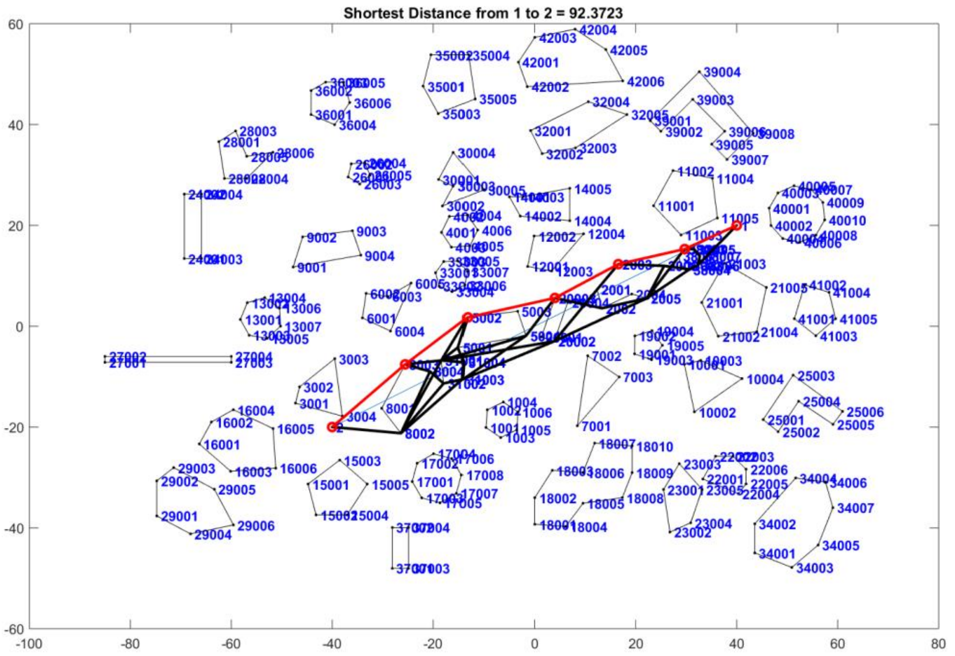

15. # objects =46

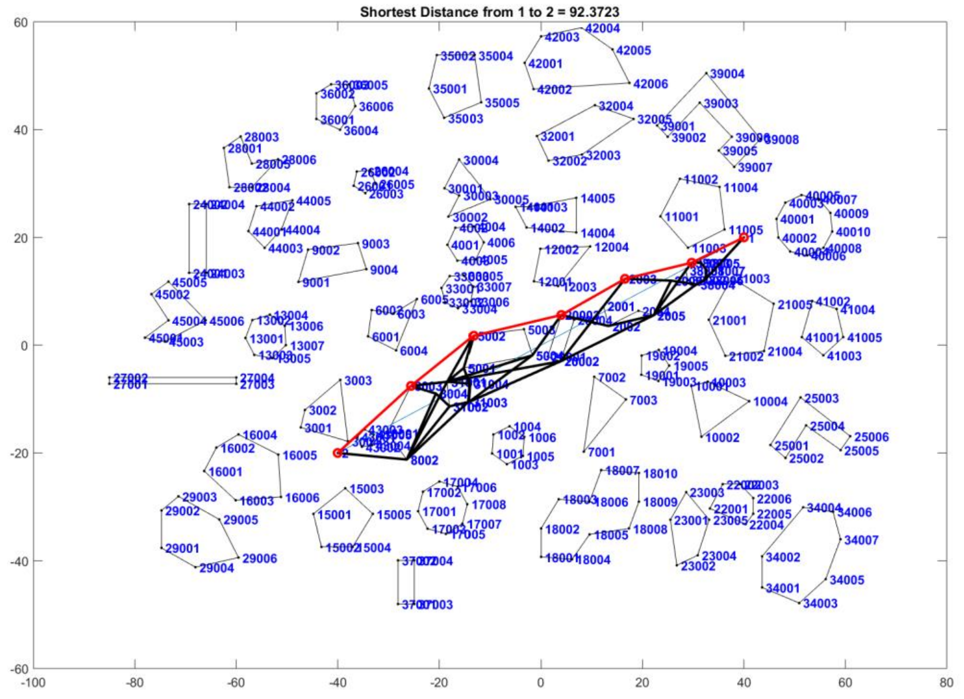

16. # objects =50

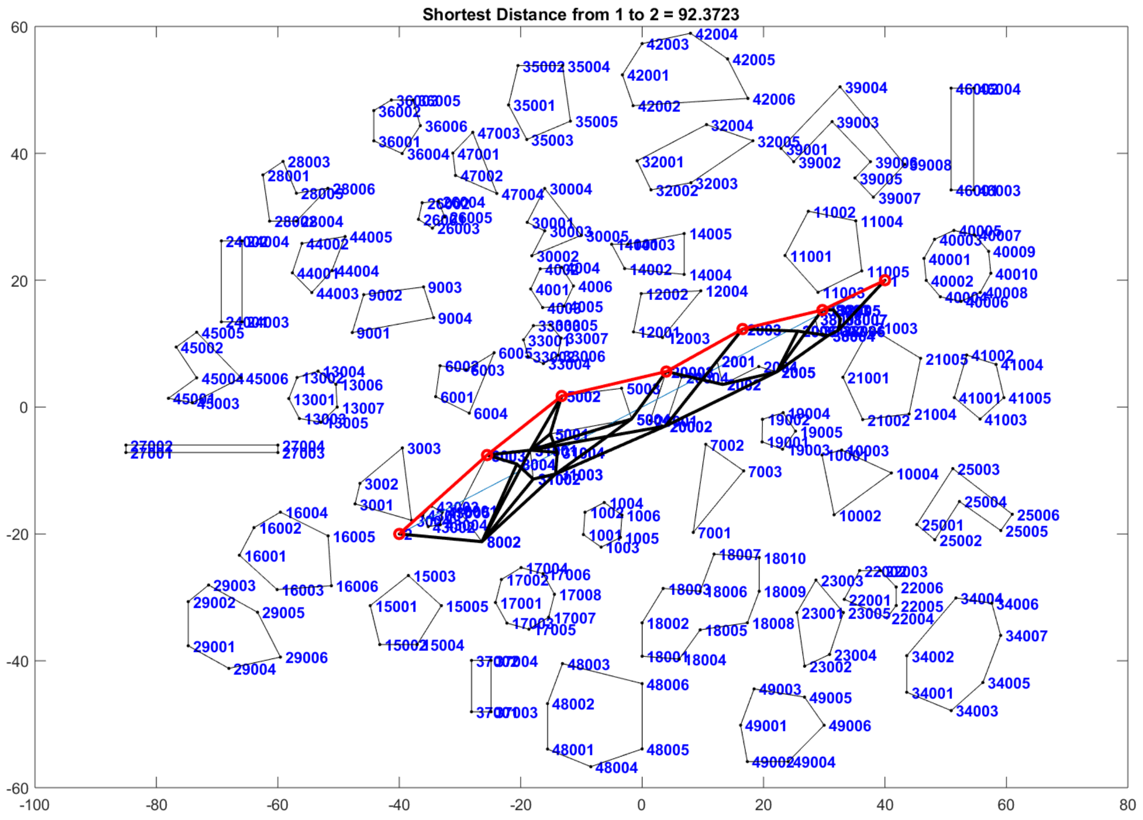

Table below summarizes the properties seen from the tests done on different planar workspaces.

Table 8.1 Test Results of the Effects of the Number of Objects and Intersections

trial#	# objects	time(sec)	shortest distance	# colliding objects
1	1	0.4874	89.5271	1
2	4	0.6548	90.192	2
3	8	0.7377	90.1622	2
4	10	0.7814	90.1622	2
5	12	0.9023	91.955	3
6	15	0.9681	91.955	3
7	18	1.0558	91.955	3
8	20	1.3201	91.955	4

9	25	1.4084	91.955	4
10	30	1.5294	91.955	4
11	34	1.7503	91.955	5
12	37	1.8128	91.955	5
13	40	2.2596	91.955	6
14	43	2.4058	91.955	6
15	46	3.4596	92.2419	7
16	50	3.604	92.2419	7

As expected, by increasing the number of obstacles, the computation time increases though increasing the number of colliding objects has a more significant influence on the time complexity than the number of objects alone. Since the configuration of the workspace roughly remains the same, the length of the shortest path barely changes by increasing the number of objects and collisions.

Second trial: effects of forbidden zones.

There are instances in which some forbidden zones exist and the path cannot go through those areas. Since these zones are typically larger than usual obstacles, they significantly affect the length of the path (with respect to the size of the workspace), for the path needs to go around such zones. An example of this situation is shown in the figure below. Forbidden zone is the shaded area shown in grey in the figure.

Forbidden zone

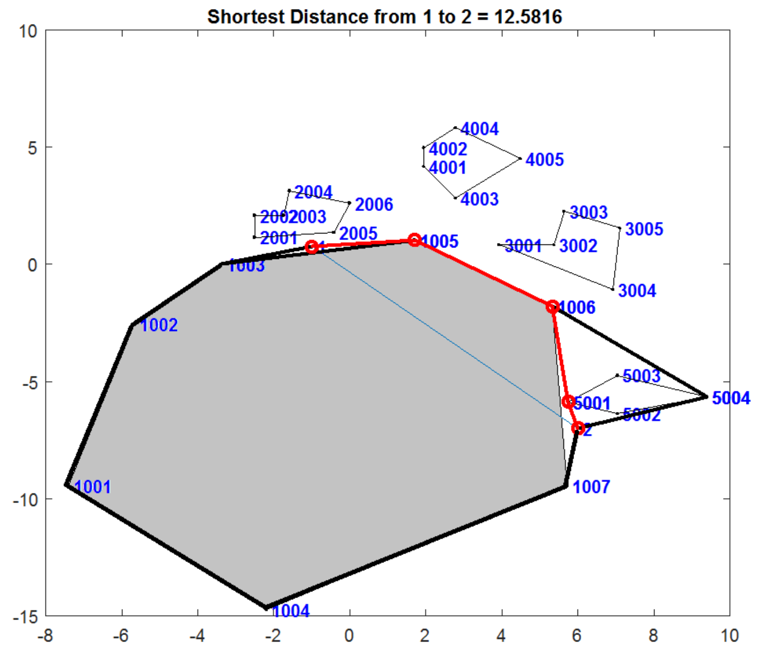

Without the forbidden zone

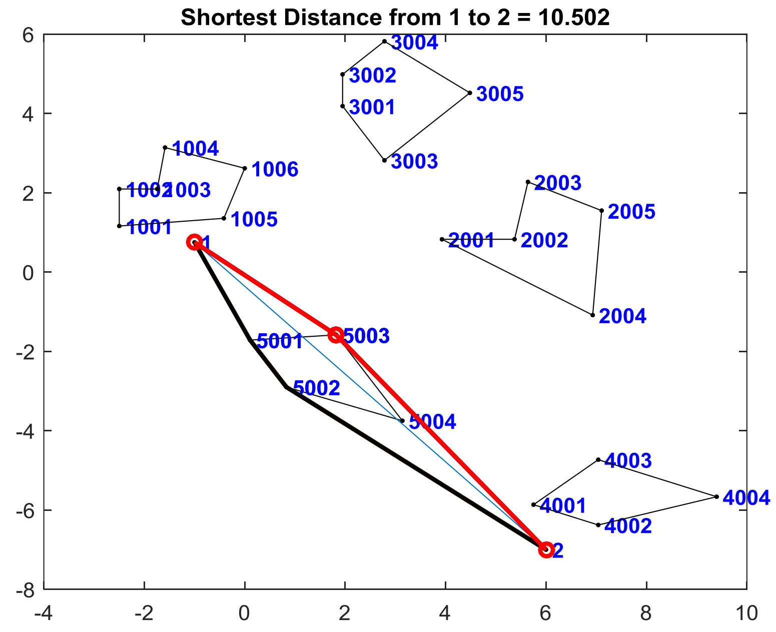

Third trial: effects of the density of the workspace.

Density of a workspace is a metric of the relative clearance between the objects of the workspace. In other words, in a dense workspace, the objects are located closer to each other than in a less dense workspace. in the following examples, a workspace containing 15 objects is tested under different densities. The first test has the least and the last has the most density. It can be observed that increasing the density, adds more edges and vertices to the graph of the free space though the length of the path may remain the same by not changing the start and end points. However, it is worth noting that by increasing the density of the workspace, more intersecting obstacles are introduced, hence, the path length may change depending on the intersecting obstacles. This also can be seen from the following tests.

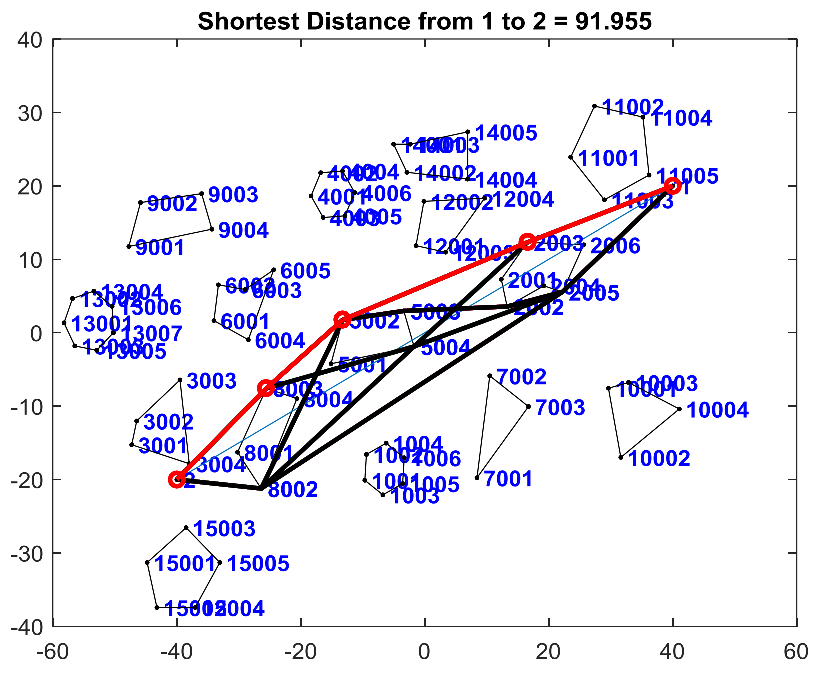

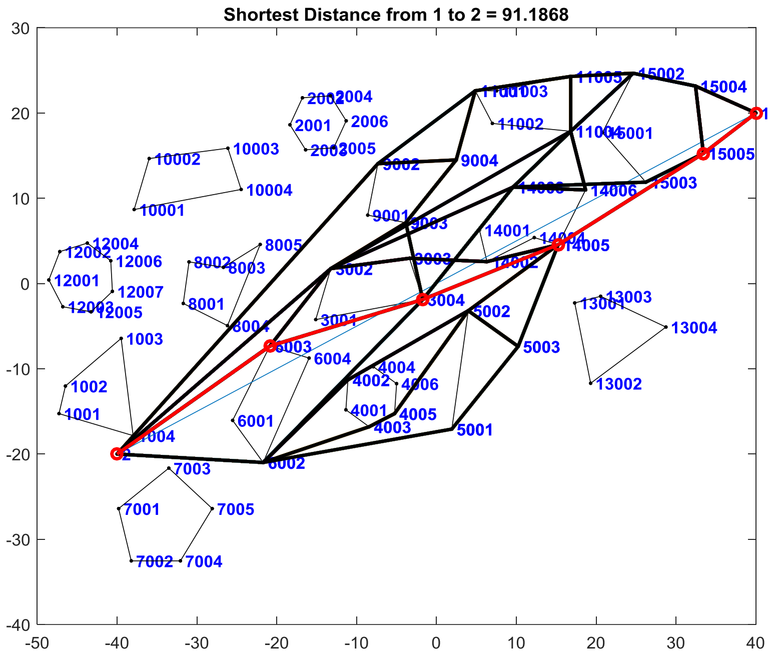
Shortest Distance from 1 to 2 = 91.1868

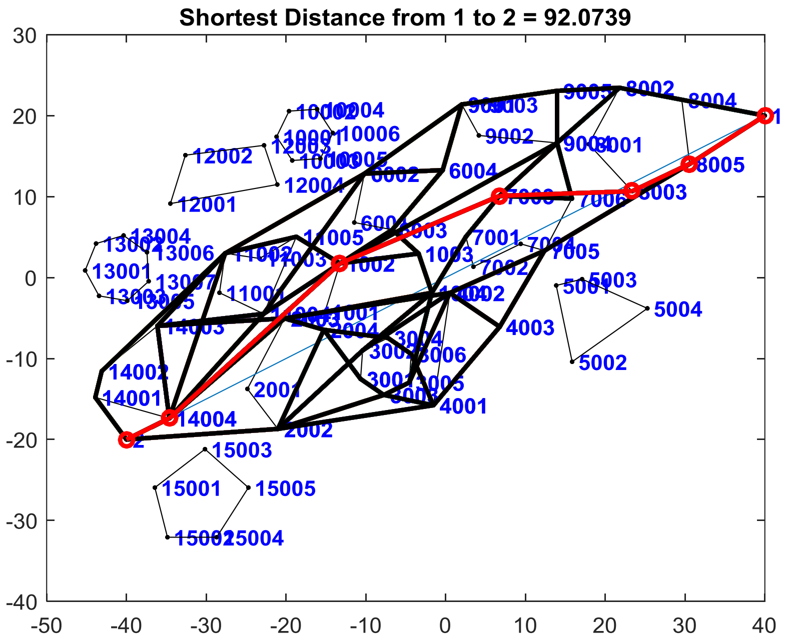
Shortest Distance from 1 to 2 = 92.0739

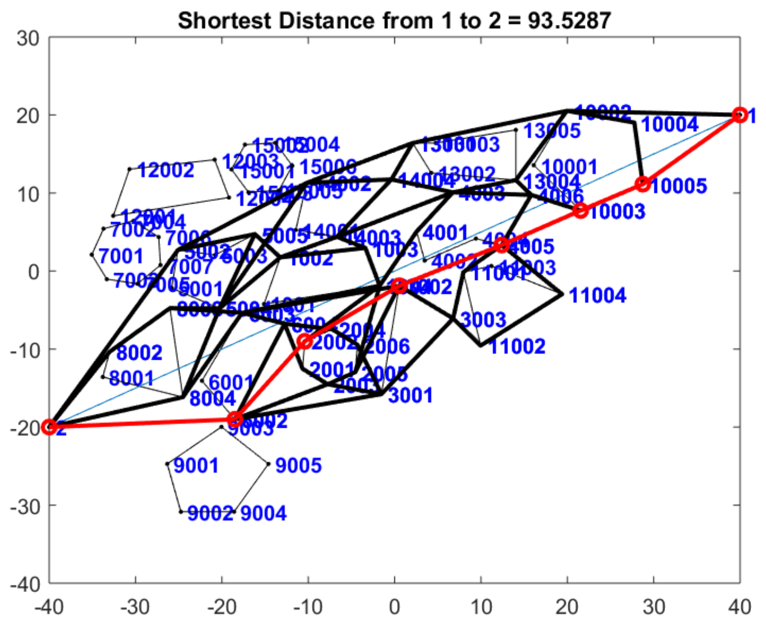

Table 8.2 Effects of the Workspace Density

trial#	Density level	time(sec)	shortest distance	# colliding objects
1	0	0.9159	91.955	3
2	1	1.7386	91.1868	8
3	2	2.0484	92.0739	10
4	3	4.6162	93.5287	11

Fourth trial: effects of increasing the average number of vertices per object.

In this trial several test are done to determine the effects of increasing the average number of vertices per object on the path length and the computation time of the algorithm. The tests are taken on a sample workspace containing 15 objects with the 0-level density. The results are summarized in the table below.

Table 8.3 Effects of Increasing the Number of Vertices per Object

trial#	n_{ave}	time(sec)	shortest distance	# colliding objects
1	5	0.9159	91.955	3
2	8	1.5085	91.3336	3
3	12	1.7811	91.2497	4
4	15	3.0323	91.9117	5

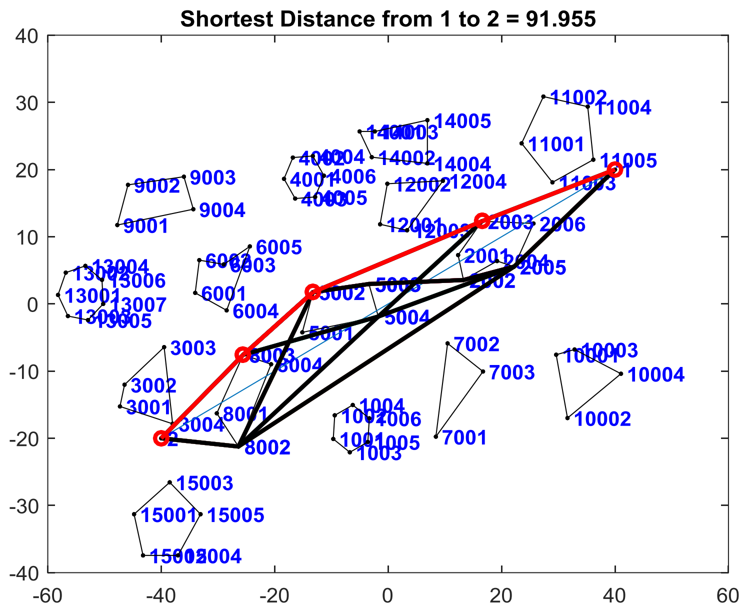

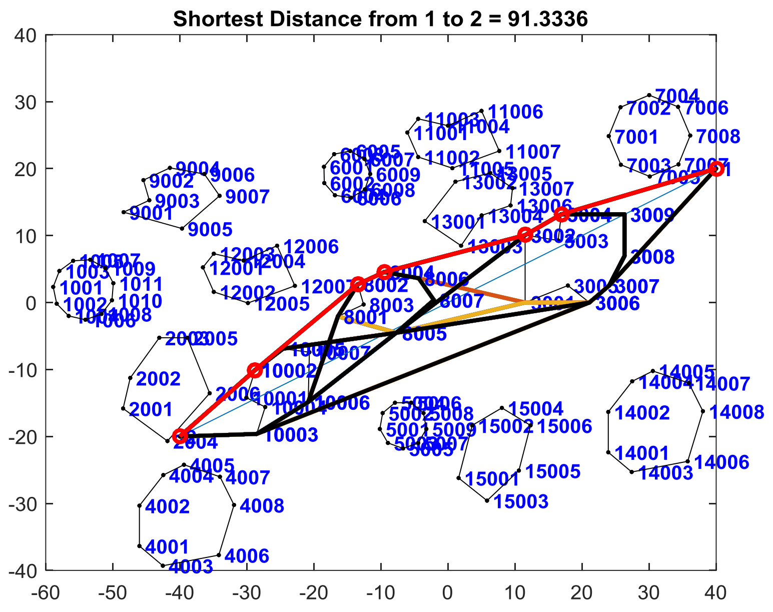

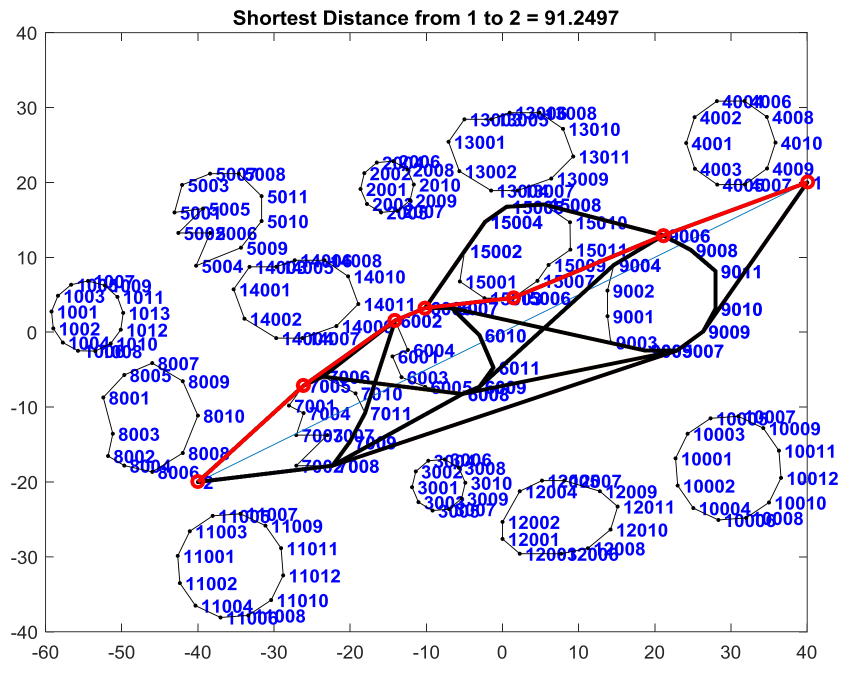

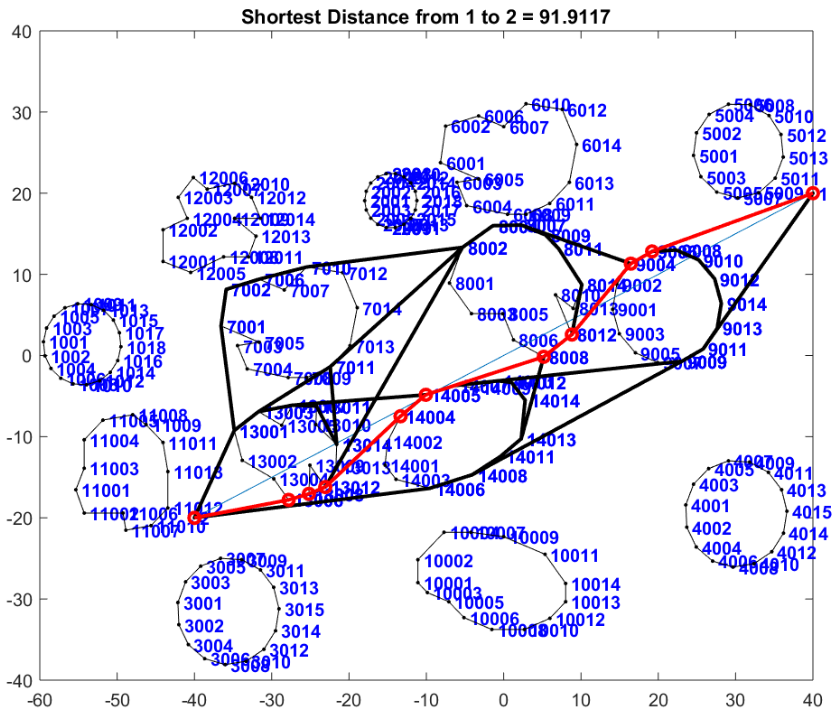
Shortest Distance from 1 to 2 = 91.9117

APPENDIX B

In this appendix, the MATLAB codes for analyzing and computing different parts of the method are presented. The authors of the read_vrml, line-segment intersection and Dijkstra's libraries are included in the respective codes.

1. Reading the VRML data

```
%/**********************************************************
************************
% FUNCTION NAME : read_vrml
% AUTHOR        : G. Akroyd
% PURPOSE  : reads a VRML or Inventor file and stores data
points and connectivity
%             in arrays ready for drawing wireframe images.
%
% VARIABLES/PARAMETERS:
%  i/p  filename       name of vrml file
%  o/p  nel            number of geometry parts (elements)
in file
%  o/p  w3d            geometry structure ;-
%                       w3d.pts   array of x y z values for
each element
%                       w3d.knx   array of connection nodes
for each element
%                       w3d.color color of each element
%                       w3d.polynum number of polygons for
each element
%                       w3d.trans  transparency of each
element
%
% Version / Date : 3.0   / 23-9-02
%                  removed triang optn & replaced face
array Nan padding
%                   with 1st value padding to correct
opengl display prob.
% Version / Date : 2.0   / 17-7-00
%                  changed output to a structure rather
than separate arrays
%                   to use less memory.
%                  1.0   / 21-6-99
%                  original version
```

```
%***********************************************************
***********************/

function [nel,w3d,infoline] = read_vrml(filename)

keynames=char('Coordinate3','point','coordIndex');

  fp = fopen(filename,'r');
  if fp == -1
      fclose all;
      str = sprintf('Cannot open file %s \n',filename);
      errordlg(str);
      error(str);
  end

%* initialise arrays & counters */
  fv = zeros(1,3);
  foundkey=zeros(1,3); %* flags to determine if keywords
found */
  endpts=0; %/* flag set when end of co-ord pts reached for
an element */
  npt=0; %/* counter for num pts or conections */
  npol=1; % counter for number of polygons in an element
  nel=1; %/* counter for num of elements */
  color(1,1:3) = [0.5 0.55 0.5]; % default color
  maxnp = 0;
  tempstr = ' ';
  lastel = 1;
  lnum = 1;
  w3d(1).name = 'patch1';
  infoline = '#';
  trnsp(1) = 1; % transparency array - one val per element

  %/* start of main loop for reading file line by line */
  while ( tempstr ~= -1)
     tempstr = fgets(fp); % -1 if eof
     if tempstr(1) == '#' & lnum == 2,
        infoline = tempstr;
     end
     lnum = lnum +1; % line counter
     if ~isempty(findstr(tempstr,'DEF')) & ~endpts,
        w3d(nel).name = sscanf(tempstr,'%*s %s %*s %*s');
     end
     if ~isempty(findstr(tempstr,'rgb')) |
~isempty(findstr(tempstr,'diffuseColor')) % get color data
         sp = findstr(tempstr,'[');
         if isempty(sp), sp = 12 +
findstr(tempstr,'diffuseColor'); end
         nc = 0;
         if ~isempty(sp)
            sp = sp +1;

[cvals,nc]=sscanf(tempstr(sp:length(tempstr)),'%f %f %f,');
         end
         if nc >= 3
            if nel > lastel+1
               for m = lastel+1:nel-1
                  color(m,1:3) = color(1,1:3); % if color
not set then make equal to 1st
               end
            end
            % if multi colors set then populate color
matrix, this is an inventor feature
            for s = 1:fix(nc/3)
                  color(s+nel-1,1:3) = cvals(3*s-2:3*s)';
               lastel = s+nel-1;
            end
         end
     end
     if ~isempty(findstr(tempstr,'transparency')), % get
transparency level
         sp = findstr(tempstr,'trans');

[tvals,nc]=sscanf(tempstr(sp+12:length(tempstr)),'%f');
         if nc > 0, trnsp(nel) = tvals(1); end
     end

     for i=1:3  %/* check for each keyword in line */
        key = deblank(keynames(i,:));
        if ~isempty(findstr(tempstr,key)) &
isempty(findstr(tempstr,'#'))
           %/* if key found again before all found there is
a problem
           %  so reset flag for that key */
           if ~foundkey(i), foundkey(i)=1;else
foundkey(i)=0; end
           if(i>1 & ~foundkey(i-1)) foundkey(i)=0; end %/*
previous key must exist first ! */
```

```
            end
         end
         if(foundkey(1) & foundkey(2)) %/* start of if A  first
2 keys found */
             if foundkey(3) %/* scan for connectivity data */
                tempstr = [tempstr,' #']; %/* last word marker
for end of line */
                skip = '';
                %/* loop puts integer values in a line into
connection array */
                word = ' ';
                while(word(1) ~= '#')
                   format = sprintf('%s %%s#',skip);
                   [word,nw] = sscanf(tempstr,format);
                   skip = [skip,'%*s'];
                   [node,nred] = sscanf(word,'%d,');
                   if nred>0
                      for p = 1:nred
                         if node(p) ~= -1
                            npt = npt +1;
                            % increment node value as matlab
counts from 1, vrml 0
                            w3d(nel).knx(npol,npt) = node(p)+1;
                         else
                            if npt > maxnp(nel), maxnp(nel) =
npt; end
                            npt = 0;
                            npol = npol + 1;
                         end
                      end
                   end
                end

                if ~isempty(findstr(tempstr,']')) %/* End of
data block marker */
                   polynum(nel)=npol-1; %/* store num of
polygons in this element */
                   endpts=0; %/* reset flag ready for next
element search */
                   npt=0;
                   npol=1;
                   foundkey = zeros(1,4); %/* reset keyword
flags for next search */
                   nel = nel+1; %/* now looking for next
element so increment counter
```

```
                 maxnp(nel) = 0;
                 w3d(nel).name = sprintf('patch%d',nel); %
name next block
              end
           end %/* end of scan for connectivity */

           %/* got 1st 2 keys but not 3rd and not end of co-
ords data */
           if(foundkey(2) & ~foundkey(3) & ~endpts) %/* scan
for pts data */
              sp = findstr(tempstr,'[');
              if isempty(sp)
                 %/* points data in x y z columns */
                 [fv,nv]=sscanf(tempstr,'%f %f %f,');
              else
                 %/* if block start marker [ in line - need
to skip over it to data
                 %   hence pointer to marker incremented */
                 sp = sp +1;

[fv,nv]=sscanf(tempstr(sp:length(tempstr)),'%f %f %f,');
              end
              if(nv>0)
                 if mod(nv,3) ~= 0
                    fclose(fp);
                    error('Error reading 3d wire co-
ordinates: should be x y z, on each line');
                 end
                 nov = fix(nv/3);
                 for p = 1:nov
                    npt = npt+1;
                    w3d(nel).pts(npt,1:3)=fv(3*p-2:3*p);
                 end
              end
              if ~isempty(findstr(tempstr,']')) %/* end of
pts data block */
                 endpts=1; %/* flag to stop entry to pts scan
while reading connections */
                 npt=0;
              end
           end %/* end of scan for data pts */
       end %/* end of if A */
    end %/* end of main loop */

   if nel == 0
```

```
        fclose(fp);
        error('Error reading 3d file: no data found');
 end
 nel = nel -1;

 % if not same number of verticies in each polygon we need
to fill
 % out rest of row in array with 1st value
 nc = size(color);
 ts = size(trnsp);

 for i = 1:nel
   facs = w3d(i).knx;
   ind1 = find(facs==0); [rown,coln] =
ind2sub(size(facs),ind1);
   facs(ind1) = facs(rown);
   w3d(i).knx = facs;
   if i > 1 & i > nc(1), color(i,1:3) = color(1,1:3); end %
extend color array to cover all elements
   w3d(i).color = color(i,1:3);
   w3d(i).polynum = polynum(i);
   if i > ts(2) | trnsp(i)==0,
       trnsp(i) = 1;
   end % extend transparency array to cover all elements
   w3d(i).trans = trnsp(i);
 end

 fclose(fp);

%  END OF FUNCTION read_vrml

%===========================================================
===========================
```

2. Bi-level collision detector

```
function intersected = BilevelDetector(line,comp_data,nel)
%% This function checks if a line identified by its start
and end points has full intersection with any of the
objects in a 2D workspace
% objects are identified either through their vertices or
their edges
% the function's inputs are the workspace data; coordinates
of each
```

```
% object's vertices and vertices link data determining the
edges of each
% object, the total number of objects in the workspace, and
the line data
% It then outputs a logical argument, 0 if no or partial
intersection and 1
% if full intersection occurs.

% the first section of this code checks if the object's
data is within the
% limits of line by looking into the bounding box
coordinates of the object
%-----------------------------------------------------------
----------------
intersected = [];
% Boundary Check
ColBB = zeros(nel,1);
for i = 1:nel
    if collision(line,comp_data{i,1}(:,(2:4))) == 1
        ColBB(i) = 1;
    else
        ColBB(i) = 0;
    end
end

% Line segment intersection detection
InBound = find(ColBB);
if isempty(InBound)
    intersected = [];
else
    XY1 = [line(1,(1:2)) line(2,(1:2))];
    for j = 1:size(InBound,1)
        XY2 = zeros(size(comp_data{InBound(j),2},1),4);
        for k = 1:size(comp_data{InBound(j),2},1)
            array = comp_data{InBound(j),2}(k,:);
            XY2(k,(1:2)) =
comp_data{InBound(j),1}(array(1),(2:3));
            XY2(k,(3:4)) =
comp_data{InBound(j),1}(array(2),(2:3));
        end

        out = lineSegmentIntersect_v2(XY1,XY2);
```

```
V = find(out.intAdjacencyMatrix);

% checking different cases of intersection: no
intersection, one-point or
% partial intersection, two-point intersection, and full
intersection
if isempty(V)
    intersected = intersected;

elseif size(V,2) == 1
    intersected = intersected;

elseif size(V,2) == 2
    x1=out.intMatrixX(V(1));
    x2=out.intMatrixX(V(2));
    y1=out.intMatrixY(V(1));
    y2=out.intMatrixY(V(2));
    if (abs(x1 - x2) <= 1e-10) && (abs(y1 - y2) <= 1e-10)

       intersected = [intersected];
    else
       intersected = [intersected InBound(j)];
    end
else
    intersected = [intersected InBound(j)];
end


end

end
end
```

Boundary check level:

```
% This function checks if a given line and polygon have a
potential of
% intersection by checking through the coordinates ranges.
% the inpts of this function are the coordinates of the
polygon and the
% line's start and end points in the form of [x1 y1 z1;x2
y2 z2]

function flag = collision(line,polygon)
```

```
theta = Line_angle(line(1,(1:2)),line(2,(1:2)));    %
calculation of the line inclination

% rotation of the coordinate system to a new system with x
axis being the given line
line_rot = CoordTransform(line,theta,-line(1,1),-
line(1,2),0);
polygon_rot = CoordTransform(polygon,theta,-line(1,1),-
line(1,2),0);
for i =1:size(polygon_rot,1)
    if abs(polygon_rot(i,2))<1e-12
        polygon_rot(i,2)=0;
    end
end


% check if the obstacle's x is within the min and max x
coordinates of the straight line
if  (min(polygon_rot(:,1)) >= max(line_rot(:,1))) ||
(max(polygon_rot(:,1)) <= min(line_rot(:,1)))
    flag = 0;
else
    if max(polygon_rot(:,2))*min(polygon_rot(:,2))<0
        flag = 1;
    else
        flag = 0;
    end
end
end
```

Line-segment intersection check level:

```
function out = lineSegmentIntersect_v2(XY1,XY2)
%LINESEGMENTINTERSECT Intersections of line segments.
%   OUT = LINESEGMENTINTERSECT(XY1,XY2) finds the 2D
Cartesian Coordinates of
%   intersection points between the set of line segments
given in XY1 and XY2.
%
%   XY1 and XY2 are N1x4 and N2x4 matrices. Rows correspond
to line segments.
%   Each row is of the form [x1 y1 x2 y2] where (x1,y1) is
the start point and
%   (x2,y2) is the end point of a line segment:
```

```
%
%                  Line Segment
%       o--------------------------------o
%       ^                                ^
%    (x1,y1)                          (x2,y2)
%
%   OUT is a structure with fields:
%
%   'intAdjacencyMatrix' : N1xN2 indicator matrix where the
entry (i,j) is 1 if
%       line segments XY1(i,:) and XY2(j,:) intersect.
%
%   'intMatrixX' : N1xN2 matrix where the entry (i,j) is
the X coordinate of the
%       intersection point between line segments XY1(i,:)
and XY2(j,:).
%
%   'intMatrixY' : N1xN2 matrix where the entry (i,j) is
the Y coordinate of the
%       intersection point between line segments XY1(i,:)
and XY2(j,:).
%
%   'intNormalizedDistance1To2' : N1xN2 matrix where the
(i,j) entry is the
%       normalized distance from the start point of line
segment XY1(i,:) to the
%       intersection point with XY2(j,:).
%
%   'intNormalizedDistance2To1' : N1xN2 matrix where the
(i,j) entry is the
%       normalized distance from the start point of line
segment XY1(j,:) to the
%       intersection point with XY2(i,:).
%
%   'parAdjacencyMatrix' : N1xN2 indicator matrix where the
(i,j) entry is 1 if
%       line segments XY1(i,:) and XY2(j,:) are parallel.
%
%   'coincAdjacencyMatrix' : N1xN2 indicator matrix where
the (i,j) entry is 1
%       if line segments XY1(i,:) and XY2(j,:) are
coincident.

% Version: 1.00, April 03, 2010
% Version: 1.10, April 10, 2010
% Author:  U. Murat Erdem

% CHANGELOG:
%
% Ver. 1.00:
%   -Initial release.
%
% Ver. 1.10:
%   - Changed the input parameters. Now the function
accepts two sets of line
%   segments. The intersection analysis is done between
these sets and not in
%   the same set.
%   - Changed and added fields of the output. Now the
analysis provides more
%   information about the intersections and line segments.
%   - Performance tweaks.

% I opted not to call this 'curve intersect' because it
would be misleading
% unless you accept that curves are pairwise linear
constructs.
% I tried to put emphasis on speed by vectorizing the code
as much as possible.
% There should still be enough room to optimize the code
but I left those out
% for the sake of clarity.
% The math behind is given in:
%
http://local.wasp.uwa.edu.au/~pbourke/geometry/lineline2d/
% If you really are interested in squeezing as much horse
power as possible out
% of this code I would advise to remove the argument checks
and tweak the
% creation of the OUT a little bit.

[n_rows_1,n_cols_1] = size(XY1);
[n_rows_2,n_cols_2] = size(XY2);

%%% Prepare matrices for vectorized computation of line
intersection points.
%-----------------------------------------------------------
---------------------
X1 = repmat(XY1(:,1),1,n_rows_2);
X2 = repmat(XY1(:,3),1,n_rows_2);
```

```
Y1 = repmat(XY1(:,2),1,n_rows_2);
Y2 = repmat(XY1(:,4),1,n_rows_2);

XY2 = XY2';

X3 = repmat(XY2(1,:),n_rows_1,1);
X4 = repmat(XY2(3,:),n_rows_1,1);
Y3 = repmat(XY2(2,:),n_rows_1,1);
Y4 = repmat(XY2(4,:),n_rows_1,1);

X4_X3 = (X4-X3);
Y1_Y3 = (Y1-Y3);
Y4_Y3 = (Y4-Y3);
X1_X3 = (X1-X3);
X2_X1 = (X2-X1);
Y2_Y1 = (Y2-Y1);

numerator_a = X4_X3 .* Y1_Y3 - Y4_Y3 .* X1_X3;
numerator_b = X2_X1 .* Y1_Y3 - Y2_Y1 .* X1_X3;
denominator = Y4_Y3 .* X2_X1 - X4_X3 .* Y2_Y1;

u_a = numerator_a ./ denominator;
u_b = numerator_b ./ denominator;

% Find the adjacency matrix A of intersecting lines.
INT_X = X1+X2_X1.*u_a;
INT_Y = Y1+Y2_Y1.*u_a;
INT_B = (u_a >= 0) & (u_a <= 1.00001) & (u_b >= 0) & (u_b
<= 1.00001);



% Arrange output.
out.intAdjacencyMatrix = INT_B;
out.intMatrixX = INT_X .* INT_B;
out.intMatrixY = INT_Y .* INT_B;
out.intNormalizedDistance1To2 = u_a;
out.intNormalizedDistance2To1 = u_b;


end
```

3. **Construction of the free space graph:**

```
% this function takes the coordinates of the two nodes to
find all safe paths
% between them; Pi = [id xi yi zi]
function AllSafeRoute =
SafeGraph_v2(P1,P2,comp_data,nel,ipath)

V1 = P1(:,(2:4));
V2 = P2(:,(2:4));
line = [V1;V2];

% Slope of the straight line
theta1 = Line_angle(V1,V2);

% collision detector
intersected = BilevelDetector(line,comp_data,nel);

%% Path Generator
if isempty(intersected)

    AllSafeRoute = [P1;P2];

else
    %% Creating the convex hulls

    % ordering the colliding obstacles
    int_info = zeros(size(intersected,2),2);    % storing
the information of intersections
    int_info(:,1) = intersected';

    % ordering the obstacles based on the distance from the
start point
    for i0 = 1:size(intersected,2)
        comp_data{intersected(i0),3} =
[comp_data{intersected(i0),1}(:,1)
CoordTransform(comp_data{intersected(i0),1}(:,(2:4)),theta1
,-P1(2),-P1(3),0)];
        int_info(i0,2) =
min(comp_data{intersected(i0),3}(:,2));
    end
    int_info_sorted = sortrows(int_info,2);

    % number of convex hulls need to be generated
    nch = 2*(size(intersected,2));

    % creating a cell to store convex hulls
    chull = cell(1,nch);

    %building the first convex hull
    chull{1} =
chull_generator(P1,comp_data{int_info_sorted(1,1),1});
    [~,Y] = max(comp_data{int_info_sorted(1,1),3}(:,3));
    start_max = comp_data{int_info_sorted(1,1),1}(Y,:);
    [~,Y] = min(comp_data{int_info_sorted(1,1),3}(:,3));
    start_min = comp_data{int_info_sorted(1,1),1}(Y,:);

    % building the max convex hulls
    for t = 2:size(int_info_sorted,1)
        chull{2*t-2} =
chull_generator(start_max,comp_data{int_info_sorted(t,1),1}
);
         [~,Y] =
max(comp_data{int_info_sorted(t,1),3}(:,3));
         start_max =
comp_data{int_info_sorted(t,1),1}(Y,:);
    end

    % building the min convex hulls
    for t = 2:size(int_info_sorted,1)
        chull{2*t-1} =
chull_generator(start_min,comp_data{int_info_sorted(t,1),1}
);
        [~,Y] =
min(comp_data{int_info_sorted(t,1),3}(:,3));
        start_min = comp_data{int_info_sorted(t,1),1}(Y,:);
    end

    % building the last convex hull using the end point of
the straight line

    chull{size(chull,2)} =
chull_generator(P2,comp_data{int_info_sorted(size(int_info_
sorted,1),1),1});

    % rotate first point
    P1_r = [P1(1) CoordTransform(P1(:,(2:4)),theta1,-
P1(2),-P1(3),0)];
```

```
    % start building the path
    children = ChildFinder(P1_r,chull,comp_data);
    if isempty(children)
        AllSafeRoute = AllSafeRoute;
        return
    else
         AllSafeRoute = {};

        for j = 1:size(children,2)

            [X,Y,Z] = node_coordinate_v2
(children(j),comp_data,1);
            ch = [children(j),X,Y,Z];
            if horimember(ch,ipath)
                continue
            else
             Path1 =
SafeGraph_v2(P1,ch,comp_data,nel,ipath);  % creating the
first segment of the path; from the initial node to the
current node

             Path2 =
SafeGraph_v2(ch,P2,comp_data,nel,Path1);  % creating the
second segment of the path; from the current node to the
final node

             % Depending on the number of Path1 and Path2
between the two
             % points, 4 different cases are possible:

             if (~iscell(Path1)) && (~iscell(Path2))
                 path = Path1;
                 for p = 2:size(Path2,1)
                     p2 = Path2(p,:);
                     path = [path;p2];
                 end


plot((path(:,2)),(path(:,3)),'LineWidth',2);
                 hold on
                 AllSafeRoute = [AllSafeRoute;path];

             elseif (~iscell(Path1)) && (iscell(Path2))

                 for t1 = 1:size(Path2,1)
```

```
                     path = Path1;
                     subpath2 = cell2mat(Path2(t1));
                     for p = 2:size(subpath2,1)
                         p2 = subpath2(p,:);
                         path = [path;p2];
                     end


plot((path(:,2)),(path(:,3)),'LineWidth',2);
                     hold on
                     AllSafeRoute = [AllSafeRoute;path];
                 end

             elseif (iscell(Path1)) && (~iscell(Path2))
                 for t2 = 1:size(Path1,1)
                     subpath1 = cell2mat(Path1(t2));
                     path = subpath1;
                     for p = 2:size(Path2,1)
                         p2 = Path2(p,:);
                         path = [path;p2];
                     end


plot((path(:,2)),(path(:,3)),'LineWidth',2);
                     hold on
                     AllSafeRoute = [AllSafeRoute;path];
                 end

             else
                 for t3 = 1:size(Path1,1)
                     subpath1 = cell2mat(Path1(t3));

                     for t4 = 1:size(Path2,1)
                         path = subpath1;
                         subpath2 = cell2mat(Path2(t4));
                         for p = 2:size(subpath2,1)
                             p2 = subpath2(p,:);
                             path = [path;p2];
                         end


plot((path(:,2)),(path(:,3)),'LineWidth',2);
                         hold on
                         AllSafeRoute =
[AllSafeRoute;path];
```

```
                    end
                end

            end
           end

       end

   end

end


end
```

4. **Dijkstra's algorithm:**

```
function [dist,path] =
dijkstra(nodes,segments,start_id,finish_id)
%DIJKSTRA Calculates the shortest distance and path between
points on a map
%   using Dijkstra's Shortest Path Algorithm
%
% [DIST, PATH] = DIJKSTRA(NODES, SEGMENTS, SID, FID)
%   Calculates the shortest distance and path between start
and finish nodes SID and FID
%
% [DIST, PATH] = DIJKSTRA(NODES, SEGMENTS, SID)
%   Calculates the shortest distances and paths from the
starting node SID to all
%     other nodes in the map
%
% Note:
%     DIJKSTRA is set up so that an example is created if
no inputs are provided,
%       but ignores the example and just processes the
inputs if they are given.
%
% Inputs:
%     NODES should be an Nx3 or Nx4 matrix with the format
[ID X Y] or [ID X Y Z]
```

```
%       where ID is an integer, and X, Y, Z are cartesian
position coordinates)
%     SEGMENTS should be an Mx3 matrix with the format [ID
N1 N2]
%       where ID is an integer, and N1, N2 correspond to
node IDs from NODES list
%       such that there is an [undirected] edge/segment
between node N1 and node N2
%     SID should be an integer in the node ID list
corresponding with the starting node
%     FID (optional) should be an integer in the node ID
list corresponding with the finish
%
% Outputs:
%     DIST is the shortest Euclidean distance
%       If FID was specified, DIST will be a 1x1 double
representing the shortest
%         Euclidean distance between SID and FID along the
map segments. DIST will have
%         a value of INF if there are no segments
connecting SID and FID.
%       If FID was not specified, DIST will be a 1xN vector
representing the shortest
%         Euclidean distance between SID and all other
nodes on the map. DIST will have
%         a value of INF for any nodes that cannot be
reached along segments of the map.
%     PATH is a list of nodes containing the shortest route
%       If FID was specified, PATH will be a 1xP vector of
node IDs from SID to FID.
%         NAN will be returned if there are no segments
connecting SID to FID.
%       If FID was not specified, PATH will be a 1xN cell
of vectors representing the
%         shortest route from SID to all other nodes on the
map. PATH will have a value
%         of NAN for any nodes that cannot be reached along
the segments of the map.
%
% Example:
%     dijkstra; % calculates shortest path and distance
between two nodes
%               % on a map of randomly generated nodes and
segments
%
```

```
% Example:
%     nodes = [(1:10); 100*rand(2,10)]';
%     segments = [(1:17); floor(1:0.5:9); ceil(2:0.5:10)]';
%     figure; plot(nodes(:,2), nodes(:,3),'k.');
%     hold on;
%     for s = 1:17
%         if (s <= 10) text(nodes(s,2),nodes(s,3),[' '
num2str(s)]); end
%
plot(nodes(segments(s,2:3)',2),nodes(segments(s,2:3)',3),'k
');
%     end
%     [d, p] = dijkstra(nodes, segments, 1, 10)
%     for n = 2:length(p)
%         plot(nodes(p(n-1:n),2),nodes(p(n-1:n),3),'r-
.','linewidth',2);
%     end
%     hold off;
%
% Author: Joseph Kirk
% Email: jdkirk630 at gmail dot com
% Release: 1.3
% Release Date: 5/18/07

if (nargin < 3) % SETUP
    % (GENERATE RANDOM EXAMPLE OF NODES AND SEGMENTS IF NOT
GIVEN AS INPUTS)
    % Create a random set of nodes/vertices,and connect
some of them with
    % edges/segments. Then graph the resulting map.
    num_nodes = 40; L = 100; max_seg_length = 30; ids =
(1:num_nodes)';
    nodes = [ids L*rand(num_nodes,2)]; % create random
nodes
    h = figure; plot(nodes(:,2),nodes(:,3),'k.') % plot the
nodes
    text(nodes(num_nodes,2),nodes(num_nodes,3),...
        [' '
num2str(ids(num_nodes))],'Color','b','FontWeight','b')
    hold on
    num_segs = 0; segments = zeros(num_nodes*(num_nodes-
1)/2,3);
    for i = 1:num_nodes-1 % create edges between some of
the nodes
```

```
        text(nodes(i,2),nodes(i,3),[' '
num2str(ids(i))],'Color','b','FontWeight','b')
        for j = i+1:num_nodes
            d = sqrt(sum((nodes(i,2:3) -
nodes(j,2:3)).^2));
            if and(d < max_seg_length,rand < 0.6)
                plot([nodes(i,2) nodes(j,2)],[nodes(i,3)
nodes(j,3)],'k.-')
                % add this link to the segments list
                num_segs = num_segs + 1;
                segments(num_segs,:) = [num_segs nodes(i,1)
nodes(j,1)];
            end
        end
    end
    segments(num_segs+1:num_nodes*(num_nodes-1)/2,:) = [];
    axis([0 L 0 L])
    % Calculate Shortest Path Using Dijkstra's Algorithm
    % Get random starting/ending nodes,compute the shortest
distance and path.
    start_id = ceil(num_nodes*rand); disp(['start id = '
num2str(start_id)]);
    finish_id = ceil(num_nodes*rand); disp(['finish id = '
num2str(finish_id)]);
    [distance,path] =
dijkstra(nodes,segments,start_id,finish_id);
    disp(['distance = ' num2str(distance)]); disp(['path =
[' num2str(path) ']']);
    % If a Shortest Path exists,Plot it on the Map.
    figure(h)
    for k = 2:length(path)
        m = find(nodes(:,1) == path(k-1));
        n = find(nodes(:,1) == path(k));
        plot([nodes(m,2) nodes(n,2)],[nodes(m,3)
nodes(n,3)],'ro-','LineWidth',2);
    end
    title(['Shortest Distance from ' num2str(start_id) ' to
' ...
        num2str(finish_id) ' = ' num2str(distance)])
    hold off

else %------------------------------------------------------------
---------------------
    % MAIN FUNCTION - DIJKSTRA'S ALGORITHM
    num_nodes = size(nodes,1);
    ids = nodes(:,1);
%     h = figure;
plot(nodes(:,2),nodes(:,3),'k.') % plot the nodes
    text(nodes(num_nodes,2),nodes(num_nodes,3),...
        [' '
num2str(ids(num_nodes))],'Color','b','FontWeight','b')
    hold on
    for j = 1:num_nodes
    text(nodes(j,2),nodes(j,3),...
        ['  ' num2str(ids(j))],'Color','b','FontWeight','b')
   hold on
    end

    % plot the edges
    for i = 1:size(segments,1)
        array = segments(i,(2:3));
        plot([nodes(find(ids==array(1)),2)
nodes(find(ids==array(2)),2)],
[nodes(find(ids==array(1)),3)
nodes(find(ids==array(2)),3)],'k.-','LineWidth',2)
        hold on
    end

    % initializations
    node_ids = nodes(:,1);
    [num_map_pts,cols] = size(nodes);
    table = sparse(num_map_pts,2);
    shortest_distance = Inf(num_map_pts,1);
    settled = zeros(num_map_pts,1);
    path = num2cell(NaN(num_map_pts,1));
    col = 2;
    pidx = find(start_id == node_ids);
    shortest_distance(pidx) = 0;
    table(pidx,col) = 0;
    settled(pidx) = 1;
    path(pidx) = {start_id};
    if (nargin < 4) % compute shortest path for all nodes
        while_cmd = 'sum(~settled) > 0';
    else % terminate algorithm early
        while_cmd = 'settled(zz) == 0';
        zz = find(finish_id == node_ids);
    end
    while eval(while_cmd)
        % update the table
        table(:,col-1) = table(:,col);
        table(pidx,col) = 0;
        % find neighboring nodes in the segments list
        neighbor_ids = [segments(node_ids(pidx) ==
segments(:,2),3);
            segments(node_ids(pidx) == segments(:,3),2)];
        % calculate the distances to the neighboring nodes
and keep track of the paths
        for k = 1:length(neighbor_ids)
            cidx = find(neighbor_ids(k) == node_ids);
            if ~settled(cidx)
                d = sqrt(sum((nodes(pidx,2:cols) -
nodes(cidx,2:cols)).^2));
                if (table(cidx,col-1) == 0) || ...
                        (table(cidx,col-1) >
(table(pidx,col-1) + d))
                    table(cidx,col) = table(pidx,col-1) +
d;
                    tmp_path = path(pidx);
                    path(cidx) = {[tmp_path{1}
neighbor_ids(k)]};
                else
                    table(cidx,col) = table(cidx,col-1);
                end
            end
        end
        % find the minimum non-zero value in the table and
save it
        nidx = find(table(:,col));
        ndx = find(table(nidx,col) ==
min(table(nidx,col)));
        if isempty(ndx)
            break
        else
            pidx = nidx(ndx(1));
            shortest_distance(pidx) = table(pidx,col);
            settled(pidx) = 1;
        end
    end
    if (nargin < 4) % return the distance and path arrays
for all of the nodes
        dist = shortest_distance';
        path = path';
    else % return the distance and path for the ending node
        dist = shortest_distance(zz);
        path = path(zz);
        path = path{1};
    end
    % If a Shortest Path exists,Plot it on the Map.
    for k = 2:length(path)
        m = find(nodes(:,1) == path(k-1));
        n = find(nodes(:,1) == path(k));
        plot([nodes(m,2) nodes(n,2)],[nodes(m,3)
nodes(n,3)],'ro-','LineWidth',2);
    end
    title(['Shortest Distance from ' num2str(start_id) ' to
' ...
        num2str(finish_id) ' = ' num2str(dist)])
%     hold off
end
```

REFERENCES

[1] Dandurand, B., Guarneri, P., Fadel, G. M., and Wiecek, M. M., 2014, “Bi-level Multibjective Packaging Optimization for Automotive Design,” J. Mech. Des., (November 2013).

[2] Wodziak, J. R., and Fadel, G. M., 1994, “Packing and optimizing the center of gravity location using a genetic algorithm,” J. Comput. Ind., **11**, pp. 2–14.

[3] Grignon, P. M., and Fadel, G. M., 1999, “CONFIGURATION DESIGN OPTIMIZATION METHOD,” Proceedings of DETC99 1999 ASME Design Engineering Technical Conferences September 12–15, 1999, Las Vegas, Nevada, pp. 1–13.

[4] Miao, Y., Blouin, V. Y., and Fadel, G. M., 2003, “Multi-objective configuration optimization with vehicle dynamics applied to midsize truck design,” Proceedings of ASME, pp. 319–327.

[5] Dong, H., Fadel, G. M., and Blouin, V. Y., 2005, “Packing optimization by enhanced rubber band analogy,” ASME International Design Engineering Technical Conferences and Computers and Information in Engineering Conference, Long Beach, California. 2005, pp. 1–9.

[6] Tiwari, S., Fadel, G., and Fenyes, P., 2008, “A fast and efficient compact packing algorithm for free-form objects,” Proceedings of the ASME International Design Engineering Technical Conferences & Computers and Information in Engineering Conference, New York, ASME Paper No. DETC2008-50097.

[7] Katragadda, R. T., Gondipalle, S. R., Guarneri, P., and Fadel, G., 2012, “Predicting the thermal performance for the multi-objective vehicle underhood packing optimization problem,” Proceedings of ASME DETC, pp. 1–8.

[8] Matheus, K., and Konigseder, T., 2015, Automotive Ethernet, Cambridge University Press.

[9] Latombe, J.-C., 1991, Robot Motion Planning, Kluwer Academic Publishers, Boston.

[10] Bhattacharya, B. Y. P., and Gavrilova, M. L., 2008, “Roadmap-Based Path Planning,” (June).

[11] Amato, N. M., and Wu, Y., 1996, “A Randomized Roadmap Method for Path and Manipulation Planning,” IEEE International Conference on Robotics and Automation, pp. 113–120.

[12] Borenstein, J., and Koren, Y., 1989, “Real-time obstacle avoidance for fast mobile robots,” {IEEE} {T}ransactions on {S}ystems, {M}an, & {C}ybernetics, **19**(5), pp. 1179–1187.

[13] Sandurkar, S., and Chen, W., 1999, “GAPRUS - genetic algorithms based pipe routing using tessellated objects,” Comput. Ind., **38**(3), pp. 209–223.

[14] O’Rourke, J., and Mallinckrodt, A. J., 1995, Computational Geometry in C, Computers in Physics.

[15] Asano, T., Asano, T., Guibas, L., Hershberger, J., and Imai, H., 1985, "Visibility-Polygon Search and Euclidean Shortest Paths," Found. Comput. Sci., pp. 155–164.

[16] Rohnert, H., 1986, "Shortest Paths in the Plane with Convex Polygonal Obstacles," Information, **23**, pp. 71–76.

[17] Fredman, M. L., and Tarjan, R. E., 1987, "Fibonacci heaps and their uses in improved network optimization algorithms.pdf," J. ACM, **34.3**, pp. 596–615.

[18] Welzl, E., 1985, "CONSTRUCTING THE VISIBILITY GRAPH FOR n-LINE SEGMENTS IN O(n 2) TIME," Inf. Process. Lett., pp. 167–171.

[19] Sharir, M., and Schorr, A., 1986, "On shortest paths in polyhedral Spaces," SIAM J. Comput., **15.1**(1), pp. 193–215.

[20] Aho, A. V., and Hopcroft, J. E., 1974, "Design and Analysis of Computer Algorithms," Pearson Education India.

[21] Butt, S. E., and Cavalier, T. M., 1996, "An efficient algorithm for facility location in the presence of forbidden regions," Eur. J. Oper. Res., **90**(1), pp. 56–70.

[22] Lozano-Pérez, T., and Wesley, M. a., 1979, "An algorithm for planning collision-free paths among polyhedral obstacles," Commun. ACM, **22**(10), pp. 560–570.

[23] Meeran, S., and Shafie, A., 1997, "O P T I M U M PATH PLANNING USING CONVEX HULL AND LOCAL SEARCH HEURISTIC ALGORITHMS," Mechatronics, **7**(8), pp. 737–756.

[24] Flood, M. M. ., 1956, "The Traveling Salesman Problem," Oper. Res., **4**(1), pp. 61–75.

[25] Bhattacharya, P., Tnn, C., and Gavrilova, M. L., 2007, "Geometric Algorithms for Clearance Based Optimal Path Computation," pp. 1–4.

[26] Dijkstra, E. W., 1959, "A note on two problems in connexion with graphs.pdf," Numer. Math., pp. 269–271.

[27] Wein, R., and Halperin, D., 2005, "The Visibility – Voronoi Complex and Its Applications," Proc. twenty-first Annu. Symp. Comput. Geom., pp. 63–72.

[28] Clarkson, K., 1987, "Approximation algorithms for shortest path motion planning," Proc. Ninet. Annu. ACM Symp. Theory Comput., pp. 56–65.

[29] Hershberger, J., and Suri, S., 1999, "An Optimal Algorithm for Euclidean Shortest Paths in the Plane," SIAM J. Comput., **28**(6), pp. 2215–2256.

[30] Yin, Y. H., Zhou, C., and Zhu, J. Y., 2010, "A pipe route design methodology by imitating human imaginal thinking," CIRP Ann. - Manuf. Technol., **59**(1), pp. 167–170.

[31] Szykman, S., and Cagan, J., 1996, "Synthesis of Optimal Nonorthogonal Routes.pdf," J. Mech. Des., **118**(3), pp. 419–424.

[32] Gottschalk, S., Lin, M. C., Manocha, D., and Hill, C., 1996, "OBBTree: A Hierarchical Structure for Rapid Interference Detection," Proceedings of the 23rd annual conference on Computer graphics and interactive techniques. ACM, pp. 171–180.

[33] Conru, A. B., and Cutkosky, M. R., 1993, "Computational Support for Interactive

Cable Harness Routing and Design," Adv. Des. Autom., **1**, pp. 551–558.

[34] Conru, A. B., 1994, "A genetic approach to the cable harness routing problem," Ieee, pp. 200–205.

[35] Lin, C., Rao, L., Giusto, P., Ambrosio, J. D., and Sangiovanni-vincentelli, A., 2014, "An Efficient Wire Routing and Wire Sizing Algorithm for Weight Minimization of Automotive Systems," Proceedings of the 51st Annual Design Automation Conference. ACM, pp. 1–6.

[36] Lin, C., Rao, L., Ambrosio, J. D., and Sangiovanni-vincentelli, A., 2014, "Electrical Architecture Optimization and Selection - Cost Minimization via Wire Routing and Wire Sizing," SAE Int. J. Passeng. Cars-Electronic Electr. Syst., pp. 502–509.

[37] Zhu, Z., 2017, "A methodology to enable automatic 3D routing of aircraft Electrical Wiring Interconnection System," CEAS Aeronaut. J., **8**(2), pp. 287–302.

[38] Chen, D. Z., 2017, "Developing Algorithms and Software for Geometric Path Planning Problems," **28**(December 1996), pp. 1–5.

[39] Zeid, I., 2005, Mastering CAD/CAM, Mc Graw Hill.

[40] Fadel, G. M., Kirschman, C., and Kirschman, C., 1996, "Accuracy issues in CAD to RP translations," Rapid Prototyp. J.

[41] Liu, E. P., and Carey, R., 1998, "The Virtual Reality Modeling Language Explained," IEEE Multimed., **5**(3), pp. 84–93.

[42] "Multidemnsional Arrays" [Online]. Available: https://www.mathworks.com/help/matlab/math/multidimensional-arrays.html#f1-87418.

[43] Aurenhammer, F., 1991, "Voronoi Diagrams — A Survey of a Fundamental Data Structure," **23**(3).

[44] K, S., 1993, "Approximation of Generalized Voronoi Diagrams by Ordinary Voronoi Diagrams," CVGIP Graph. Model. Image Process., **55 (6)**, pp. 522–531.

[45] Mounts, D. M., 1991, "AN OUTPUT SENSITIVE ALGORITHM FOR COMPUTING VISIBILITY GRAPHS *," **20**(5), pp. 888–910.

[46] Sniedovich, M., 2006, "Dijkstra ' s algorithm revisited : the dynamic programming connexion by," **35**(3), pp. 87–92.

[47] 2009, "Lecture 18 Solving Shortest Path Problem : Dijkstra ' s Algorithm" [Online]. Available: http://www.ifp.illinois.edu/~angelia/ge330fall09_dijkstra_l18.pdf.